



Mechanisms of DNA damage by redox active Cr(III) complexes  
by Kent Dennis Sugden

A thesis submitted in partial fulfillment of the requirements for the degree of Doctor of Philosophy  
Chemistry

Montana State University

© Copyright by Kent Dennis Sugden (1992)

Abstract:

Investigations of the mechanisms and interactions of chromium complexes with DNA are essential for the better understanding of how these complexes may induce carcinogenesis as well as their possible negative environmental impacts. The prevalence of chromium in the +3 oxidation state both environmentally and intracellularly implicate this oxidation state as a potentially important biologically active complex.

A series of biologically active and inactive Cr(III) complexes were synthesized and used to determine structure/activity relationships and the role that ligands have in conferring biological activity.

The biological activity of these complexes has been measured in a Salmonella reversion assay. Those complexes that tested positive were assayed in an anaerobic Salmonella assay to determine if mutagenic activity was dependent on oxygen. Loss of activity, upon assaying under anoxic conditions, implicates reactive oxygen species in the mechanism of DNA damage. Mutant frequencies were determined for the active complexes to give a relative reversion order irrespective of toxicity.

Cyclic voltammetry was employed to determine the redox kinetics of Cr(III) complexes and the relationship of this physical parameter with the generation of oxygen radicals. Cyclic voltammetry has shown that the ligands contribute to the formation of these radical species by "activating" the metal center.

Plasmid relaxation assays have been carried out to demonstrate that the complexes can produce a radical that uses DNA as a substrate. This radical can be shown to induce relaxation of supercoiled DNA consistent with a mechanism of oxygen radical generation.

Interactions of Cr(III) complexes with DNA are required for a radical mechanism of damage. The type of DNA interactions associated with mutagenic Cr(III) complexes have been shown using equilibrium dialysis, electrophoretic mobilities and UV-VIS spectrophotometry. Some of the mutagenic Cr(III) complexes show physical properties which implicate an intercalation mode of interaction with DNA.

A predictive model is proposed that allows ranking of efficacy of potentially mutagenic Cr(III) complexes based on their redox characteristics and interactions with DNA.

**MECHANISMS OF DNA DAMAGE BY REDOX  
ACTIVE Cr(III) COMPLEXES**

by

Kent Dennis Sugden

A thesis submitted in partial fulfillment  
of the requirements for the degree

of

Doctor of Philosophy

in

Chemistry

**MONTANA STATE UNIVERSITY  
Bozeman, Montana**

June 1992



**STATEMENT OF PERMISSION TO USE**

In presenting this thesis in partial fulfillment of the requirements for a doctoral degree at Montana State University, I agree that the Library shall make it available to borrowers under rules of the library. I further agree that copying of the thesis is allowable only for scholarly purposes, consistent with "fair use" as prescribed in the U.S. Copyright Law. Request for extensive copying or reproduction of this thesis should be referred to University Microfilms International, 300 North Zeeb Road, Ann Arbor, Michigan 48106, to whom I have granted "the exclusive right to reproduce and distribute copies of the dissertation in and from microfilm and the right to reproduce and distribute by abstract in any format."

Signature 

Date 7/22/97

## TABLE OF CONTENTS

	<u>Page</u>
LIST OF TABLES.....	vii
LIST OF FIGURES.....	viii
ABSTRACT.....	xiii
INTRODUCTION.....	1
Chromium Mutagenesis.....	1
History.....	1
Theory.....	2
Activity Of Cr(III) Versus Cr(VI).....	2
Selective Uptake/Reduction Model.....	3
Mechanisms Of DNA Damage By Other Compounds.....	6
Cis-Platinum.....	7
Alkylating Agents (MNNG And MMS).....	8
Bleomycin.....	9
Paraquat.....	10
Oxygen Radicals.....	11
Characterization.....	11
Superoxide Anion Radical.....	12
Hydroxyl Radical.....	13
Formation.....	14
The Haber-Weiss Reaction.....	14
The Fenton Reaction.....	14
DNA Interactions.....	15
Models Of Interaction.....	16
Covalent Dimers.....	16
Intercalation.....	16
Coulombic Attraction.....	17
Reduction Adducts.....	18
Electrochemical Behavior Of Metals.....	18
Theory.....	18
STATEMENT OF THE PROBLEM.....	22
EXPERIMENTAL.....	25

	<u>Page</u>
Synthesis, Purification And Characterization Of Cr(III) Complexes.	25
[Cr(bpy) <sub>2</sub> Cl <sub>2</sub> ]Cl And [Cr(bpy) <sub>2</sub> (H <sub>2</sub> O) <sub>2</sub> ]Cl <sub>3</sub> .....	25
Synthesis Of Substituted Bipyridyls.....	26
[Cr(dmbpy) <sub>2</sub> Cl <sub>2</sub> ]Cl.....	30
[Cr(dcbpy) <sub>2</sub> Cl <sub>2</sub> ]Cl.....	30
[Cr(dmebpy) <sub>2</sub> Cl <sub>2</sub> ]Cl.....	31
[Cr(dmabpy) <sub>2</sub> Cl <sub>2</sub> ]Cl.....	31
[Cr(bpy) <sub>2</sub> F <sub>2</sub> ]F.....	32
[Cr(bpy) <sub>2</sub> Br <sub>2</sub> ]Br.....	32
[Cr(bpy) <sub>2</sub> I <sub>2</sub> ]I.....	32
[Cr(phen) <sub>2</sub> Cl <sub>2</sub> ]Cl And [Cr(phen) <sub>2</sub> (H <sub>2</sub> O) <sub>2</sub> ]Cl <sub>3</sub> .....	33
[Cr(bpy) <sub>3</sub> ](ClO <sub>4</sub> ) <sub>3</sub> .....	34
[Cr(en) <sub>3</sub> ]Cl <sub>3</sub> .....	37
[Cr(en) <sub>2</sub> Cl <sub>2</sub> ]Cl.....	37
[Cr(NH <sub>3</sub> ) <sub>4</sub> Cl <sub>2</sub> ]Cl.....	38
K <sub>3</sub> Cr(CN) <sub>6</sub> .....	39
[Cr(py) <sub>4</sub> Cl <sub>2</sub> ]Cl.....	39
Biological Assays For Mutagenicity .....	40
Salmonella Reversion Assay.....	40
Aerobic Assay.....	41
Anaerobic Assay.....	42
Mutation Frequency.....	43
SOS Response.....	44
Aerobic Assay.....	45
Anaerobic Assay.....	46
Toxicity Testing.....	47
Mutagenesis In Mammalian Cells.....	47
Cyclic Voltammetry.....	48
Instrumentation.....	48
Software.....	49
Electrochemical Cells And Electrodes.....	50
CV Methods And Parameters.....	52
Electrode Area.....	52
Data Analysis.....	53
Electrophoresis.....	53
Instrumentation.....	54
Plasmid Transformations.....	54
DNA Plasmid Extraction.....	55
Electrophoretic Experimental Procedures.....	57
Metal Interactions With DNA.....	58
UV-VIS Spectrophotometry.....	58
Equilibrium Dialysis And Polarimetry.....	58

	<u>Page</u>
Electrophoretic Mobilities.....	60
Membrane Permeability.....	60
RESULTS AND DISCUSSION.....	61
Structures Of The Cr(III) Complexes.....	61
Biological Assays.....	69
Membrane Permeability.....	94
Cyclic Voltammetry.....	98
Plasmid Relaxation Studies.....	126
Interactions Of Mutagenic Cr(III) Complexes With DNA.....	132
Electrophoretic Mobility.....	133
Equilibrium Dialysis And Polarimetry.....	135
Spectrophotometric Changes Upon Intercalation.....	137
SUMMARY.....	140
LITERATURE CITED.....	144
APPENDIX.....	151

## LIST OF TABLES

<u>Table</u>		<u>Page</u>
I.	Relative reversion rates of original Cr(III) complexes.....	70
II.	Reversion rate of halogenated bipyridyl complexes.....	85
III.	Relative reversion rates of substituted bipyridyls.....	90
IV.	Mammalian toxicity and mutagenesis of selected chromium compounds.....	94
V.	Half-wave potentials of the Cr(III)/Cr(II) redox couple for original Cr(III) complexes.....	115
VI.	Half-wave potentials of the Cr(III)/Cr(II) redox couple for the different halogenated complexes of bipyridyl.....	117
VII.	Half-wave potentials of the Cr(III)/Cr(II) redox couple for the substituted bipyridyl complexes.....	123
VIII.	Chiral enrichment of Cr(III) isomers after dialysis.....	137

## LIST OF FIGURES

<u>Figure</u>	<u>Page</u>
1. Schematic representation of selective uptake/reduction of Cr(VI)...	6
2. cis-Pt dimer formation with adjacent guanosine DNA bases.....	8
3. Alkylating agents and alkylated lesions on DNA bases.....	9
4. Structure of bleomycin.....	10
5. Structure of paraquat (methyl viologen).....	11
6. Intercalation between coplanar DNA bases.....	17
7. Reversible, quasi-reversible and irreversible waves in the cyclic voltammeter.....	21
8. Synthesis of substituted bipyridyls.....	29
9. Structures of Cr(III) complexes.....	66
10. Structures of Cr(III) complexes.....	67
11. Structures of Cr(III) complexes.....	68
12. Salmonella reversion assay of original mutagenic complexes in TA102.....	71
13. Salmonella reversion assay of original mutagenic complexes in TA2638.....	71
14. Salmonella reversion assay of nonmutagenic Cr(III) complexes in TA102.....	72
15. Salmonella reversion assay of nonmutagenic Cr(III) complexes in TA2638.....	72
16. Mutation frequency of original Cr(III) complexes in TA102.....	73
17. Mutation frequency of original Cr(III) complexes in TA2638.....	73

LIST OF FIGURES-continued

<u>Figure</u>	<u>Page</u>
18. Salmonella reversion assay of bipyridyl and phenanthroline ligands in TA102.....	75
19. Salmonella reversion assay of bipyridyl and phenanthroline ligands in TA2638.....	75
20. Salmonella reversion assay of Cr(VI) and a representative Cr(III) complex in TA100.....	76
21. Salmonella reversion assay of Cr(VI) both aerobic and anaerobic in TA102.....	79
22. Salmonella reversion assay of a representative Cr(III) complex both aerobic and anaerobic in TA102.....	79
23. Salmonella reversion assay of Cr(VI) both aerobic and anaerobic in TA2638.....	80
24. Salmonella reversion assay of a representative Cr(III) complex both aerobic and anaerobic in TA2638.....	80
25. Salmonella reversion assay of MNNG both aerobic and anaerobic in TA2638.....	81
26. SOS response of a representative Cr(III) complex both aerobic and anaerobic with GE-94.....	81
27. Salmonella reversion assay of the different halogenated complexes of Cr(bpy) <sub>2</sub> X <sub>2</sub> in TA102.....	83
28. Salmonella reversion assay of the different halogenated complexes of Cr(bpy) <sub>2</sub> X <sub>2</sub> in TA2638.....	83
29. Mutation frequency of different halogenated complexes of Cr(bpy) <sub>2</sub> X <sub>2</sub> in TA102.....	84
30. Mutation frequency of different halogenated complexes of Cr(bpy) <sub>2</sub> X <sub>2</sub> in TA2638.....	84

## LIST OF FIGURES-Continued

<u>Figure</u>	<u>Page</u>
31. Salmonella reversion assay of substituted bipyridyl complexes of Cr(III) in TA102.....	87
32. Salmonella reversion assay of substituted bipyridyl complexes in TA2638.....	87
33. Mutation frequency of substituted bipyridyl complexes of Cr(III) in TA102.....	91
34. Mutation frequency of substituted bipyridyl complexes of Cr(III) in TA2638.....	91
35. Membrane permeability of mutagenic chromium compounds in mammalian cells.....	95
36. Membrane permeability of nonmutagenic Cr(III) complexes in mammalian cells.....	95
37. DMSO induced uptake in relation to mutation rate.....	97
38. Single scan cyclic voltammogram of paraquat showing potential and current parameters.....	102
39. Reaction coordinate versus energy diagram for reversible and irreversible electrochemical reactions.....	102
40. Cyclic voltammogram of 1.0 mM Cr(phen) <sub>2</sub> Cl <sub>2</sub> .....	104
41. Cyclic voltammogram of 1.0 mM Cr(phen) <sub>2</sub> (OH) <sub>2</sub> .....	104
42. Cyclic voltammogram of 1.0 mM Cr(bpy) <sub>2</sub> Cl <sub>2</sub> .....	105
43. Cyclic voltammogram of 1.0 mM Cr(bpy) <sub>2</sub> (OH) <sub>2</sub> .....	105
44. Cyclic voltammogram of 1.0 mM Cr(bpy) <sub>3</sub> .....	106
45. Cyclic voltammogram of 1.0 mM Cr(en) <sub>2</sub> Cl <sub>2</sub> .....	106
46. Cyclic voltammogram of 1.0 mM Cr(en) <sub>3</sub> .....	107

LIST OF FIGURES -continued

<u>Figure</u>	<u>Page</u>
47. Cyclic voltammogram of 1.0 mM $\text{Cr}(\text{NH}_3)_4\text{Cl}_2$ .....	107
48. Cyclic voltammogram of 1.0 mM $\text{Cr}(\text{CN})_6$ .....	108
49. Cyclic voltammogram of 1.0 mM $\text{Cr}(\text{py})_4\text{Cl}_2$ .....	108
50. Cyclic voltammogram of 1.0 mM phenanthroline ligand.....	110
51. Cyclic voltammogram of 1.0 mM bipyridyl ligand.....	110
52. Cyclic voltammogram of 1.0 mM $\text{Cr}(\text{bpy})_2\text{F}_2$ .....	116
53. Cyclic voltammogram of 1.0 mM $\text{Cr}(\text{bpy})_2\text{Br}_2$ .....	116
54. Cyclic voltammogram of 1.0 mM $\text{Cr}(\text{bpy})_2\text{I}_2$ .....	117
55. Correlation between absorbance maxima of first visible absorption band and half-wave potential.....	120
56. Correlation of half-wave potentials with mutational frequency.....	120
57. Cyclic voltammogram of 1.0 mM $\text{Cr}(\text{dmbpy})_2\text{Cl}_2$ .....	124
58. Cyclic voltammogram of 1.0 mM $\text{Cr}(\text{dmabpy})_2\text{Cl}_2$ .....	124
59. Cyclic voltammogram of 1.0 mM $\text{Cr}(\text{dcbpy})_2\text{Cl}_2$ .....	125
60. Cyclic voltammogram of 1.0 mM $\text{Cr}(\text{dmebpy})_2\text{Cl}_2$ .....	125
61. Plasmid relaxation of supercoiled DNA in the presence of mutagenic and nonmutagenic Cr(III) complexes with a reductant...	129
62. Plasmid relaxation of supercoiled DNA in the presence of mutagenic and nonmutagenic Cr(III) complexes without a reductant.....	130
63. Plasmid relaxation of supercoiled DNA in the presence of different halogenated complexes of bipyridyl with and without a reductant.....	131

LIST OF FIGURES-continued

<u>Figure</u>		<u>Page</u>
64.	Electrophoretic mobility of supercoiled DNA in the presence of a metal gradient of select Cr(III) compounds.....	135
65.	Ultraviolet absorption of Cr(bpy) <sub>2</sub> Cl <sub>2</sub> with and without the presence of DNA.....	139
66.	Ultraviolet absorption of Cr(bpy) <sub>3</sub> with and without the presence of DNA.....	139

**ABSTRACT**

Investigations of the mechanisms and interactions of chromium complexes with DNA are essential for the better understanding of how these complexes may induce carcinogenesis as well as their possible negative environmental impacts. The prevalence of chromium in the +3 oxidation state both environmentally and intracellularly implicate this oxidation state as a potentially important biologically active complex.

A series of biologically active and inactive Cr(III) complexes were synthesized and used to determine structure/activity relationships and the role that ligands have in conferring biological activity.

The biological activity of these complexes has been measured in a *Salmonella* reversion assay. Those complexes that tested positive were assayed in an anaerobic *Salmonella* assay to determine if mutagenic activity was dependent on oxygen. Loss of activity, upon assaying under anoxic conditions, implicates reactive oxygen species in the mechanism of DNA damage. Mutant frequencies were determined for the active complexes to give a relative reversion order irrespective of toxicity.

Cyclic voltammetry was employed to determine the redox kinetics of Cr(III) complexes and the relationship of this physical parameter with the generation of oxygen radicals. Cyclic voltammetry has shown that the ligands contribute to the formation of these radical species by "activating" the metal center.

Plasmid relaxation assays have been carried out to demonstrate that the complexes can produce a radical that uses DNA as a substrate. This radical can be shown to induce relaxation of supercoiled DNA consistent with a mechanism of oxygen radical generation.

Interactions of Cr(III) complexes with DNA are required for a radical mechanism of damage. The type of DNA interactions associated with mutagenic Cr(III) complexes have been shown using equilibrium dialysis, electrophoretic mobilities, and UV-VIS spectrophotometry. Some of the mutagenic Cr(III) complexes show physical properties which implicate an intercalation mode of interaction with DNA.

A predictive model is proposed that allows ranking of efficacy of potentially mutagenic Cr(III) complexes based on their redox characteristics and interactions with DNA.

## INTRODUCTION

### Chromium Mutagenesis

#### History

Chromium-related health problems have been the subject of many epidemiological studies in the past 100 years. Early recognition of chromium compounds as possible carcinogens due to occupational exposure has led to one of the most extensive investigations which continue to this day.<sup>1,2</sup> These studies have shown a direct relationship between chromium exposure and an increase in lung cancer. The major occupations affected by chromium exposure are the chrome-plating, leather tanning and pigment industries.<sup>3-5</sup> Epidemiological studies of workers in these industries have shown that the consequence of exposure to chromium can be cancer (mainly of the lung and digestive tract) as well as kidney failure, depression of the immune response and ulceration of the skin and nasal septa.<sup>6</sup> Chromium, in contrast to its carcinogenic potential, functions as an essential mineral in the body. The trivalent form of chromium, Cr(III), is a trace element that has a proposed enzymatic role as a cofactor in the metabolism of glucose.<sup>7</sup>

Chromium, in the environment, is found primarily in the form of chromite ore,  $\text{FeCr}_2\text{O}_4$ . Complexes of chromium can exist in a variety of oxidation states from minus 2 to +6 with the +6 and +3 states being the most stable and most common. These chromium complexes exhibit a wide range of geometries

including, square planar, tetrahedral, octahedral and various distorted geometries.

Chromium has the potential to be an economically important mineral in Montana since the only known exploitable ore deposits in North America are located in the Absaroka/Beartooth Wilderness Area.<sup>8</sup> Conversely, it is a major constituent in the hazardous mine tailings of the Berkely Pit Superfund site located in Butte, MT.<sup>9</sup> These opposing views of chromium as both an exploitable natural resource and an environmental hazard show the unique role that chromium plays in our region.

### Theory

Activity Of Cr(III) Versus Cr(VI) The two major oxidation states of chromium that have been investigated for their biological activity are the hexavalent, +6, chromates and the trivalent, +3, chromic complexes. This focus on only two of the oxidation states is due to the stability of these two forms of chromium in the environment.<sup>10</sup> Historically, it was assumed that Cr(VI) was the only oxidation state of chromium that had a significant toxic and carcinogenic potential while the trivalent chromium species were generally considered to be biologically inert. Chromates have been shown to induce tumors in rats and mice,<sup>11</sup> cause mutations in bacterial, yeast and mammalian systems,<sup>12</sup> show differential lethality in a repair assay,<sup>13</sup> cause infidelity of *in vitro* DNA replication<sup>14</sup> and cause induction of lambda prophage.<sup>15</sup> Cr(III) salts, such as CrCl<sub>3</sub>, have shown little or no activity in these same assays.<sup>16-19</sup> At the genetic level, Cr(VI) has been shown to produce a variety of lesions in DNA including single-strand

breaks, DNA-DNA and DNA-protein crosslinks.<sup>20-22</sup> Cr(III) salts have shown either no activity or a much lower degree of DNA lesion induction in these same assays.

In contrast to the Cr(III) salts commonly used to assess activity of this oxidation state, hexacoordinate Cr(III) complexes with bidentate aromatic amine ligands have shown a significant degree of biological activity.<sup>23,24</sup> These complexes, possessing bipyridyl and phenanthroline ligands, have demonstrated mutagenicity in a variety of bacterial strains, genetic toxicity in a differential lethality assay and induction of the SOS response in *E. coli*.<sup>25</sup> In assays of mutagenicity against certain bacterial strains, these complexes have demonstrated activity comparable to that of the chromates.

**Selective Uptake Reduction Model** The mechanisms of DNA damage by chromium(VI) have been generally defined by the selective uptake/reduction model, figure 1.<sup>16</sup> This model proposes that the intracellular stable oxidation state of chromium is Cr(III) and it is this complex, or reactive intermediates formed in the reduction process of Cr(VI), that is the ultimate DNA damaging component *in vivo*. The inability of Cr(III) salts to induce mutagenesis or carcinogenesis directly has been attributed to a lack of membrane permeability. Whereas Cr(VI) readily traverses the plasma membrane of a cell via the sulfate anion transport system, Cr(III) salts have a limited plasma membrane permeability.<sup>16</sup> Cr(VI), once selectively taken up, can be reduced intracellularly by natural reductants such as flavonucleotides, microsomes, ascorbate, or sulfhydryls such as glutathione to generate the proposed biologically active intracellular Cr(III) complex and/or

produce reactive intermediates.<sup>16,26</sup> Once reduced, the active intracellular Cr(III) complex is unable to leave the cell because of this same membrane impermeability. This subsequent impermeability upon reduction of Cr(VI) leads to an intracellular accumulation of chromium.<sup>16</sup> Reactive intermediates, such as oxygen radicals, have been associated with Cr(VI) species and may account for some or all of the observed activity. Electron spin resonance (ESR) studies of Cr(VI) complexes *in vitro* have shown that a "stable" +5 oxidation state complex, tetraperoxochromate(V), Cr(V), can be formed that has the potential to generate oxygen radicals. In the presence of intracellular reductants such as ascorbate, reduced nucleotides and glutathione, the +5 oxidation state chromium complex can produce the short-lived hydroxyl radical that is captured using radical spin trapping compounds.<sup>27-30</sup> Some debate, however, has arisen as to whether the radical is generated by the Cr(V) alone or is an artifact of the system. Different systems have produced a variety of different radicals. Aiyar et al. and Shi and Dalal, using glutathione as a reductant, have detected the Cr(V) species and a glutathione thiol radical but no hydroxyl radical.<sup>31,32</sup> It appears that the glutathione thiol radical can react with molecular oxygen to generate the superoxide anion species. Cr(VI) in the presence of excess hydrogen peroxide will form the hydroxyl radical as shown by using DMPO, 5,5-dimethyl-1-pyrroline N-oxide as the radical spin trap.<sup>28</sup> No Cr(V) EPR signal was seen, however. Kawanishi et al. observed the formation of singlet oxygen, hydroxyl radical and the Cr(V) species using hydrogen peroxide as the reductant of Cr(VI).<sup>33</sup> It was proposed by Kawanishi et al. that the hydroxyl

radical could be formed by these products using iron as the catalyst between superoxide and hydrogen peroxide.<sup>33</sup> It should be pointed out, that all reactions were run in phosphate buffer that is known to have significant quantities of contaminating iron. Reduced nucleotides, such as NADPH reacted with Cr(VI) and hydrogen peroxide have shown significant production of the hydroxyl radical that was not significantly affected by addition of superoxide dismutase. This suggests that the iron-catalyzed reaction between superoxide and hydrogen peroxide is not the pathway through which hydroxyl radicals are generated. Jones et al. showed that a Cr(V) complex formed with glutathione,  $\text{Na}_4\text{Cr}(\text{GSH})_2 \cdot (\text{GSSG}) \cdot 8\text{H}_2\text{O}$ , in the presence of molecular oxygen can result in the production of the hydroxyl radical that is further increased upon addition of hydrogen peroxide.<sup>34</sup> This same complex, when run under anoxic conditions inhibited all radical formation. These same types of assays have been carried out with Cr(III) salts in the presence of hydrogen peroxide and have shown a limited production of hydroxyl radicals.<sup>35</sup> This, however, could only be accomplished using a pH 2 buffer which is an unlikely condition intracellularly and the significance of this work is questionable. The ability of certain hexacoordinate Cr(III) species to be biologically active by themselves may disturb the current model of Cr(VI) mutagenicity. If a redox active, or DNA binding Cr(III) compound is formed from the Cr(VI) reduction intracellularly, then it can be argued that this may be the actual DNA damaging complex formed *in vivo*. Until recently, little real evidence has been presented to uphold this theory.

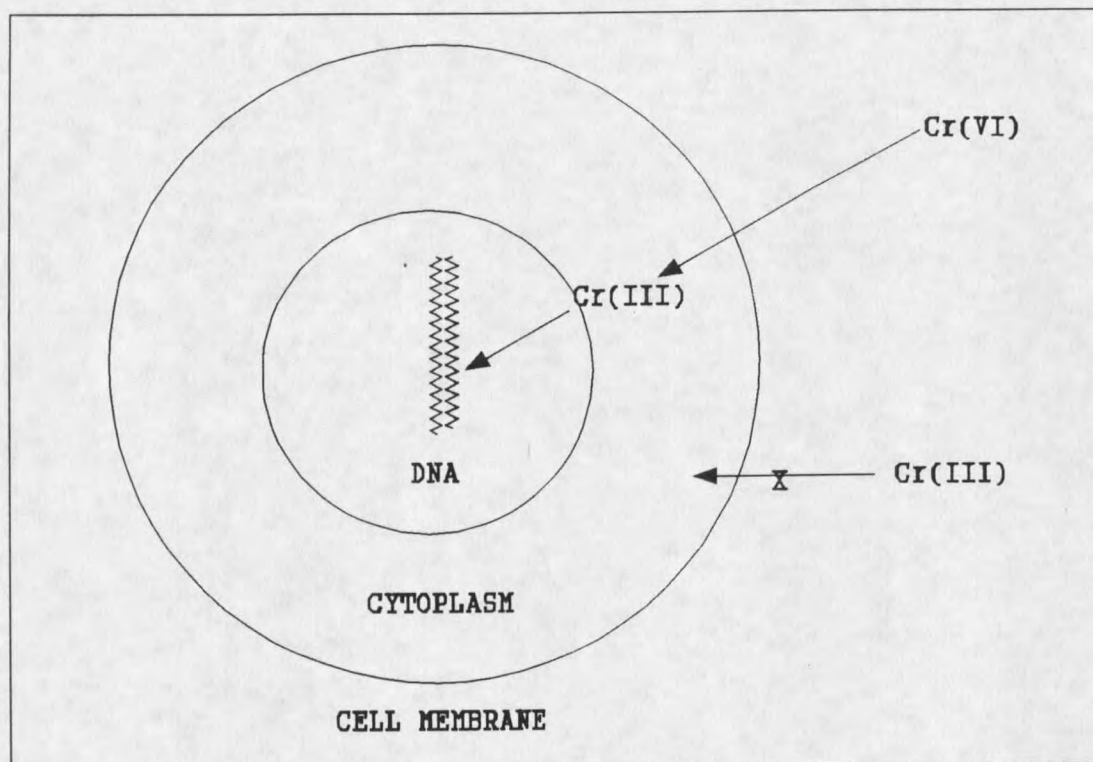


Figure 1: Schematic representation of selective uptake and reduction of Cr(VI).

### Mechanisms Of DNA Damage By Other Compounds

While extensive studies have been carried out on Cr(VI) and Cr(III), the mechanism by which these complexes damage DNA have yet to be adequately elucidated. Research on a variety of other classes of mutagenic compounds have identified several mutagenic themes that serve as a basis for this study. While this does not preclude a wholly different method of DNA damage for these compounds, it does give us a rational starting point for this investigation. The different types of DNA damaging mechanisms that are most common are illustrated with examples on the following pages.

## Cis-Platinum

Cisplatin, *cis*-DDP or *cis*-dichlorodiammineplatinum(II), is a commonly used anti-tumor agent. The activity of this compound was first discovered, serendipitously, by Barnett Rosenberg when he noticed that *E. coli*, in the presence of a platinum electrode, showed the induction of filamentation.<sup>36</sup> Filamentation is a known bacterial response to stress, mediated by environmental conditions or DNA damage. Further studies revealed that the biologically active species of Pt included the *cis* isomer of diamminedichloroplatinum(II), as well as a tetraamminedichloroplatinum(IV) compound. The remarkable effectiveness of this compound as an anti-tumor drug has led to an extensive investigation into the mechanism of its DNA damaging activity. Cisplatin has been shown to form dimeric crosslinks with a variety of substrates. These are interstrand DNA-DNA crosslinks, intrastrand DNA-DNA crosslinks and DNA-protein crosslinks.<sup>37</sup> The most common lesion, believed to be responsible for the majority of the activity with this compound, is an intrastrand crosslink between two adjacent guanine nucleotides, figure 2.<sup>38</sup> The genetic consequence of this type of lesion is at least two-fold. The guanine-guanine Pt crosslink must be repaired and an error prone repair could lead to mutation. Since repair of this lesion is quite slow, this same lesion could cause infidelity of replication by the DNA polymerase by blocking polymerase read through along the effected strand.<sup>39-42</sup>

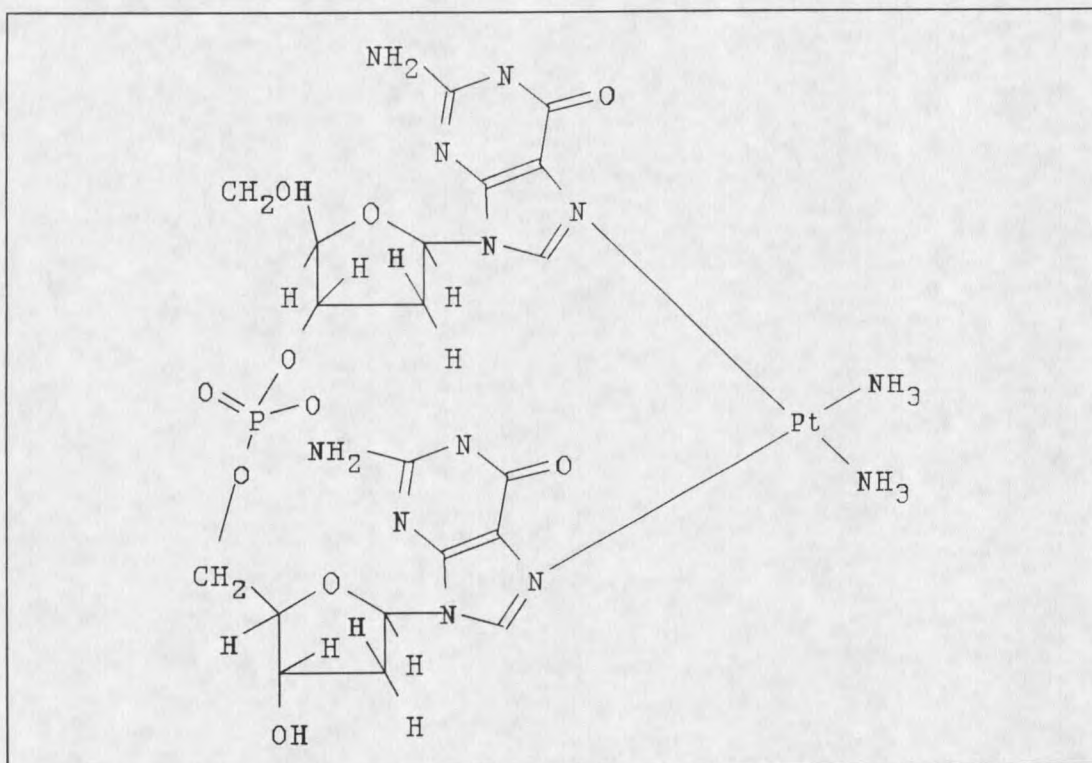


Figure 2: cis-Pt dimer formation with adjacent guanosine DNA bases.

### Alkylating Agents (MNNG And MMS)

The alkylating agents, MNNG, N-methyl-N'-nitro-nitrosoguanidine, and MMS, methyl-methanesulfonate, are both powerful mutagenic agents. They potentiate their action by alkylation of DNA nucleotides.<sup>43</sup> While all nucleotides are susceptible to this type of alkylation reaction, the best substrate for this reaction is the guanine nucleotide. More specifically, the alkylation is shown to occur at the O-6 or N-7 position of guanine, figure 3.<sup>44,45</sup> The consequence of this type of lesion leads is lack of read through by the DNA polymerase and subsequent poor fidelity of replication.<sup>46,47</sup> Unlike Cisplatin, these type of lesions are readily repaired by endogenous alkyltransferase enzymes.<sup>48</sup>

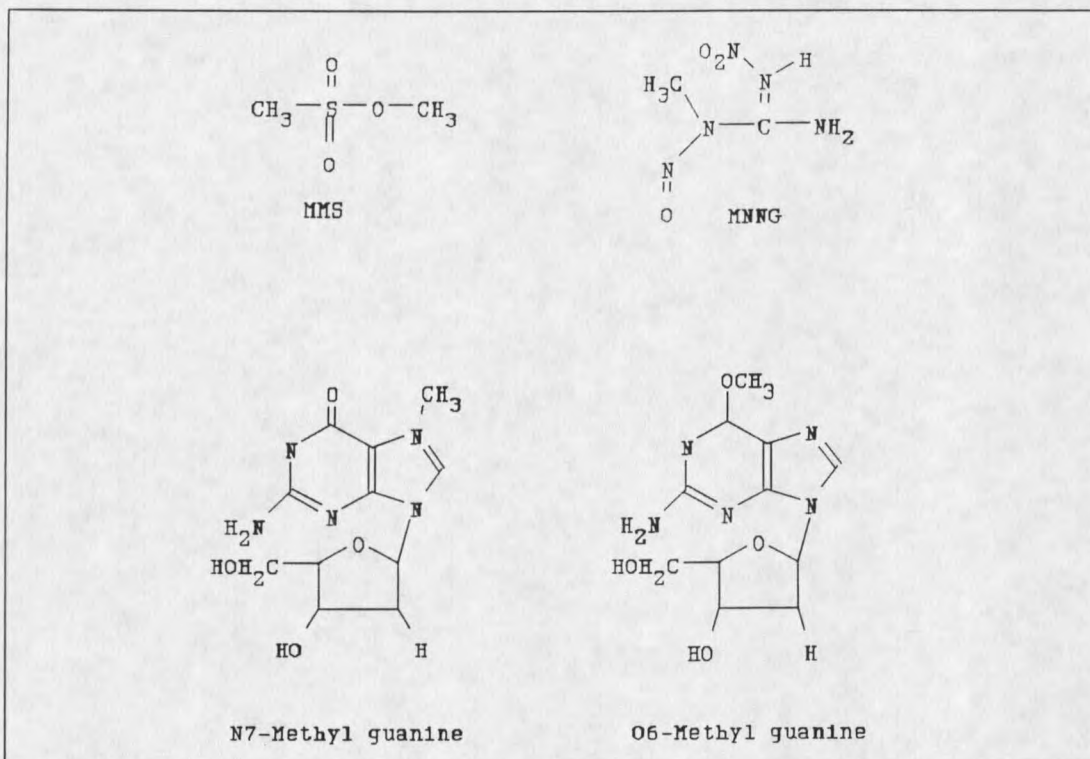


Figure 3: Alkylating agents and alkylated lesions on DNA bases.

### Bleomycin

Bleomycin is a metalloglycopeptide that is an effective anti-tumor drug currently in clinical use, figure 4. The biological activity of this drug can be attributed to its ability to induce strand-cleavage of DNA. Bleomycin consists of a glycopeptide, a small peptide with attached sugar units, that can interact with DNA by intercalating between the purine and pyrimidine bases to allow the active redox center of bleomycin, consisting of Fe(II), to generate oxygen radicals through a Fenton reaction.<sup>49</sup> These active oxygen radicals generated at the DNA surface interact with the DNA to induce strand scission. This iron catalyzed strand cleavage is the proposed mechanism by which bleomycin potentiates its mutagenic

and anti-tumor activity.

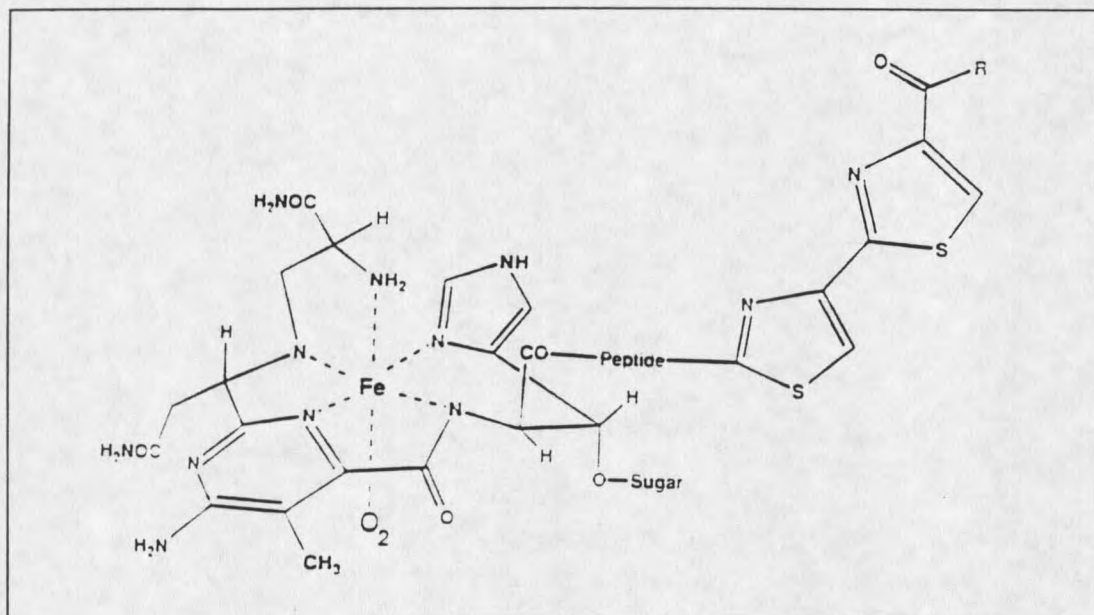


Figure 4: Structure of bleomycin.

### Paraquat

Paraquat, or methyl viologen, is a commonly used herbicide, Figure 5. Paraquat itself shows very little mutagenicity but is a highly toxic compound. The toxicity of this compound is considered to be a function of its ability to generate superoxide anion radicals.<sup>50</sup> These radicals, while not as biologically active as some of the other oxygen radical species, show a high degree of toxicity which may be related to their affinity and damaging capability for membrane components.<sup>51</sup> Generation of lipid radicals is a well defined system that can lead to cell death by disruption of membrane integrity. This would account for paraquat's low to nonexistent mutagenicity yet high toxicity as seen in bioassays. There is, however, a body of evidence that suggests that the superoxide anion

may have a capacity for DNA damage that would give it a mutagenic and carcinogenic potential.<sup>52</sup> It is possible that the high degree of toxicity of this compound simply masks the more subtle mutagenic effect. Little evidence for this type of interaction exists, however, and the actual effect could be attributed to an iron-catalyzed reaction between superoxide and hydrogen peroxide to form the hydroxyl radical.

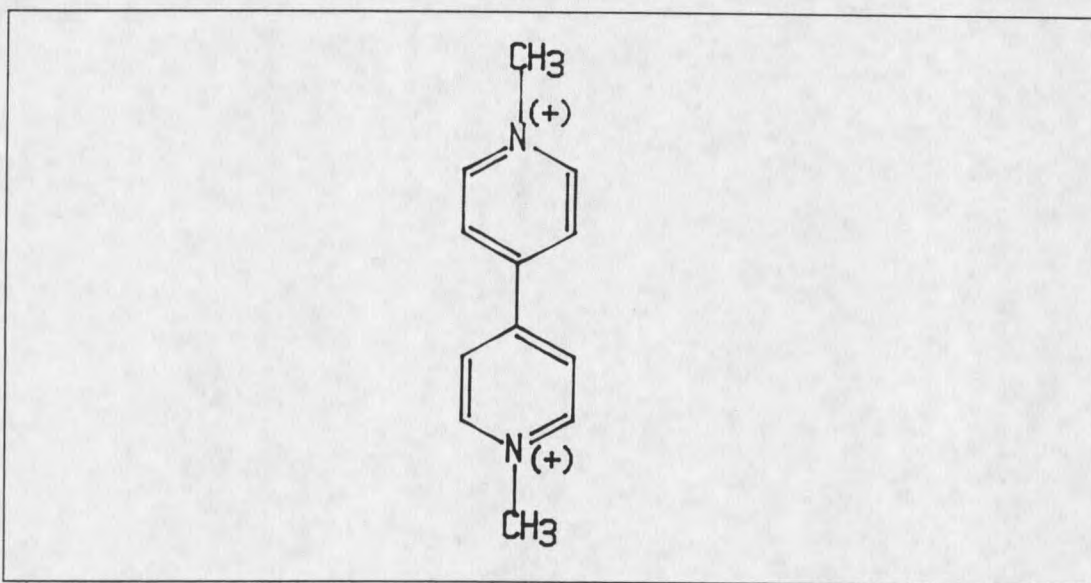


Figure 5: Structure of paraquat (methyl viologen).

## Oxygen Radicals

### Characterization

Oxygen radicals are common constituents intracellularly because they are byproducts of cellular metabolism and respiration.<sup>53</sup> The high degree of reactivity of oxygen radicals are a constant threat to all aerobic organisms and their production has been implicated in both carcinogenesis and ageing.<sup>54</sup> Because of

this threat, organisms have evolved methods for removing oxygen radicals from susceptible tissues. Simultaneously, certain cells, such as neutrophils, have used the reactive properties of oxygen radicals as a defense mechanism against foreign antigens.<sup>55</sup> For self-protection, aerobic organisms have developed a distinct set of enzymes that are specific for the removal of oxygen radicals. These include peroxidases, superoxide dismutases and catalases. Further steps to minimize deleterious oxygen radical generation have evolved as well. These include, packaging of redox active metal complexes in a form which renders them inert i.e. complexation of iron in hemoglobin and burying redox active metal centers inside proteins such as ferritin. The two major forms of oxygen radicals that we will be concerned with are the superoxide anion and the hydroxyl radical.

**Superoxide Anion Radical** Superoxide anion,  $O_2^{\bullet -}$ , is produced *in vivo* by both enzymatic and spontaneous processes as well as through photochemical oxidation reactions.<sup>53</sup> Formation of superoxide anion takes place via a one electron reduction of molecular oxygen. Superoxide anion is capable of initiating and propagating free-radical chain reactions which can lead to damage of cellular components.<sup>56</sup> Failure to control the production of superoxide anions leads to cessation of growth, mutagenesis and death. Specific enzymes, superoxide dismutases, have evolved to scavenge superoxide anions before they can damage a cell.<sup>53</sup> There are two families of SOD's, these being the Zn, Cu SOD's and the Fe, Mn SOD's. Both of these enzymes catalyze the dismutation of superoxide anion to HOOH and  $O_2$ . While superoxide anion is deleterious to an organism, it

is considered, by some, not to have the appropriate reactivity and electrophilicity to be a direct DNA damaging component.<sup>57</sup> This, however, does not preclude a mechanism in which it is a vital reactive intermediate.

**Hydroxyl Radical** The hydroxyl radical, OH<sup>•</sup>, is the most reactive of all the oxygen radical species known. It has a rare combination of high electrophilicity and reactivity that allows it to react with DNA in a variety of ways, all of which are deleterious to an organism.<sup>57</sup> The hydroxyl radical has the potential to abstract a proton from the C-4 position of a deoxyribose sugar which results in single strand cleavage.<sup>58</sup> Alternatively, it may abstract a proton from a DNA base, i.e. conversion of thymine to dihydroxymethyluracil, that would result in an inability for the DNA polymerase to copy a daughter strand with high fidelity.<sup>59</sup> The hydroxyl radical can also add electrophilically to DNA bases to produce hydroxylated lesions such as 8-hydroxyguanine.<sup>60</sup> Once again, this type of DNA damage may lead to infidelity of replication or cause single strand cleavage.

For damage to occur, the hydroxyl radical must be generated in the vicinity of DNA. This is due to the high reactivity of the hydroxyl radical. It is estimated that the hydroxyl radical will only diffuse 5-10 molecular diameters before a reaction will take place.<sup>57</sup> Thus, for a direct acting oxygen radical generating mechanism of damage, the hydroxyl radical is the most likely candidate.

Oxygen radical damage is readily repaired by a set of enzymes called the *UVR* enzymes.<sup>61</sup> This set of enzymes recognize and repair single strand breaks in DNA. This same set of enzymes are activated by ionizing radiation induced

DNA damage since the resulting damage to DNA is similar. This is why oxygen radical generating compounds are said to be radiomimetic, i.e. they mimic the type of damage seen with radiation.

### Formation

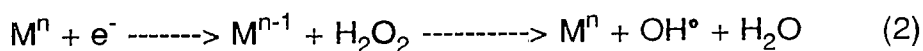
**The Haber-Weiss Reaction** The Haber-Weiss reaction (1) describes a series of single electron reductions to take molecular oxygen, through a series of radical intermediates, to its ultimate reduced form, water.<sup>62</sup>



In comparison to water, molecular oxygen is in a strongly oxidative form. However, the oxidative potential of molecular oxygen is constrained by its two unpaired, spin-parallel electrons. The consecutive monovalent reductions to produce superoxide, hydrogen peroxide and hydroxyl radical exempt these species from the kinetic restrictions to allow electron exchange. The superoxide anion,  $\text{O}_2^{\bullet -}$ , can act as either an oxidant or a reductant, hydrogen peroxide is relatively stable but the hydroxyl radical,  $\text{HO}^\bullet$ , is a powerful oxidant that can react at diffusion-limited rates. The stability of hydrogen peroxide does not normally allow for easy formation of the hydroxyl radical. Thus, the Haber-Weiss reaction is limited in the direct production of this damaging species. However, in the presence of a redox active metal, this equilibrium can be shifted dramatically.

**The Fenton Reaction** The Fenton reaction (2) involves the use of a redox

active metal center that catalyzes the decomposition of hydrogen peroxide to the hydroxyl radical and water.<sup>63</sup>



The metal most commonly associated with the Fenton reaction is iron although many metals, such as Cu and Ni, have shown the potential to participate in this type of reaction.<sup>64-66</sup> One of the requirements for a good Fenton catalyst is the ability to redox cycle between two oxidation states to serve as a cyclical electron generator. The only limitation for this type of reaction is availability of an electron source which, intracellularly, is freely accessible in the form of reduced nucleotides (NADPH), ascorbate or sulfhydryl containing groups (glutathione and cysteine). It is this type of reaction that is considered to be the most deleterious to an organism. This would account for the elaborate system of enzymes and metal chelators used by an organism to prevent this type of reaction from occurring.

### DNA Interactions

The type of interaction a compound has with DNA can directly influence the mechanism of DNA damage. Identification of the type of interaction can be helpful in determining and supporting a mechanism of damage. The questions to be considered when examining DNA interactions are: 1) is the interaction part of the overall mechanism of damage or 2) is the interaction itself wholly responsible for the biological activity observed. Below, is a list of a few of the different types of

interactions that have been identified for certain biologically active compounds.

### Models Of Interactions

**Covalent Dimers** The formation of covalent dimers with DNA is probably the best known and studied of all the interactions with DNA. Some of the compounds which undergo this type of interaction are *cis*-platinum and Mitomycin C. In this case, it is the interaction itself that causes the DNA lesions leading to DNA damage, mutagenesis and carcinogenesis. Dimer formation with *cis*-platinum has been discussed earlier, with the primary damaging adduct being an intrastrand crosslink formed between two adjacent guanine residues. Mitomycin C intercalates with DNA and has the primary damaging adduct as an interstrand crosslink formed by nucleophilic attack of a DNA amino group on the azocyclopropane ring of Mitomycin C followed by a Michael addition of an amino group from the complementary strand of the DNA to a conjugated diene functional group.<sup>67</sup>

**Intercalation** Intercalation is best known for compounds such as bleomycin, ethidium bromide and metal complexes of bipyridyl, phenanthroline and terpyridyl.<sup>68-71</sup> By definition, intercalation is the process by which a compound stacks between the coplanar DNA bases, figure 6. Intercalation, unlike the formation of covalent dimers, is not necessarily mutagenic in and of itself depending on how tightly the complex will bind between the DNA bases. It does, however, have the capability to spatially orient a reactive compound near enough to the DNA for damage to take place. In the case of hydroxyl radical formation,

intercalation may serve to orient the reactive center the 5-10 Å° needed for a reaction to take place.

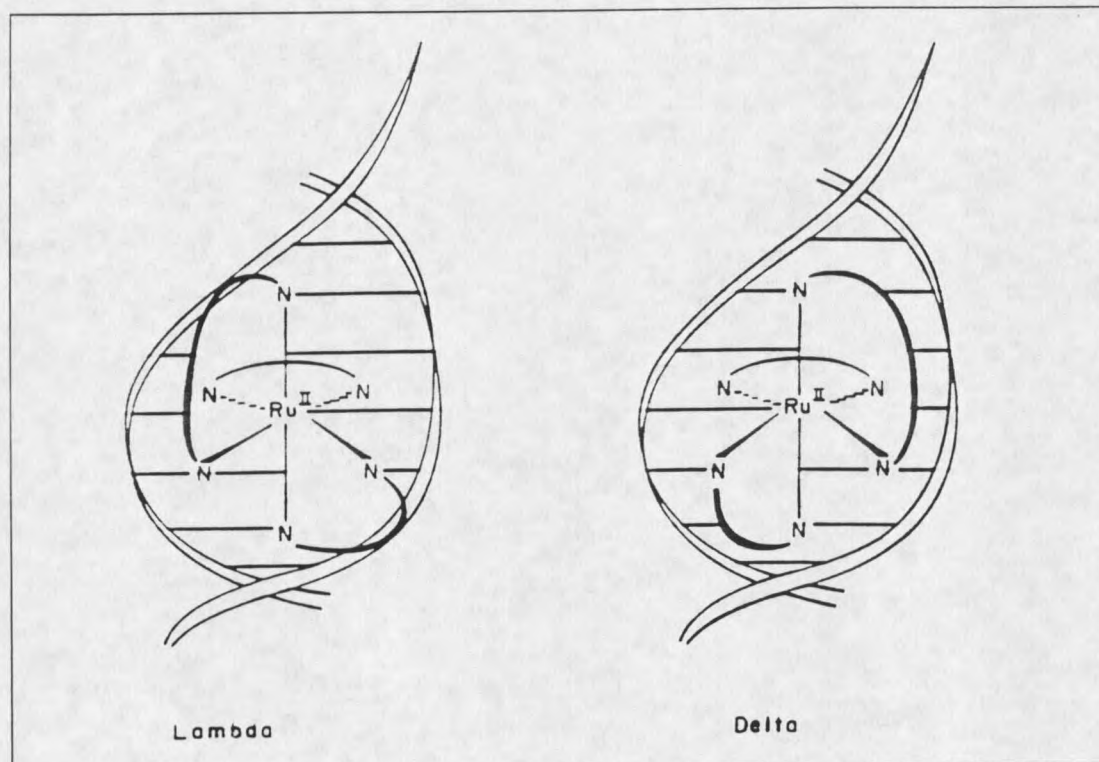


Figure 6: Intercalation between coplanar DNA bases.

**Coulombic Attraction** Coulombic attraction is simply the attraction that two oppositely charged particles have for each other. Free metal ions and many metal complexes have a net positively charged oxidation state. DNA, on the other hand, has a net negative charge arising from the negatively charged phosphates on the backbone of DNA. Coulombic attraction arising from the opposite charges between the metal and the DNA can allow electrostatic interactions between metal and DNA. This association is predominantly ionic in character and no real bond formation need occur between the two species.

**Reduction Adducts** Reduction adducts are formed when a metal, in the presence of DNA, becomes reduced resulting in labilization of the ligands and rearrangement to form a ligand complex with DNA. The best known example of this type of interaction is with Cr(VI) complexes.<sup>72</sup> Reduction of the tetrahedral Cr(VI) complexes in the presence of DNA can result in a rearrangement of the inner sphere ligands to give an octahedral Cr(III) complex with one or more of its ligands becoming a DNA base. These type of adducts with Cr(VI) have been detected *in vitro* upon reduction with cellular reductants.<sup>72</sup> Whether this type of adduct can occur *in vivo* has not yet been demonstrated. As well, the significance of this type of adduct in mutagenesis is currently unknown but may play a role in the overall mechanism of chromium mutagenesis.

### **Electrochemical Behavior Of Metals**

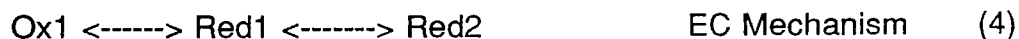
Formation of oxygen radicals in a system is fundamentally based on a series of electron transfers. Invoking the Fenton reaction to explain the formation of DNA damaging radicals *in vivo* implies the use of metal complexes as cyclical electron donors. Thus, the electrochemical behavior of metals is an important aspect in understanding the overall damaging process which takes place to cause mutagenesis and carcinogenesis via oxygen radicals.

### **Theory**

An electron transfer is expected to result in an accompanying change in the reactant molecule. In many cases, the changes in bond length and connectivity

will not be extreme and the redox process will be a simple one displaying rapid charge transfer kinetics. In certain cases, there is a recognizable change in the structure such as isomerization and change in bond connectivity. In the case of a structure change, it is important to ascertain whether it has occurred before or after the electron transfer step. Any structural changes that occur between the two forms of the redox couple will contribute to the height of the activation barrier if the transition state is intermediate between reactant and product. If the energetics of the rearrangement are low, the electron transfer is usually fast and the system is termed electrochemically reversible. Slow charge transfer reactions give rise to an irreversible electrochemical reaction relating to large structural changes in the molecule. An intermediate degree of charge transfer yields a quasi-reversible electrochemical reaction. These three type of charge transfer kinetics, reversible, quasi-reversible and irreversible are shown in Figure 7.<sup>73</sup>

Electrochemical reversibility does not preclude chemical reactivity during the reaction. There are two types of mechanism, EC (4) or CE (3) that can alter the reversibility of a compound if it is in equilibrium.



In the CE mechanism (chemical/electrochemical), the reactant, Ox2 (oxidized complex), undergoes a chemical reaction to Ox1 prior to electron transfer to form Red1 (reduced complex). In the EC (electrochemical/chemical) mechanism, the

reactant, Ox1, undergoes electron transfer to a chemically labile reduced form, Red1, which can then undergo a chemical reaction to form the ultimate product, Red2. This scenario assumes that Ox2 and Red2 are themselves electrochemically inert. Reversible proton or ligand loss is an example of this type of mechanism. For reversible ligand loss, the ligand must be in saturating quantities in the supporting electrolyte to give the same compound in the anodic sweep for an EC mechanism. When the ligand is not in saturating concentrations, a mixed electrochemical equilibrium will be observed.

Reversibility and standard reduction potentials are the two most common parameters measured in cyclic voltammetry. However, these two parameters are not physical constants. Both of these parameters can be dramatically influenced by the solvent, the electrode system and the nature of the ligand.<sup>74</sup> In this study, it is the nature of the ligand and how it affects the redox characteristics i.e. reversibility and reduction potentials, that we are interested in.

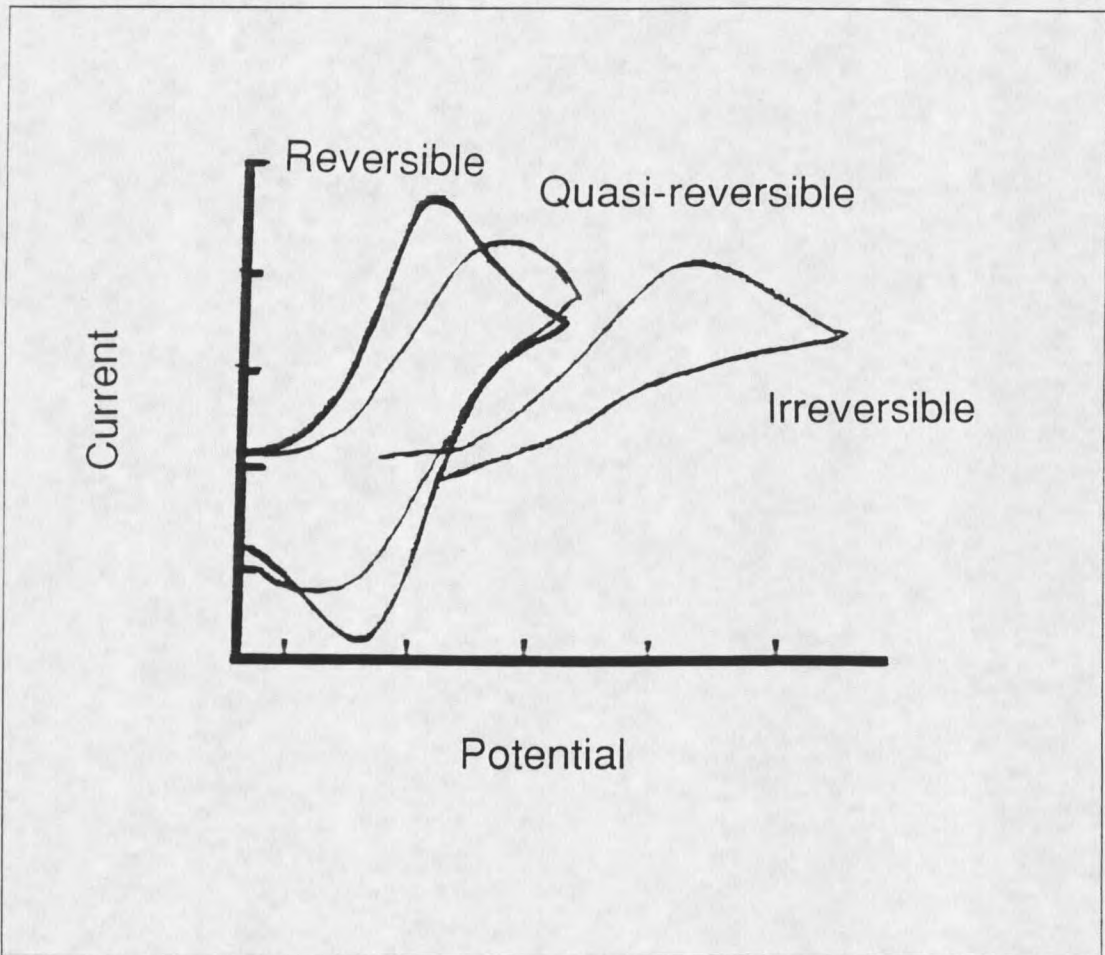


**Figure 7:** Reversible, quasi-reversible and irreversible waves in the cyclic voltammeter

## STATEMENT OF THE PROBLEM

The mechanism by which chromium complexes cause mutations in DNA and thus carcinogenesis has been sought since epidemiological studies first identified them as cancer causing compounds. The widespread use of chromium in industry coupled with its environmental stability has made chromium exposure and remediation a critical issue. While some progress has been made on the mechanism of DNA damage and toxicity of the +6 oxidation state chromates, the ubiquitous +3 oxidation state chromium complexes have been virtually ignored. This neglect of the more common +3 complexes is understandable since the easily obtained complexes of this oxidation state, such as  $\text{CrCl}_3$  have shown no propensity towards biological activity.

In 1981, this research group was the first to identify Cr(III) complexes that demonstrate mutagenesis in biological assays. Two complexes,  $[\text{Cr}(\text{bpy})_2\text{Cl}_2]^+$  and  $[\text{Cr}(\text{phen})_2\text{Cl}_2]^+$  both showed a high degree of activity in both a Salmonella reversion assay and a differential repair assay. At this point, no mechanism was defined for these compounds although it was proposed that it might induce mutations much like cis-platinum since both had *cis* halogen ligands.

In 1987, I entered this research group with the goal of determining the mechanism by which these compounds potentiate their activity. We believed that the mechanism of Cr(III) mutagenesis would not only help to define the mechanism by which the more active Cr(VI) species causes cancer but would also prove that Cr(III) complexes could not be considered innocuous in the environment. We also

hoped to determine distinct physical characteristics associated with the mutagenic Cr(III) complexes that allow us to predict whether certain complexes would be biologically active.

Determination of the mechanism of DNA damage for the Cr(III) complexes was accomplished by investigating the following areas: 1) The dependence on oxygen for the induction of mutagenicity, 2) The structure/activity relationships between mutagenic and nonmutagenic Cr(III) species, 3) The redox behavior of the Cr(III) complexes in aqueous solutions, 4) The conformation changes of supercoiled plasmid DNA induced *in vitro*, and 5) The interactions of the Cr(III) complexes with DNA.

The oxygen dependence on the induction of mutagenicity was accomplished by developing an anaerobic Salmonella reversion assay. Use of this method, with appropriate controls, demonstrates that an oxygen radical mechanism of DNA damage may be occurring.

Many Cr(III) complexes are nonmutagenic in the assay systems used. An apparent structure/activity relationship, conferred by the ligand, exists for these complexes. Synthesis and testing of a variety of related Cr(III) complexes have given insight into the factors that influence both mutagenesis and those physical parameters associated with a particular metal-ligand complex that promote biological activity.

Electrochemical analysis by cyclic voltammetry has determined that there is a relationship between ligand type and electrochemical behavior. The

electrochemical behavior observed for the mutagenic Cr(III) complexes are: 1) shifts in the reduction potentials and 2) reversibility of the redox couple. Correlation of this electrochemical behavior with mutagenesis data provides a measurable physical parameter by which biological activity can be predicted and also demonstrates the effects a certain ligand has on formation of a redox active center.

Electrophoretic plasmid relaxation assays show both the interactions and possible damage conferred upon supercoiled plasmid DNA. Formation of relaxed or linear conformations of DNA from the supercoiled plasmid upon incubation with the metal is considered the result of oxygen radical attack on either the DNA bases themselves or on the deoxyribose sugar.

Metal-DNA interactions were monitored using UV-VIS spectrophotometry, electrophoresis and equilibrium dialysis/polarimetry. Previous work on similar metal-ligand complexes have shown an interaction with DNA via intercalation. These results are confirmed for the mutagenic Cr(III) complexes used in this study.

These type of data will help us both model and predict the possibility of a metal complex to act as a mutagen. Definition of stringent physical characteristics which allow a complex to be mutagenic can then be applied towards risk assessment and possibly towards the rational design of a new generation of metal antitumor drugs.

## EXPERIMENTAL

Synthesis, Purification And Characterization Of Cr(III) Complexes[Cr(bpy)<sub>2</sub>Cl<sub>2</sub>]Cl And [Cr(bpy)<sub>2</sub>(H<sub>2</sub>O)<sub>2</sub>]Cl<sub>3</sub>

*cis*-bis-2,2'-bipyridyldichlorochromium(III) chloride dihydrate, *cis*-[Cr(bpy)<sub>2</sub>Cl<sub>2</sub>]Cl·2H<sub>2</sub>O, and its aquated analogue, *cis*-bis-2,2'-bipyridyldiaquochromium(III) trichloride, *cis*-[Cr(bpy)<sub>2</sub>(H<sub>2</sub>O)<sub>2</sub>]Cl<sub>3</sub>, was synthesized using a previously described method.<sup>75</sup> 1.5 g of anhydrous CrCl<sub>3</sub> and 4.7 g of 2,2'-bipyridyl were mixed in 50 ml of 95% ethanol and heated to boiling in the presence of a catalytic amount of zinc dust. The reaction mixture was allowed to boil for 10 min and then cooled. The red-brown crystals were collected by filtration and allowed to air dry. Purification was achieved by liquid chromatography on a Sephadex LH-20 support with 9:1 H<sub>2</sub>O:MeOH eluent. Two major bands were observed with both LC and subsequent HPLC analysis on a reverse phase C-18 bondapack column. The fastest eluting red band corresponded to the aquated species [Cr(bpy)<sub>2</sub>(H<sub>2</sub>O)<sub>2</sub>]Cl<sub>3</sub>. The second brown band corresponded to the original product [Cr(bpy)<sub>2</sub>Cl<sub>2</sub>]Cl·2H<sub>2</sub>O. Characterization of these two complexes was accomplished using ultraviolet and visible (UV-VIS) spectrophotometry and Fast Atom Bombardment Mass Spectrometry (FAB-MS).

Ultraviolet absorption spectra for the two compounds were measured in millipore H<sub>2</sub>O using a 1.0 nm slit width and matched quartz cuvettes. The wavelengths were scanned at 25 nm/min with a chart speed of 1.0 inch/min

between 380-220 nm. The  $[\text{Cr}(\text{bpy})_2\text{Cl}_2]\text{Cl}$  species showed the following wavelength maxima with the log of  $\epsilon_m$ , (molar extinction coefficient in parenthesis); 335s, (3.87); 324s, (3.98); 308, (4.27); 245, (4.34).

The  $[\text{Cr}(\text{bpy})_2(\text{H}_2\text{O})_2]\text{Cl}_3$  species, scanned under the same conditions, gave wavelength maxima and the logarithm of the extinction coefficients of; 305, (4.32); 245, (4.28).

Visible absorption spectra was measured using the same parameters as above. Wavelengths between 700 and 380 nm were scanned at a 50 nm/min scan rate and 0.5 inch/min chart speed. The wavelength maxima and the extinction coefficient,  $\epsilon_m$ , in parenthesis for the dichloro species; 552, (44.8); 447s, (91.6); 418s, (239); 394, (314). The diaquo species gave wavelength maxima and extinction coefficients of; 525, (41.0); 447s, (77.8); 417s, (197); 393, (285). These UV-VIS wavelength maxima and extinction coefficients are similar to that reported previously for these complexes.<sup>76</sup>

FAB-MS on these complexes in a glycerol matrix, using xenon as the particle accelerant, gave a molecular ion of  $m/z$  434 for both the dichloro and the diaquo species.

### Synthesis Of Substituted Bipyridyls

4,4'-dimethyl-2,2'-bipyridyl was synthesized using a palladium catalyzed oxidative coupling reaction of 4-picoline essentially as reported previously, figure 8.<sup>77</sup> 150 ml of 4-picoline was refluxed with 6.2 g of 5% palladium on alumina for four days. The reaction mixture was allowed to cool and 60 ml of hot benzene

was added through the top of the condenser. The mixture was refluxed for an additional 0.5 hr and the palladium was removed by filtration while the solution was still hot. Upon cooling, a yellow-white precipitate was formed that could be filtered off. Further product was obtained by evaporating the remaining picoline/benzene reaction mixture in the hood. The impure yellow-white precipitate was recrystallized twice from hot absolute methanol. The % yield for this reaction was 5% although greater yields could be obtained by using 10% palladium on carbon as the catalyst or by longer reflux periods.

The pure product had a melting point of 172°C and was characterized using  $^1\text{H}$  and  $^{13}\text{C}$  NMR.  $^1\text{H}$ ; 2.4s, 7.1d, 8.2s, 8.4d.  $^{13}\text{C}$ ; 21, 122, 124, 148, 149, 156.

4,4'-dicarboxy-2,2'-bipyridyl was synthesized from the corresponding 4,4'-dimethyl-2,2'-bipyridyl compound by oxidation with  $\text{KMnO}_4$ , figure 8. 3.8 g of 4,4'-dimethyl-2,2'-bipyridyl and 12.0 g of  $\text{KMnO}_4$  was refluxed in 150 ml of  $\text{dH}_2\text{O}$  overnight. The unreacted starting products were filtered off while still hot. The remaining aqueous layer was then extracted with 3x50 ml portions of anhydrous diethyl ether. The aqueous layer was acidified with concentrated HCl to give a flocculent white precipitate. The white precipitate was filtered off, washed with water and allowed to air dry. The yield for this synthesis was 25%, the melting point was greater than 320°C and the compound was characterized using  $^1\text{H}$  NMR.  $^1\text{H}$ ; 7.6d, 8.0s, 8.5d.

4,4'-dimethylester-2,2'-bipyridyl was synthesized from the 4,4'-dicarboxy-2,2'-bipyridyl compound, figure 8. 0.4 g of 4,4'-dicarboxy-2,2'-bipyridyl and 4.0 ml

of thionyl chloride were refluxed for 3 h. The resulting solution was cooled and dried under argon. 6.0 ml of absolute methanol was added slowly to the reaction flask and allowed to stand for 30 min. Excess methanol was evaporated under argon and the solid product was taken up in aqueous 0.1 M NaOH. Addition of anhydrous diethyl ether precipitated a pinkish-white solid. This solid was filtered off and recrystallized from hot acetone. The compound was characterized using  $^1\text{H}$  NMR.  $^1\text{H}$ ; 3.9s, 7.2d, 8.8s, 9.0d.

4,4'-di(dimethylamino)-2,2'-bipyridyl was synthesized using a palladium catalyzed oxidative coupling reaction with 4-dimethylaminopyridine, figure 8. 25 g of 4-dimethylaminopyridine was heated until liquid. 1.5 g of 10% Pd on activated carbon was added and allowed to reflux for 3 days. The palladium was filtered off while the solution was hot and the remaining filtrate was allowed to cool. A yellow-white precipitate formed upon cooling which was filtered and recrystallized from acetone. The compound was characterized using  $^1\text{H}$  NMR.  $^1\text{H}$ ; 3.2s, 7.8d, 8.2s, 8.4d.

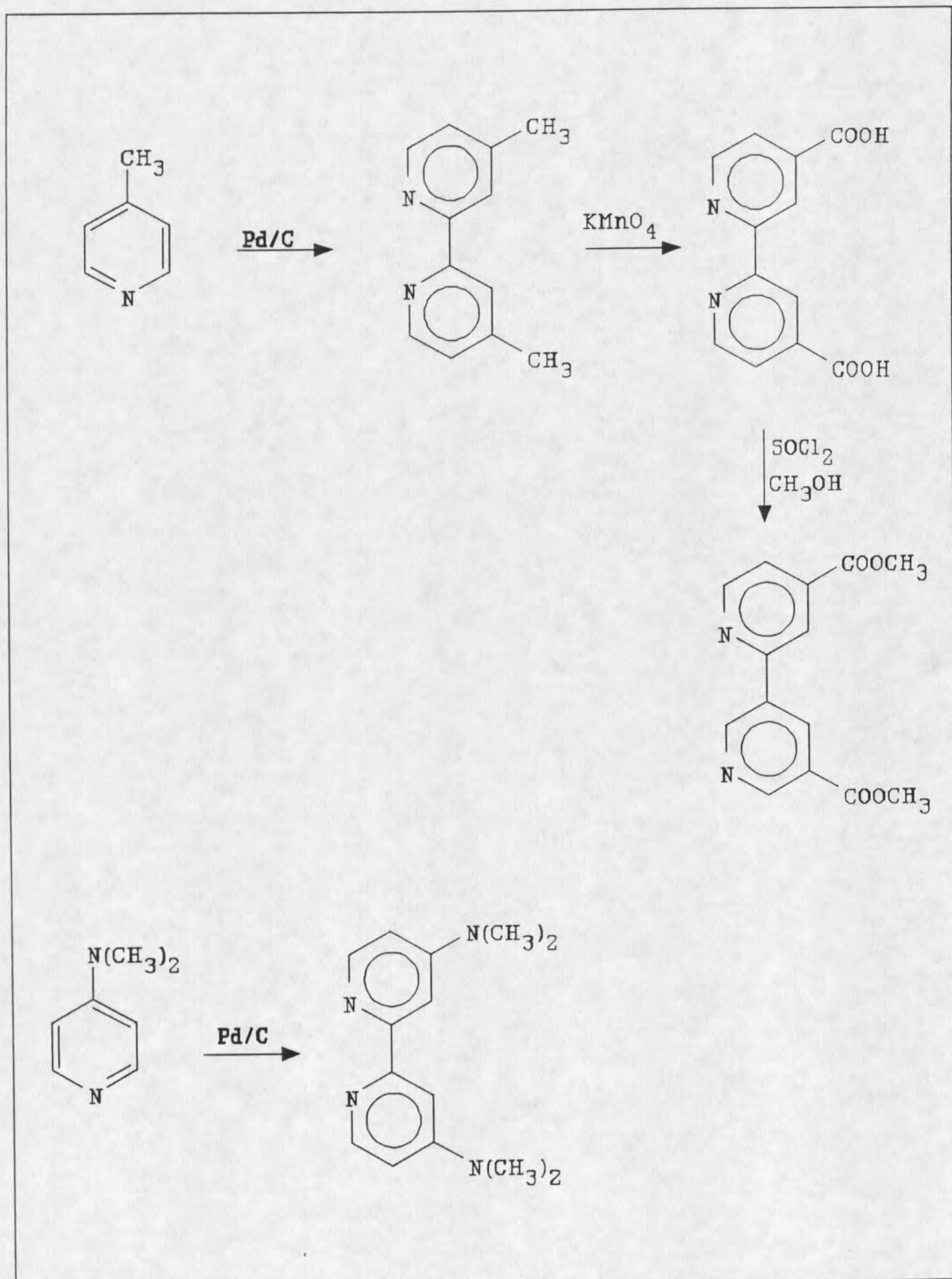


Figure 8: Synthesis of substituted bipyridyls.

**[Cr(dmbpy)<sub>2</sub>Cl<sub>2</sub>]Cl**

*cis*-bis-4,4'-dimethyl-2,2'-bipyridyldichlorochromium(III) chloride was synthesized using a modification of the method of Burstall and Nyholm.<sup>75</sup> 0.5 g of 4,4'-dimethyl-2,2'-bipyridyl and 0.15 g of anhydrous CrCl<sub>3</sub> was added to 6.0 ml of 95% ethanol. The solution was brought to a boil and a catalytic amount of zinc dust was added to the solution. The solution was boiled for 10 min and allowed to cool. Upon cooling, a brown-green precipitate formed which was filtered off. The product was dissolved in absolute methanol and purified using LC with a Sephadex LH-20 support and methanol as the eluent. The brown-green band was collected and allowed to crystallize by standing on the bench. HPLC analysis using a C-18 bondapack column revealed essentially one peak.

**[Cr(dcbpy)<sub>2</sub>Cl<sub>2</sub>]Cl**

*cis*-bis-4,4'-dicarboxy-2,2'-bipyridyldichlorochromium(III) chloride was synthesized using the method of Burstall and Nyholm.<sup>75</sup> 0.8 g of 4,4'-dicarboxy-2,2'-bipyridyl, 3.0 ml of 95% ethanol and 0.3 g of anhydrous CrCl<sub>3</sub> were heated to boiling. A catalytic amount of zinc dust was added and the solution was allowed to boil for 10 min. Upon cooling, a dark green compound precipitated which was filtered off. The dark green precipitate was dissolved in absolute methanol and purified by LC with a Sephadex LH-20 support and methanol as eluent. The dark green band was allowed to air dry on the bench. HPLC analysis using a C-18 bondapack column revealed essentially one peak.

**[Cr(dmebpy)<sub>2</sub>Cl<sub>2</sub>]Cl**

*cis*-bis-4,4'-dimethylester-2,2'-bipyridyldichlorochromium(III) chloride was synthesized using the method of Burstall and Nyholm.<sup>75</sup> 0.5 g of 4,4'-dimethylester-2,2'-bipyridyl, 2.5 ml of 95% ethanol and 0.25 g of anhydrous CrCl<sub>3</sub> were heated to boiling. A catalytic amount of zinc dust was added and the solution was allowed to boil for 10 min. Upon cooling, a light green compound precipitated which was filtered off. The light green precipitate was dissolved in absolute methanol and purified by LC with a Sephadex LH-20 support and methanol as eluent. The light green band was allowed to air dry on the bench. HPLC analysis using a C-18 bondapack column revealed essentially one peak.

**[Cr(dmabpy)<sub>2</sub>Cl<sub>2</sub>]Cl**

*cis*-bis-4,4'-di(dimethylamino)-2,2'-bipyridyldichlorochromium(III) chloride was synthesized using the method of Burstall and Nyholm.<sup>75</sup> 0.22 g of 4,4'-di(dimethylamino)-2,2'-bipyridyl, 5.0 ml of 95% ethanol and 0.08 g of anhydrous CrCl<sub>3</sub> were heated to boiling. A catalytic amount of zinc dust was added and the solution was allowed to boil for 10 min. Upon cooling, a yellow-orange compound precipitated which was filtered off. The yellow-orange precipitate was dissolved in absolute methanol and purified by LC with a Sephadex LH-20 support and methanol as eluent. The yellow band was allowed to air dry on the bench. HPLC analysis using a C-18 bondapack column revealed essentially one peak.

**[Cr(bpy)<sub>2</sub>F<sub>2</sub>]F**

*cis*-bis-2,2'-bipyridyldifluorochromium(III) fluoride was synthesized and purified by Dr D. Bancroft and J. Kerns. The compound was used without any further purification. Ultraviolet and visible spectroscopy was performed to define the complex. Ultraviolet spectroscopy yielded absorbance maxima and the logarithm of the extinction coefficient,  $\log \epsilon_m$ , in parenthesis of; 335s, (4.58); 324s, (4.68); 310, (4.86). Visible spectroscopy gave absorbance maxima, with the extinction coefficient  $\epsilon_m$  in parenthesis of; 392, (289); 414s, (220); 443s, (90.0); 540b, (43.0).

**[Cr(bpy)<sub>2</sub>Br<sub>2</sub>]Br**

*cis*-bis-2,2'-bipyridyldibromochromium(III) bromide was synthesized and purified by Dr D. Bancroft and J. Kerns. The compound was used without any further purification. Ultraviolet and visible spectroscopy was performed to define the complex. Ultraviolet spectroscopy yielded absorbance maxima and the logarithm of the extinction coefficient,  $\log \epsilon_m$ , in parenthesis of; 335s, (4.75); 324s, (4.83); 310, (4.94). Visible spectroscopy gave absorbance maxima, with the extinction coefficient  $\epsilon_m$  in parenthesis of; 393, (397); 416s, (309); 445s, (129); 554b, (62.0).

**[Cr(bpy)<sub>2</sub>I<sub>2</sub>]I**

*cis*-bis-2,2'-bipyridyldiiodochromium(III) iodide was synthesized and purified by Dr D. Bancroft and J. Kerns. The compound was used without any further

purification. Ultraviolet and visible spectroscopy was performed to define the complex. Ultraviolet spectroscopy yielded absorbance maxima and the logarithm of the extinction coefficient,  $\log \epsilon_m$ , in parenthesis of; 335s, (4.62); 324s, (4.71); 310, (4.85). Visible spectroscopy gave absorbance maxima, with the extinction coefficient  $\epsilon_m$  in parenthesis of; 393, (461); 416s, (363); 443s, (148); 560b, (70.0).

### [Cr(phen)<sub>2</sub>Cl<sub>2</sub>]Cl And [Cr(phen)<sub>2</sub>(H<sub>2</sub>O)<sub>2</sub>]Cl<sub>3</sub>

*cis*-bis-1,10-phenanthroline dichlorochromium(III) chloride dihydrate, *cis*-[Cr(phen)<sub>2</sub>Cl<sub>2</sub>]Cl·2H<sub>2</sub>O and its aquated analogue, *cis*-bis-1,10-phenanthroline diaquochromium(III) trichloride were synthesized as described previously.<sup>75</sup> 1.5 g of anhydrous CrCl<sub>3</sub> was mixed with 5.42 g of 1,10-phenanthroline in 50 ml of 95% ethanol. The reaction mixture was allowed to boil in the presence of a catalytic amount of zinc dust for 10 min. Upon cooling a greenish-brown precipitate formed which was collected by filtration and allowed to air dry. Purification was achieved by liquid chromatography on a Sephadex LH-20 support using a 9:1, H<sub>2</sub>O:MeOH eluent. Two major bands were observed in both LC and subsequent HPLC analysis on a reverse phase C-18 bondapack column. The first red band to elute from the column was the diaquo species, [Cr(phen)<sub>2</sub>(H<sub>2</sub>O)<sub>2</sub>]Cl<sub>3</sub>. The second green band corresponded to the dichloro species, [Cr(phen)<sub>2</sub>Cl<sub>2</sub>]Cl. Characterization of these complexes was accomplished using UV-VIS absorption spectrophotometry and FAB-MS.

Ultraviolet absorption spectra for the two compounds were measured in Millipore H<sub>2</sub>O using a 1.0 nm slit width and matched quartz cuvettes. The

wavelength area between 380-220 nm was scanned at 25 nm/min with a chart speed of 1.0 inch/min. The  $[\text{Cr}(\text{phen})_2\text{Cl}_2]\text{Cl}$  species showed the following wavelength maxima,  $\log \epsilon_m$ , in parenthesis; 276, (4.55); 226, (4.64). The diaquo species,  $[\text{Cr}(\text{phen})_2(\text{H}_2\text{O})_2]\text{Cl}_3$  showed very similar wavelength maxima and extinction coefficients; 276, (4.56); 226, (4.73).

Visible absorption spectra were measured using the same parameters as above. The wavelengths between 700 and 380 nm were scanned at 50 nm/min scan rate and a chart speed of 0.5 inches/min. The wavelength maxima and extinction coefficient ( $\epsilon_m$  in parenthesis) for the dichloro species were; 556, (38.6); 420s, (176); 392s, (260). The diaquo complex gave the following wavelength maxima and extinction coefficients; 530, (39.6); 420s, (137); 392s, (228). These UV-VIS wavelength maxima and extinction coefficients are similar to that reported previously for these complexes.<sup>76</sup>

FAB-MS performed on these complexes in a glycerol matrix using xenon gas as the particle accelerant gives a molecular ion of  $m/z$  482 for both the diaquo and dichloro complexes.

### $[\text{Cr}(\text{bpy})_3](\text{ClO}_4)_3$

Tris-2,2'-bipyridylchromium(III) Perchlorate was synthesized using two different methods. The first method, which has been described previously, has been slightly modified.<sup>75</sup> In the first method, the chromous bromide intermediate was formed directly from chromium metal using a 1:10 w/v mixture of chromium metal and hydrobromic acid. These two compounds were allowed to react under

an inert argon atmosphere until the solution was dark blue and all of the metal had dissolved (some heating may be required). The solution, while still under an inert atmosphere was cooled in an ice bath for 30 min or until a blue crystalline precipitate of chromous bromide formed. While maintaining an inert atmosphere, the excess solvent is filtered off and the chromous bromide is washed twice with air-free, ice-cold distilled water. 1.0 g of 2,2'-bipyridyl in 10 ml of water with 4 drops of con HCL was degassed and added with stirring to the chromous bromide mixture followed by an excess of sodium bromide. The solution was allowed to stand for 30 min at 0° C prior to filtration of the black crystalline Tris-2,2'-bipyridylchromium(II) Dibromide Tetrahydrate species. This complex was washed with cold distilled water and cold chloroform and then oxidized by shaking with a aqueous 5% perchloric acid in air. The resulting species was the yellow Tris-2,2'-bipyridylchromium(III) perchlorate. This yellow compound was recrystallized from hot water and a single band was observed with liquid chromatography on a Sephadex LH-20 support and 9:1 H<sub>2</sub>O:MeOH eluent. A single peak was observed as well using HPLC on a reverse phase C-18 bondapack column.

The second method used, which provided a higher yield, involved the use of a Jones Reductant (a zinc-mercury amalgam) to generate the labile chromous species. 1.0 g of CrCl<sub>3</sub>·6H<sub>2</sub>O in 20 ml of distilled H<sub>2</sub>O was allowed to pass slowly through a column containing the Jones Reductant. The green CrCl<sub>3</sub>·6H<sub>2</sub>O solution became bright blue after passing through the column and was allowed to drip into 50 ml of an aqueous 5% perchloric acid solution containing 4.0 g of 2,2'-bipyridyl.

The whole system was kept under an inert atmosphere of argon. The black complex of tris-2,2'-bipyridylchromium(II) perchlorate was removed from the inert atmosphere, filtered and washed with cold distilled water and chloroform. The black crystals were then heated in the presence of a small amount of aqueous 5% perchloric acid while stirring in air. After several minutes, the solution became a homogenous bright orange color and was then allowed to cool. The orange crystals collected by filtration were washed with cold water and subsequently recrystallized from hot water. The resulting yellow tris-2,2'-bipyridylchromium(III) perchlorate complex proved to be of high purity upon LC and HPLC with parameters listed previously.

Once again, the structure was confirmed using UV-VIS spectrophotometry and FAB-MS. The wavelength maxima and logarithm of the extinction coefficient,  $\log \epsilon_m$ , in parenthesis in the ultraviolet spectra for this compound were; 345, (3.89); 308, (4.33); 280, (4.15). The parameters used were the same as cited for previous compounds. The wavelength maxima and extinction coefficient,  $\epsilon_m$ , (in parenthesis) for the visible absorption spectrum were; 453s, (892); 425s (640); 402s, (269). The parameters were the same as that mentioned previously. The wavelength maxima and extinction coefficients for this complex closely matches previous work.<sup>76</sup>

FAB-MS of this compound was carried out in a glycerol + trifluoroacetic acid (TFA) matrix using xenon as the particle accelerant. A molecular ion at  $m/z$  520 corresponding to  $[\text{Cr}(\text{bpy})_3]$  was detected.

### [Cr(en)<sub>3</sub>]Cl<sub>3</sub>

Tris-ethylenediamminechromium(III) trichloride was synthesized using a modification of a previous method.<sup>78</sup> 10 g of CrCl<sub>3</sub>·6H<sub>2</sub>O was dissolved in 50 ml of absolute methanol. The solution was placed in a reflux apparatus with a catalytic amount of zinc dust and allowed to reflux for 10 min. 30 ml of anhydrous ethylenediamine was then added dropwise through the top of the condenser. The vigorous exothermic reaction yielded an immediate bright yellow precipitate which, upon cooling, was filtered, washed with cold methanol and air dried. The complex was recrystallized from hot water which yields yellow-orange needle-like crystals.

UV-VIS absorption spectra for [Cr(en)<sub>3</sub>]Cl<sub>3</sub> shows wavelength maxima and extinction coefficients (in parenthesis) of; 458, (69.2); 350, (56.3). These values are nearly identical with those reported previously for this complex.<sup>76</sup> The parameters for obtaining the spectra are identical with those used previously.

FAB-MS of this complex in glycerol/water and magic bullet/water does not show a molecular ion of m/z 232 as expected, instead a rearrangement upon ionization is taking place to form the bis-ethylenediamminedichlorochromium(III) complex of m/z 242. It also shows the formation of dimers of this bis complex.

### [Cr(en)<sub>2</sub>Cl<sub>2</sub>]Cl

*cis*-bis-ethylenediamminedichlorochromium(III) chloride was synthesized from the tris-ethyleneidamminechromium(III) trichloride species using a previous method.<sup>79</sup> The [Cr(en)<sub>2</sub>Cl<sub>2</sub>]Cl complex was prepared by recrystallizing the [Cr(en)<sub>3</sub>]Cl<sub>3</sub> from a 1% aqueous solution of ammonium chloride. After air drying,

the recrystallized product was heated at 210°C for 2-3 hr. The red-violet compound produced was recrystallized from hot distilled water and used without further purification.

No absorption was seen in the ultraviolet spectrum for this complex. Visible absorption spectra gave wavelength maxima and extinction coefficients (in parenthesis) of; 528, (40.6); 400s, (43.2). Parameters and scan rates are same as reported previously.<sup>76</sup>

FAB-MS for this complex, using magic bullet + water shows a molecular ion at m/z of 242 corresponding to the  $[\text{Cr}(\text{en})_2\text{Cl}_2]$  species.

### $[\text{Cr}(\text{NH}_3)_4\text{Cl}_2]\text{Cl}$

The *cis*-tetraamminedichlorochromium(III) chloride complex was synthesized as described previously.<sup>80</sup> Stock compound of chloroaquatetraamminechromium(III) chloride was heated in an oven at 120°C for 4 h. The reddish-purple chloroaquo complex changed to a violet color upon formation of the dichloro species. The crystal were washed with 10% hydrochloric acid, ethanol and ether in turn and allowed to air dry. No further purification was attempted on this complex.

Characterization of this complex was accomplished using visible absorption spectrophotometry. Wavelength maxima and extinction coefficients using parameters previously described were; 512, (22.7); 382, (34.6). These values closely match those previously reported for this complex.<sup>76</sup> Ultraviolet absorption spectrophotometry showed no peaks in the 380-220 nm wavelength scanned.

$K_3Cr(CN)_6$ 

Potassium hexacyanochromate(III) was synthesized using a modification of a previous method.<sup>81</sup> 1.5 g of chromium(III) acetate was dissolved in a small amount of distilled water and slowly added to a flask containing a boiling solution of 3.0 g of potassium cyanide in 15.0 ml of water. The hot solution was allowed to cool and evaporate in the hood overnight. The pale-yellow crystals formed upon cooling were filtered and recrystallized from hot water. No further purification was attempted with this complex.

Characterization was accomplished using ultraviolet absorption spectrophotometry. Wavelength maxima and the logarithm of the extinction coefficients (in parenthesis) were; 264, (3.15); 230, (2.70). FAB-MS for this complex was not possible due to the potassium associated with this complex.

 $[Cr(py)_4Cl_2]Cl$ 

*cis*-tetrapyridyldichlorochromium(III) chloride was synthesized and purified by Dr D. Bancroft and J. Kerns. No further purification was made on this complex.

## Biological Assays For Mutagenicity

### Salmonella Reversion Assay

The Salmonella reversion assay is a biological assay system developed by Dr. Bruce N. Ames. This development was in response to the need for a rapid and inexpensive system that can be used to show whether a compound or set of compounds is mutagenic. Dr. Ames accomplished this by developing several strains of *Salmonella typhimurium* with a mutation in the histidine operon which makes these bacterial strains dependent on added histidine to their growth medium. Plasmids with resistance genes to ampicillin and tetracycline were also added for selection of various strains of bacteria. A second mutation in the gene coding for membrane synthesis, *rfa*, causes partial loss of the lipopolysaccharide structure that makes the membranes more permeable. The AT or GC point mutation in the histidine operon is at the *hisG428* locus for tester strains TA102 and TA2638 and at *hisG46* locus for TA100. Depending on the strain, this mutation can be located either on a plasmid or in the genome. In TA102, the *hisG428* mutation resides on the *pAQ1* plasmid which also contains a gene for tetracycline resistance. The strains, TA102 and TA100 also contain an R-factor plasmid, *pKM101*, that increases chemical and spontaneous mutagenesis by enhancing an error-prone DNA repair system which is normally present in these organisms. This allows for detection of mutagens that are detected weakly or not at all in the parent, or nonplasmid containing strains.

The revertible DNA base pairs can be of two types, either an AT base pair

mutation or a GC base pair mutation. Those strains with the AT base pair mutations have been found to be much more sensitive to oxidative damage than the GC base pair mutations.<sup>82</sup> TA100 has a GC substitution in the histidine operon. This allows it to primarily detect base pair substitutions. TA102 and TA2638 have an AT base pair substitution. This type of mutation is sensitive to point mutations and small deletions derived from such things as X rays, UV light, bleomycin and other radical generators.

In the assay, enough histidine is added to a minimal media plate to allow several cycles of replication for the bacteria. Upon challenging the bacteria with a putative mutagenic compound, a positive result is regarded as formation of viable histidine producing colonies. The growth of colonies, above that of background, means that a mutation has occurred which has allowed the bacteria to revert back to the wild type, histidine producing, strain. Thus, the colonies that are seen on a plate are called His revertants.

**Aerobic Assay** In the aerobic assay, *S. typhimurium* strains TA102 and TA2638 were chosen for their sensitivity to oxidative mutagens. These strains were constructed by Levin et. al., and were gifts of Dr. B.N. Ames.<sup>82</sup> Both TA102 and TA2638 have an A-T base pair at the site of the mutation in *hisG428*. The *hisG428* allele in TA102 resides on the plasmid *pAQ1* and is in its normal genomic location in TA2638. For the assay, 100  $\mu$ l of an overnight culture of the Salmonella strain grown in nutrient broth, was challenged with varying concentrations of the chemical in 0.5 ml of M9 buffer (see appendix pg. 158). The

mixture was allowed to preincubate for 30 min at room temperature prior to plating in standard plate overlays (see appendix pg. 158).<sup>83</sup> The plates were counted for *His*<sup>+</sup> revertant colonies after incubation at 37°C for 72 hr. The colonies were counted automatically using a BioTran II automated colony counter with a colony size of 0.2 mm, sensitivity of 675 and area of 580.

**Anaerobic Assay** The anaerobic assay was developed to test for oxygen dependence of the mutagenic complexes seen aerobically. Since *S. typhimurium* is a facultative anaerobe, meaning it is capable of growth in both an anaerobic and aerobic environment, we are able to use this strain in much the same way that it is used aerobically. To run this assay anaerobically, several modifications to the original aerobic system had to be made. In this assay, the Salmonella bacteria were grown aerobically in nutrient broth (see appendix pg. 161). The bacteria, plates, M9 buffer and metal solution were then placed into an anaerobic Coy chamber. The Coy chamber contained a stock anaerobic gas mixture of 5.17% CO<sub>2</sub>, 10.1% H<sub>2</sub> and 84.73% N<sub>2</sub>. The solutions were allowed to equilibrate for several minutes with stirring prior to use. The actual assay was then run in the Coy chamber in the same manner as the aerobic assay. The plates were allowed to remain in the Coy chamber for 24 hr and then removed and incubated aerobically at 37°C for 72 hr prior to counting for His revertant colonies. Colonies were counted using an automated colony counter with the same parameters listed for the aerobic assay. To assure that morphological and physiological changes upon introducing the Salmonella bacteria anaerobically had no appreciable effect

upon mutation rate, an oxygen independent mutagen was used as a control. The choice for this positive control was the DNA alkylating agent, MNNG.

### Mutation Frequency

Mutation frequency is a measure of the number of mutants per number of live cells. Cell toxicity is measured in one of the Ames strains described above and the assay is set up similar to the Salmonella reversion assay. One hundred  $\mu\text{l}$  of an overnight culture of *S. typhimurium* is suspended in 0.5 ml of M9 buffer.

The bacteria are challenged with the appropriate concentration of mutagen and allowed to incubate at ambient temperature for 30 min. After 30 min, the solutions were diluted to 1.0 ml and thoroughly vortexed. Ten  $\mu\text{l}$  of the mixture was removed, diluted to 1.0 ml and vortexed. This 100 fold dilution was repeated once more on the solutions. One hundred  $\mu\text{l}$  of the resulting diluted solution was removed and uniformly streaked on LB agar petri plates (see appendix pg. 158). The plates were counted after 24 hr at 37° C to give the total number of cells. The dilution from the beginning cell density is 1 million fold. A late logarithmic phase culture of bacteria has a cell density of  $1 \times 10^7$  to  $1 \times 10^9$  per ml. The million fold dilution should then give us a cell count of between 10 and 1000 colonies. The number of His revertants from the preceding Salmonella assay can then be divided by the cell density to give the mutational frequency for the compound tested. Use of the mutation frequency assay has the advantage over a straight Salmonella reversion assay of taking into account any differences arising from differential toxicity among the compounds.

## SOS Response

The SOS response is a term given to a multi-gene global response by enteric bacteria to agents that cause DNA damage or interfere with DNA replication. The SOS response is controlled by the RecA and LexA proteins.<sup>61</sup> These two proteins control the expression of genes whose products play roles in excision repair, daughter-strand gap repairs, strand break repair, methyl-directed mismatch repair and SOS processing.<sup>61</sup> The exact mechanism of response and repair is quite complicated and will not be discussed here. However, an overview of the control system would be useful. The LexA protein serves as a repressor of all SOS genes. The RecA protein interacts with LexA and cleaves the LexA repressor to activate gene expression.

In the SOS repair assay which we use, a construct of *E. coli*, GE-94, has the repressor/operator portion of the *sulA* operon (a gene coding for expression of a filamentation protein) fused with the *lacZ* portion of the lactose operon (a gene coding for the production of  $\beta$ -galactosidase). When an agent is introduced into the system which would activate the SOS response, the cell responds by producing  $\beta$ -galactosidase. This production of  $\beta$ -galactosidase can then be measured by adding ONPG, o-nitrophenyl- $\beta$ -D-galactoside, which is a substrate for  $\beta$ -galactosidase. Cleavage of ONPG by the  $\beta$ -galactosidase results in the yellow colored o-nitrophenol group which can be measured quantitatively using visible spectrophotometry.<sup>84</sup> Induction of  $\beta$ -galactosidase, if in the appropriate concentration range, is linear with the amount of mutagen added.

**Aerobic Assay** The aerobic assay is simply the normal assay developed to measure the SOS response. This categorization is only meant to distinguish the normal (aerobic assay) from the anaerobic assay which we have developed.

In this assay, an overnight culture of GE-94 in nutrient broth was subcultured into M9 complete media at a ratio of 1.0 ml of the overnight culture per 50 ml of fresh media. The subculture is placed in a shaking water bath at 37°C until the cell count reaches  $2-5 \times 10^8$  cells/ml ( $OD_{600}$  of 0.28-0.70). It is crucial to obtain this range of cell density prior to assaying because this is the range where logarithmic growth is occurring and the point at which the cells are most susceptible to DNA damage. Further growth can be prevented once you reach this range by cooling the culture in an ice bucket. Ten ml of culture was challenged with the mutagen and incubated for 1.0 hr. Optical density at  $OD_{600}$  of the aliquots was measured after the one hour incubation. Aliquots of cells were distributed in tubes containing Z buffer (see appendix pg. 158), one drop of 0.1 % SDS and two drops of chloroform were added. The tubes were vortexed and incubated at room temperature for 20 min. After the 20 min incubation time, a drop of chloroform was added to each tube and vortexed. This results in partial disruption of the cell membranes. A 0.2 ml aliquot of ONPG, o-nitrophenol- $\beta$ -galactoside, (4 mg/ml) was added to each tube and the reaction was allowed to take place for 5 min. After 5 min, the reaction was stopped by adding 0.5 ml of 1.0 M  $Na_2CO_3$ . The optical density at 420 nm and 550 nm were recorded on a Varian Series 634 dual beam spectrophotometer. To compensate for light scattering by cell debris a

correction factor of  $1.75 \times \text{O.D.}_{550}$  is used. The final formula for finding the  $\beta$ -galactosidase units produced from this reaction is (5):

$$\text{Miller Units} = 1000 \times \text{OD}_{420} - 1.75 \times \text{OD}_{550} / t \times v \times \text{OD}_{600} \quad (5)$$

Where  $t$ =time of the reaction in minutes and  $v$ = volume of culture used in the assay, in ml. The factor of 1000 is added because a fully induced culture grown on glucose medium has approximately 1000 units of galactosidase activity/min and an uninduced culture has approximately 1.0 unit. A control that has been uninduced is run to give the basal level of  $\beta$ -galactosidase activity which can be subtracted out.

**Anaerobic Assay** The anaerobic assay is run in much the same manner as the aerobic assay but with several modifications. GE-94 *Escherichia coli* is a facultative anaerobe that grows nearly equally well in aerobic or anaerobic conditions. This ability is utilized by growing the culture to be assayed anaerobically. This is accomplished by inoculating the LB media with the culture, capping the flask with a rubber septa and purging the atmosphere with argon for several minutes. The subsequent cell growth can be monitored by removal of small aliquots of the culture with a syringe. Once the bacteria obtain the appropriate optical density, the 0.1 ml aliquots of the culture can be removed and placed into septa capped test tubes that have been purged with argon. Addition of the Z buffer, ONPG and  $\text{Na}_2\text{CO}_3$  can be added by syringe. Once the  $\text{Na}_2\text{CO}_3$  is added, the test tubes can be uncapped since the reaction has been terminated.

The optical density readings can then be made and converted to Miller units (5) using the same procedure as for the aerobic assay. The negative control for this experiment was Mitomycin C since its mechanism of action is independent of oxygen. The positive control for this experiment was paraquat since it is a known oxygen radical generator. Since paraquat is not a good inducer of the SOS response, it was used only as an indicator of anaerobiosis by observing the decrease in toxicity for this compound when assayed anaerobically.

### Toxicity Testing

Toxicity testing on select compounds was carried out by Jia Chen of the Massachusetts Institute of Technology via Gentest Corporation. The toxicity of Cr(VI),  $[\text{Cr}(\text{bpy})_2\text{Cl}_2]\text{Cl}$  and  $[\text{Cr}(\text{phen})_2\text{Cl}_2]\text{Cl}$  were measured against TK6 human lymphoblast cells and CH V-79 chinese hamster lung fibroblast cells. The toxicity is based on a simple survival % versus concentration of metal. This assay is accomplished in much the same way as that described previously for the bacterial strains.

### Mutagenesis In Mammalian Cells

The mutagenicity of select chromium compounds were measured by Jia Chen of the Massachusetts Institute of Technology via Gentest Corporation. The mutant fraction of both TK6 human lymphoblast cells and CH V-79 chinese hamster cells were measured for Cr(VI),  $[\text{Cr}(\text{bpy})_2\text{Cl}_2]\text{Cl}$  and  $[\text{Cr}(\text{phen})_2\text{Cl}_2]\text{Cl}$ . Only those doses which showed a significant survival rate could be assayed for the

mutant fraction. This assay is done in much the same way as that described for the bacterial mutant frequency.

### Cyclic Voltammetry

Cyclic Voltammetry, CV, is an electroanalytical technique used to study electroactive species in solution. Fundamentally, CV consists of cycling the potential of an electrode in a stationary solution and measuring the resulting current. The basis of a voltammogram is the measure of the amount of current transferred to an analyte versus the potential at which this current transfer occurred. The amount of current transferred in a forward sweep is a measure of the number of electrons that are accepted by the analyte. The reduction potential is the potential at which these electrons were accepted and reversibility deals with the tendency for the analyte to give up those electrons and reform the original complex on the reverse sweep. A more in depth discussion of these concepts will be presented later in this thesis.

### Instrumentation

Cyclic voltammetric data were obtained using a cyclic voltammeter interfaced with an Apple IIe computer. This system was built by Dr. R. Geer and R. A. Bonsteel and consists of 10 parts that both operate the cyclic voltammeter and collect data for further workup.<sup>85</sup> These ten parts consisted of:

1. Computer interface
2. Initial DC potential

3. DC step potential
4. Sweep generator
5. Sine wave generator
6. Potentiostat
7. AC and DC response separator
8. Gain control and positive feedback
9. Sample and hold with a 12 bit D/A converter
10. X and Y recorder output

The Apple IIe controlled CV used a FORTH-based software program to run the CV package and was written by Dr. R. Geer.

### Software

The FORTH-based software package is menu-driven and could be loaded into memory by typing *runcv*. The main menu gives a variety of options for electrochemical experiments as well as a calibrate instrument option. The calibration of the instrument is necessary prior to any series of CV runs. The output data from the calibrate instrument option is:

1. Gain tables
2. Sweep tables
3. Cell constants

The data thus obtained, is essential for later conversion of the raw voltage data to actual current data.

After calibration of the instrument, an actual experiment can be initiated by

using the *cv run* option. A second menu appears allowing the operator to choose the experimental parameters. The pertinent experimental parameters are:

1. Starting and ending potentials
2. Reversing potentials
3. Sweep resolution
4. Sweep rates
5. Signal to Gain

Once these parameters were selected, the experiment could be initiated. Data from the experiment was recorded both as a data file on a floppy disk and a hardcopy of the voltammogram from an Omnigraphic 2000 XY recorder.

### **Electrochemical Cell And Electrodes**

The cell used for the sample solution for the cyclic voltammetry experiments was a 25 ml sample vial with a screw cap having four holes bored in it for the three electrodes used in this system as well as a hole for degassing of the solution. The three electrodes consisted of:

1. Working electrode
2. Counter electrode
3. Reference electrode

Both the working and counter electrodes were platinum flag electrodes that were plated with mercury using the method of Enke et al.<sup>86</sup> The reference electrode was a 1.0 M Ag/AgCl electrode constructed by placing a small piece of porous vycor glass in the end of a section of 3.9 mm glass tubing. The hollow glass tube

was then filled with 1.0 M KCl and a AgCl coated Ag wire was inserted into the glass tube. The process of coating the silver wire with silver chloride has been described previously by Sawyer.<sup>87</sup>

The process of making a CV run consisted of adding 10 ml of the analyte solution to the electrochemical cell with a small teflon stirring bar. The solution was then degassed using argon for 5-15 minutes prior to running. The temperature was maintained at approximately 25°C throughout the experiment. Once the solution was degassed, the CV run could be initiated as described previously. Prior to running the solution of interest, several background runs must be made. These are the electrolyte alone, for background subtraction and a 0.001 M solution of CdCl<sub>2</sub> for determination of the electrode area. CdCl<sub>2</sub> was used for the determining the electrode area because the diffusion coefficient for this compound is well known. The electrode area, in cm<sup>2</sup>, could be found then by using the following equation (6).

$$i_p = (2.69 \times 10^5) n^{3/2} A D_o^{1/2} v^{1/2} C_o^* \quad (6)$$

Where  $i_p$  is current in amperes,  $n$  is the number of electrons transferred,  $A$  is the area of the electrode in cm<sup>2</sup>,  $D_o$  is the diffusion coefficient in cm<sup>2</sup>/sec,  $v$  is potential in V/sec and  $C_o^*$  is the ionic concentration in mol/cm<sup>3</sup>. Determination of the electrode area is essential for later use in determining various physical parameters for compounds which do not have a well defined diffusion coefficient. In this work, it is primarily used to determine the number of electrons transferred in the

reduction process.

### CV Methods And Parameters

The sample was prepared by dissolving the metal complex in 10 ml of 0.1 M KCl electrolyte. The final concentration of the metal was 0.001 M. If necessary, the pH of the solution was adjusted to 7.0 using 1.0 M NaOH. Buffers cannot be used due to their tendency to be good ligands. The solution was placed in the 25 ml sample vial with the electrodes and allowed to degas for 5-15 min. The CV run was initiated and the following parameters were inputted. Initial and end potentials were -250 mV with reversing potentials at -1500 and -50 mV versus a 1.0 M Ag/AgCl reference electrode. Sweep resolution was 1.00 mV/data point with 4-5 sweep rates between 100 and 1500 mV/sec. The signal to gain was set at 0 and the initial sweep direction was negative. Prior to running any of the chromium complexes, both a 0.1 M KCl solution, for background subtraction and a 0.001M CdCl<sub>2</sub> solution, for electrode area were run.

### Electrode Area

The electrode area was determined using 0.001 M CdCl<sub>2</sub> with the 0.1 M KCl electrolyte subtracted so that all peak heights were due completely to the cadmium. The initial and end potentials were set at -250 mV and the reversing potentials were set at -1300 and -50 mV versus a 1.0 M Ag/AgCl reference electrode. The sweep resolution was 1.00 mV/data point, the initial sweep direction was negative and the sweep rates were between 100 and 1100 mV/sec.

Using equation (3) and using the peak current measured from the subtracted output we can solve for the electrode area. The number of electrons transferred is two and the diffusion coefficient is  $7.15 \times 10^{-6} \text{ cm}^2/\text{sec}$ . An electrode area was determined for each sweep rate and the values averaged together. This value was then used for the rest of the experiments.

### Data Analysis

Data analysis of the digital data acquired on floppy disk during the CV run required several steps to process. The initial data was saved to disk as an Apple DOS 3.3 file. This Apple DOS file had to be converted to an Apple ASCII text file using a FORTH program written by R. Geer called *CD1X*. The Apple ASCII text file could then be converted to a MS-DOS ASCII text file using *CROSS-WORKS*. Once the MS-DOS ASCII text file was made, the data could be imported into Quattro Pro for analysis and graphing. The steps involved in analyzing the CV data require the calibration data discussed previously. The actual steps used to generate the CV data will be discussed in detail in the appendix.

### Electrophoresis

Electrophoresis is an analytical technique used to separate molecules based on their charge and size. The velocity ( $V$ ) at which a molecule moves in an electric field is dependent on the strength of the electric field ( $E$ ), the net electrical charge ( $Z$ ) which resides on that molecule and the frictional resistance ( $f$ ) i.e. size and shape of the molecule. This can be expressed in the following equation (7):

$$V = EZ/f \quad (7)$$

This technique can be used not only for separation of molecules but can also be used to determine if a molecule has undergone a conformational change, that would either increase or decrease its frictional resistance.

### Instrumentation

The instrumentation for electrophoresis consists of a gel box, either vertical or horizontal, with two electrodes on either end serving as a cathode and an anode. A power supply is needed to supply the voltage and the current across the gel box. The matrix for electrophoresis is commonly either polyacrylamide for proteins or agarose for DNA. The matrix is a gel-like consistency which is immersed in an ionic buffer solution to allow charge transfer.

### Plasmid Transformations

Our electrophoretic work involved the analysis of DNA. More specifically, we needed the supercoiled conformation of a plasmid DNA of known size and sequence. We also needed a large enough concentration to run a large number of assays. This was accomplished by transforming *E. coli* with *pUC-18* plasmid. *pUC-18* is a multi-copy plasmid which has been well characterized in terms of size, sequence and enzymatic restriction sites. It also has a genetic sequence coding for ampicillin resistance which allows for selection of this genotype.

For the plasmid transformation, we chose *E. coli* HB101 as the cloning vehicle. The procedure involved inoculating 10 ml of LB broth with a single

bacterial colony and allowing it to grow overnight. 50 ml of fresh LB broth was then inoculated with 0.5 ml of the overnight culture and incubated at 37°C until the  $OD_{600}$  reached 0.4-0.6. The cells were then centrifuged at 7000g for 5 min and resuspended in cold 50 mM  $CaCl_2$ . The cells were kept on ice for 15-60 min, centrifuged at 7000g and resuspended in 4 ml of 50 mM  $CaCl_2$  and kept on ice for several hours. At this time, the cells are competent, i.e. ready to be transformed. 1-50 ng of *pUC-18* DNA was added to 50  $\mu$ l of TE buffer. 100  $\mu$ l of the competent cells were added to this solution and placed on ice for 10 min. The cells were taken off the ice and immediately immersed in a 42°C water bath for 2 hr. After this time, the cells were streaked on a LB + ampicillin plate and allowed to grow overnight at 37°C. Those cells which formed viable colonies were the transformed cells containing the *pUC-18* plasmid.

### DNA Plasmid Extraction

Extraction of the *pUC-18* plasmid for electrophoretic work was accomplished using a method described by Maniatis.<sup>88</sup> A single colony of transformed *E. coli* HB101 was cultured overnight in 50 ml of LB broth containing 100  $\mu$ g/ml of ampicillin. Eppendorf tubes containing 3.0 ml of cells were centrifuged for 15 sec or until the cells formed a pellet on the bottom. The supernatant was discarded and the cells were resuspended in 1.0 ml of LB media, recentrifuged and the supernatant discarded. Two hundred  $\mu$ l of solution I (see appendix pg. 157) containing 10 mg/5 ml of lysozyme was added to the eppendorf tube. The solution was mixed and incubated at room temperature for 5 min. Four hundred  $\mu$ l of

solution II (see appendix pg. 157) was then added, gently shaken and kept on ice for 10 min. Three hundred  $\mu\text{l}$  of solution III (see appendix pg. 157) was then added, mixed once by inversion and kept on ice for 15 min. At this point, a clot of genomic DNA should be visible. The solution was centrifuged for 10 min, the supernatant was transferred to a new eppendorf tube and the genomic DNA pellet was discarded. To the supernatant, 1.0 ml of ice-cold isopropanol was added and kept at  $-20^{\circ}\text{C}$  for 20 min. The tube was centrifuged for 15 min and the supernatant was discarded. The pellet, which now should contain only plasmid DNA and RNA was dissolved in 300  $\mu\text{l}$  of  $\text{T}_{50}\text{NaOAc}$  (see appendix pg. 158). Once in solution, 1.0 ml of ice-cold 95% EtOH was added and the solution was kept at  $-20^{\circ}\text{C}$  overnight. The solution was then centrifuged, the supernatant discarded and the pellet redissolved in 150  $\mu\text{l}$  of TE (see appendix pg. 157). At this point, the DNA was ready for use in our assay and electrophoresis.

The concentration of DNA was determined spectrophotometrically. The RNA which is present in our DNA samples absorbs at a similar wavelength so steps had to be taken to remove it before measuring. This was accomplished by incubating 50  $\mu\text{l}$  of the DNA/RNA fraction collected in the above described extraction scheme with 2  $\mu\text{l}$  of a 10mg/ml solution of boiled RNAse for 2 hr. One ml of ice-cold 95% EtOH was then added to the solution and kept at  $-20^{\circ}\text{C}$  for 2 hr. The solution was centrifuged for 15 min and the pellet resuspended in 2.0 ml of distilled water. The absorbance was measured at 260 nm using ultraviolet absorption spectrophotometry and a concentration could then be determined using

a standard extinction coefficient of  $6600 \text{ cm}^{-1} \text{ M}^{-1}$ / nucleotide pair.

### Electrophoretic Experimental Procedures

Electrophoresis experiments were carried out using either a Bethesda Research Laboratories Model 100 Power supply hooked to an 8 well BioRad Mini-Sub DNA Cell horizontal gel box or a Heathkit Regulated High Voltage Power Supply hooked to a Bethesda Research Laboratories Horizon 20-25 30 well horizontal gel box. The potential applied in both cases was 100 mV and 30 mA. The gel consisted of 1% agarose in 0.5X TBE buffer with  $0.5 \mu\text{l}$  of a 10 mg/ml solution of ethidium bromide per 100 ml of agarose gel. The ethidium bromide allows resolving of the DNA bands when viewed under ultraviolet light. The electrophoresis buffer was 0.5X TBE with  $0.5 \mu\text{l}$  of a 10 mg/ml solution of ethidium bromide added per 100 ml of solution. Gel electrophoresis experiments were carried out on  $10 \mu\text{l}$  reaction mixtures. Typical reaction mixtures contained  $2.0 \mu\text{l}$  of 6.0 mM plasmid DNA,  $2.0 \mu\text{l}$  of 2.0 mM metal,  $2.0 \mu\text{l}$  of 5.0 mM 1:1 ascorbate/ $\text{H}_2\text{O}_2$  as the reductant/oxidant and  $4.0 \mu\text{l}$  of TE buffer. The metal-DNA solutions were incubated at  $37^\circ\text{C}$  for 30 min; the reductant/oxidant was then added and the solutions were allowed to incubate at ambient temperature for 15 min prior to electrophoresis. DNA alone and DNA + the Ascorbate/ $\text{H}_2\text{O}_2$  reductant/oxidant were both used as controls in this experiment.

## Measurement Of Metal Interactions With DNA

### UV-VIS Spectrophotometry

Spectrophotometric measurements have been made to determine if a compound can intercalate between the DNA base pairs. This type of measurement is limited by the type of compound that is being investigated. Metal complexes that have an intense MLCT (metal-ligand charge transfer) band in the visible or ultraviolet spectrum show a hypochromic shift of this absorption band upon intercalation. UV wavelengths between 360 and 280 nm were scanned using a Series 634 Varian UV-VIS spectrophotometer. The wavelength of maximum absorbance was determined using a 0.03 mg/ml solution of the metal in a pH 7.2 Tris-HCl buffer. A 0.15 mg/ml of calf thymus DNA was added to the solution and the wavelengths rescanned. A solution containing 0.15 mg/ml of calf thymus DNA alone was then scanned and used as a background subtraction.

### Equilibrium Dialysis And Polarimetry

Equilibrium dialysis of the mutagenic metal complexes, coupled with polarimetry, will allow us to determine if there is any chiral specificity in the interaction of these complexes with DNA. Dialysis was performed using a dual chambered BellCo dialysis unit with 3.0 ml volume compartments. The two chambers were separated by a dialysis membrane with a molecular weight cut-off of 12000-14000. The dialysis membrane was pretreated by boiling successively in 1%  $\text{Na}_2\text{CO}_3$ , 1% EDTA and 1% SDS. The membrane was rinsed successively

in Millipore water, 80°C 0.3% Na<sub>2</sub>SO<sub>3</sub>, 60°C 2% H<sub>2</sub>SO<sub>4</sub> and again with Millipore water. A 1.0 mg/ml solution of calf thymus DNA in a 5mM Tris-HCl, 50 mM NaCl pH 7.1 buffer was "exhaustively" dialyzed against pure buffer to remove any fragments of DNA. The side containing the buffer and DNA fragments was removed and the compartment rinsed with distilled water. A 3.33 mg/ml solution of metal was added to the compartment and dialyzed for 24 hr against the DNA. After dialysis, the contents of the compartment containing the metal complex was removed and the concentration determined spectrophotometrically. A racemic mixture of the metal with the same concentration was then made as a control.

Polarimetry was performed using both the racemic mixture and the dialyzed mixture of metal. The polarimeter was set at the sodium D line using a 2 cm path length cell. Thirty data points were taken for the racemic mixture and averaged to get the zero baseline. The cell was rinsed with water and acetone before addition of the dialyzed solution. Thirty data points were then taken for the dialyzed solution and the values were averaged. The optical rotation of the solution could then be found by using the following equation (8).

$$[\alpha]_D = \alpha/lc \quad (8)$$

Where  $[\alpha]_D$  is the optical rotation in degrees at the sodium D line wavelength,  $\alpha$  is the rotation in degrees from control,  $l$  is the pathlength of the cell in decimeters and  $c$  is the concentration in grams/100 ml.

### Electrophoretic Mobilities

Gel electrophoresis of supercoiled *pUC-18* plasmid DNA in a 1% agarose gel was carried out to measure the changes in mobility of the DNA in the presence of a constant metal gradient. This constant metal gradient was maintained by the positive charge on the metal migrating horizontally in the opposite direction from that of the negatively charged DNA. This movement limits the natural diffusion out of the gel vertically over time. A series of electrophoretic gels were run with different concentrations of metal added directly to the agarose gel prior to pouring. The gel was run in 0.5X TBE buffer in an eight well DNA mini-Sub cell for 1.0 h. The gel was then stained by soaking in a 0.1  $\mu\text{l/ml}$  solution of ethidium bromide and the relative positions of the DNA bands were measured versus their origin. Changes in the mobility of the DNA can be interpreted as an interaction taking place between the metal and the DNA.

### Membrane Permeability

Membrane permeability was measured for selected Cr(III) complexes used in this study as well as for  $\text{CrCl}_3$  and Cr(VI) by Dr. Marguerite Sognier of the University of Texas at Galveston Medical Branch. Data was obtained by pretreating V79 Chinese Hamster Lung Fibroblasts with varying concentrations of the chromium compound in a low serum media. After 180 min, the cells were washed, lysed and analyzed with inductively coupled plasma mass spectrometry to obtain the concentration of chromium which had accumulated intracellularly.

## RESULTS AND DISCUSSION

For presentation, the results and discussion section has been divided into a number of categories. These categories will consist of: 1) Structures of the different complexes used in the experiments, 2) Biological assays for the different compounds, 3) Membrane permeability of metal complexes, 4) Cyclic voltammetry of metals in relation to production of oxygen radicals, 5) Electrophoresis of metal-treated DNA and the significance to the mechanism of damage, and 6) The interactions of mutagenic metal complexes with DNA.

### Structures Of The Cr(III) Complexes

In order to determine the structure/activity relationships between the Cr(III) species, it was necessary to synthesize structurally related compounds and relate structure to biological activity. The structures for the ten Cr(III) complexes used originally are shown in figures 9 and 11. Later reference to the original complexes are these ten compounds that were used to develop the structure/activity model. Other structurally related compounds were synthesized to refine this model following the basic principles developed from the original complexes.

With the exception of the hexacyano complex, there is a common theme among these compounds. This common theme is the amine ligands associated with the chromium metal. Five of the compounds have associated ligands which are bis-bidentate aromatic amines. They differ only in the number of these amine ligands and the corresponding halogen or aquo species needed to saturate the six-

coordinate structure. These compounds are,  $[\text{Cr}(\text{bpy})_3](\text{ClO}_4)_3$ ,  $[\text{Cr}(\text{bpy})_2\text{Cl}_2]\text{Cl}$ ,  $[\text{Cr}(\text{bpy})_2(\text{H}_2\text{O})_2]\text{Cl}_3$ ,  $[\text{Cr}(\text{phen})_2\text{Cl}_2]\text{Cl}$  and  $[\text{Cr}(\text{phen})_2(\text{H}_2\text{O})_2]\text{Cl}_3$ . The bipyridyl and phenanthroline ligands are structurally analogous, with the only difference being an additional ring system associated with the phenanthroline ligand. A consequence of this extra ring structure in phenanthroline is a more planar ligand, the significance of which will be discussed in a later section. Both the bipyridyl and phenanthroline ligands are characterized as rigid chelates. A single tris-bidentate compound was used in this study,  $[\text{Cr}(\text{bpy})_3](\text{ClO}_4)_3$ , although a second tris-bidentate compound,  $[\text{Cr}(\text{phen})_3](\text{ClO}_4)_3$ , was synthesized but not used due to its low solubility in the aqueous buffer systems used in the biological assays.

One complex containing aromatic amine ligands, but having monodentate instead of bidentate bonding to chromium was synthesized to test the effects of the aromatic structure associated with the ligands. This compound was  $\text{Cr}(\text{py})_4\text{Cl}_2$  which contains the monodentate aromatic amine ligand pyridine. With the exception of the bridging carbon-carbon bond between two pyridyls, this compound closely resembles the bis-bidentate complex  $\text{Cr}(\text{bpy})_2\text{Cl}_2$ .

Complexes with bidentate aliphatic amine ligands have been synthesized and tested as well. These include the bis-bidentate  $[\text{Cr}(\text{en})_2\text{Cl}_2]\text{Cl}$  complex and the tris-bidentate complex,  $[\text{Cr}(\text{en})_3]\text{Cl}_3$ . The ethylenediamine ligand mimics the bipyridyl and phenanthroline ligand system with its bidentate structure but differs considerably by lack of aromaticity, overall size and planarity. The ethylenediamine ligand in contrast to the aromatic bis-bidentate ligands is classified

as a flexible chelate.

A monodentate complex with four amine ligands and two halogens in its hexacoordinate structure was synthesized and tested as well. This complex was,  $[\text{Cr}(\text{NH}_3)_4\text{Cl}_2]\text{Cl}$ . It was synthesized to test what, if any effect a simple monodentate complex had on the activity. The ligand size differs only by two carbons from that of the bidentate ethylenediamine complex but, unlike the ethylenediamine ligand, the amine groups have free rotation about the Cr-N bond.

The odd compound in this group was  $\text{K}_3\text{Cr}(\text{CN})_6$ . While this is not an amine ligand, it was synthesized to test what, if any, effect a high spectrochemical series ligand has on the activity and redox behavior of the chromium metal center. The spectrochemical series is a measure of a ligand's ability to split the octahedral d-orbitals. The order of splitting due to ligand field strength is given below.

$$\text{CN}^- > \text{phen, bpy, NO}_2^- > \text{en} > \text{NH}_3, \text{pyr} > \text{H}_2\text{O} > \text{C}_2\text{O}_4 > \text{OH}^- > \text{F}^- > \text{S}^{2-} > \text{Cl}^- > \text{Br}^- > \text{I}^-$$

The effect of a high spectrochemical series ligand is due to  $\pi$  bonding between the metal and the ligand.<sup>89</sup> This  $\pi$  bonding results in donation of electrons from one of the  $t_{2g}$  orbitals of the metal to a vacant orbital of the ligand. This donation of electrons can increase the effective positive charge on the metal ion as well as shorten the M-X bond distance. Thus, the choice of the hexacyano chromium complex was based on its position in the spectrochemical series so that if there was an effect due to ligand field splitting, it should be seen in this complex. The

work of Herzog and others, have calculated that the degree of  $\pi$  bonding between the metal and the ligand is nominal for Cr(III) complexes and the highest occupied orbital is a delocalized molecular orbital composed mainly of the metal  $t_{2g}$ -orbital.<sup>90-93</sup> This assignment was based on the ESR spectra for amine based ligands of chromium. Semi-empirical molecular orbital calculations, while not presented in this work, tend to agree with that of Herzog et al. The significance of this work, however, is at best suggestive since a minimized structure was never obtained.

Further structures were synthesized to test the model derived from the previous group of compounds. These compounds tested two different themes; 1) The effect of splitting the octahedral symmetry with different halogens and 2) The effect of electron withdrawing and electron donating substituents on the bipyridyl ligand. Splitting of the octahedral symmetry was accomplished using different halogens in the *cis* position of the hexacoordinate geometry. Splitting of the octahedral symmetry should increase as the separation between the different ligands in the spectrochemical series increases.<sup>94</sup> The different halogen complexes of the bis-bipyridyl Cr(III) complex were used, figure 9. These were  $[\text{Cr}(\text{bpy})_2\text{F}_2]^{+1}$ ,  $[\text{Cr}(\text{bpy})_2\text{Cl}_2]^{+1}$ ,  $[\text{Cr}(\text{bpy})_2\text{Br}_2]^{+1}$ , and  $[\text{Cr}(\text{bpy})_2\text{I}_2]^{+1}$ .

The effect of electron withdrawing and electron donating groups on the bipyridyl ligand were shown by substituting the 4 and 4' position of bipyridyl with different groups, figure 10. Two electron donating groups  $-\text{CH}_3$  and  $-\text{N}(\text{CH}_3)_2$  and the two electron withdrawing groups  $-\text{COOH}$  and  $-\text{COOCH}_3$  were synthesized.

The bis-bidentate dichloro Cr(III) complex of these species were synthesized and tested. These are,  $[\text{Cr}(\text{dmbpy})_2\text{Cl}_2]^+1$ ,  $[\text{Cr}(\text{dmabpy})_2\text{Cl}_2]^+1$ ,  $[\text{Cr}(\text{dcbpy})_2\text{Cl}_2]^+1$  and  $[\text{Cr}(\text{dmebpy})_2\text{Cl}_2]^+1$ . Where dmbpy is 4,4'-dimethyl-2,2'-bipyridyl, dmabpy is 4,4'-di(dimethylamino)-2,2'-bipyridyl, dcbpy is 4,4'-dicarboxy-2,2'-bipyridyl and dmebpy is 4,4'-dimethylester-2,2'-bipyridyl. The *cis* halogens in all of these compounds were chloride for consistency.

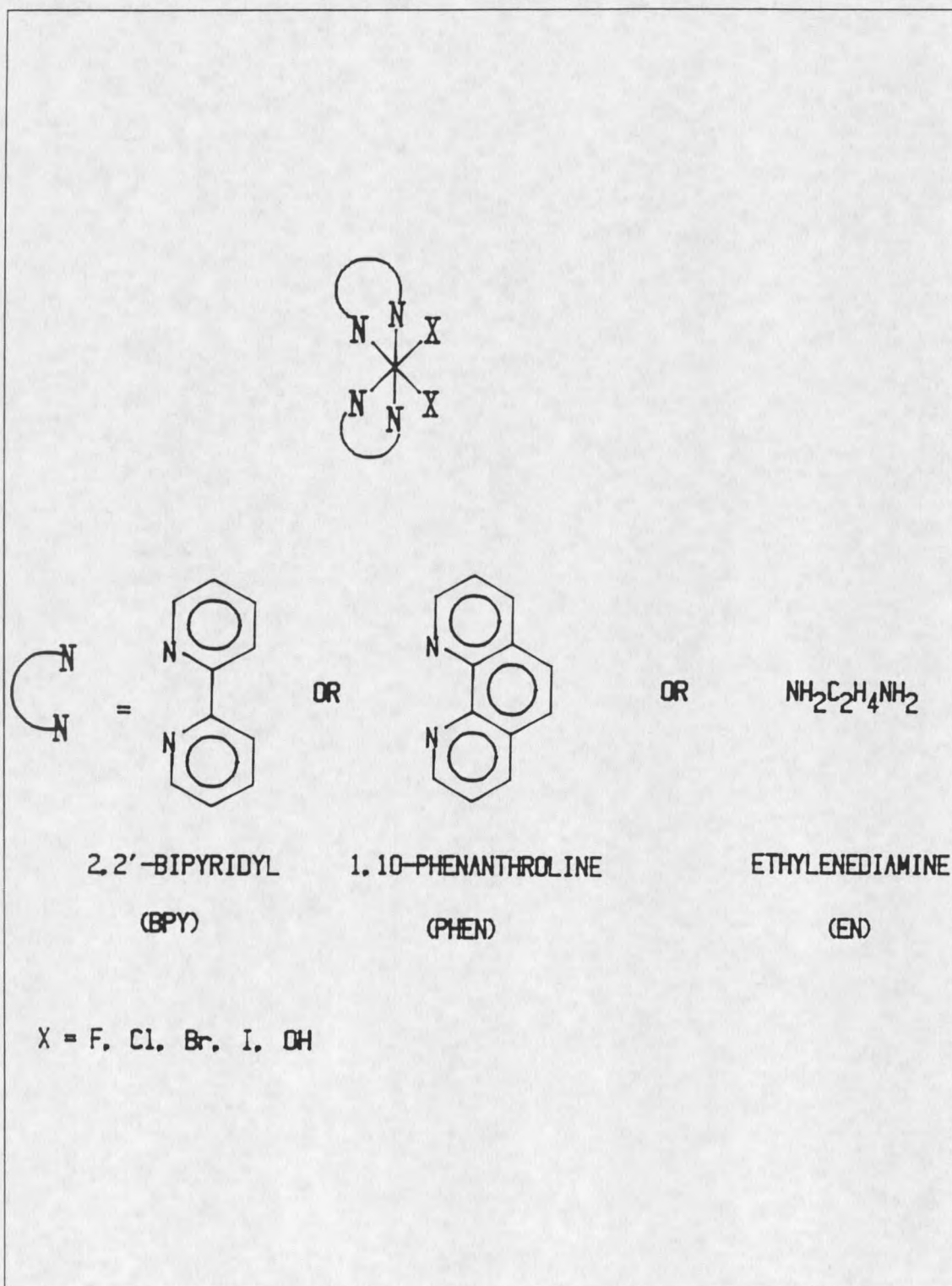


Figure 9: Structures of Cr(III) complexes.

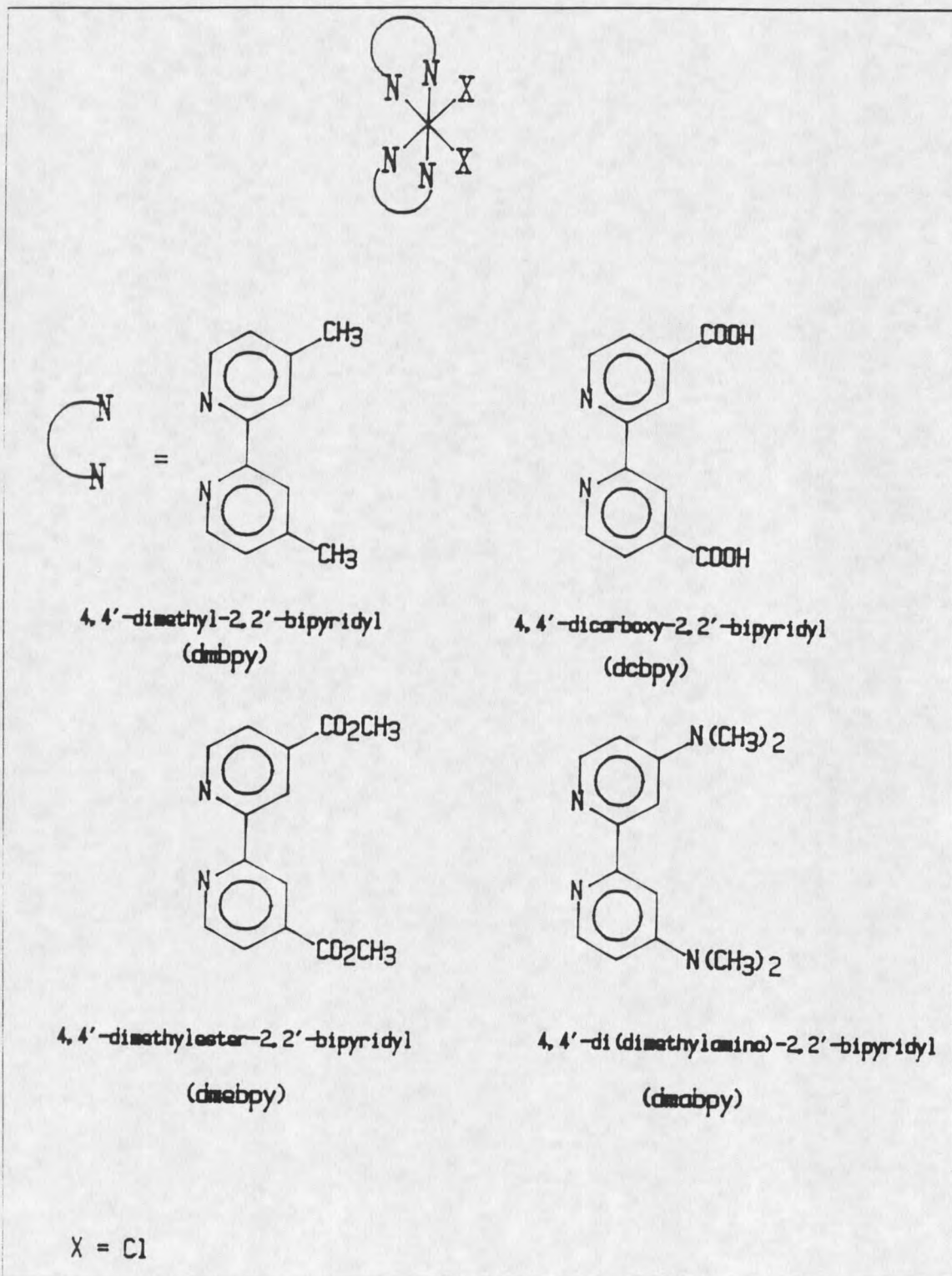


Figure 10: Structures of Cr(III) Complexes.

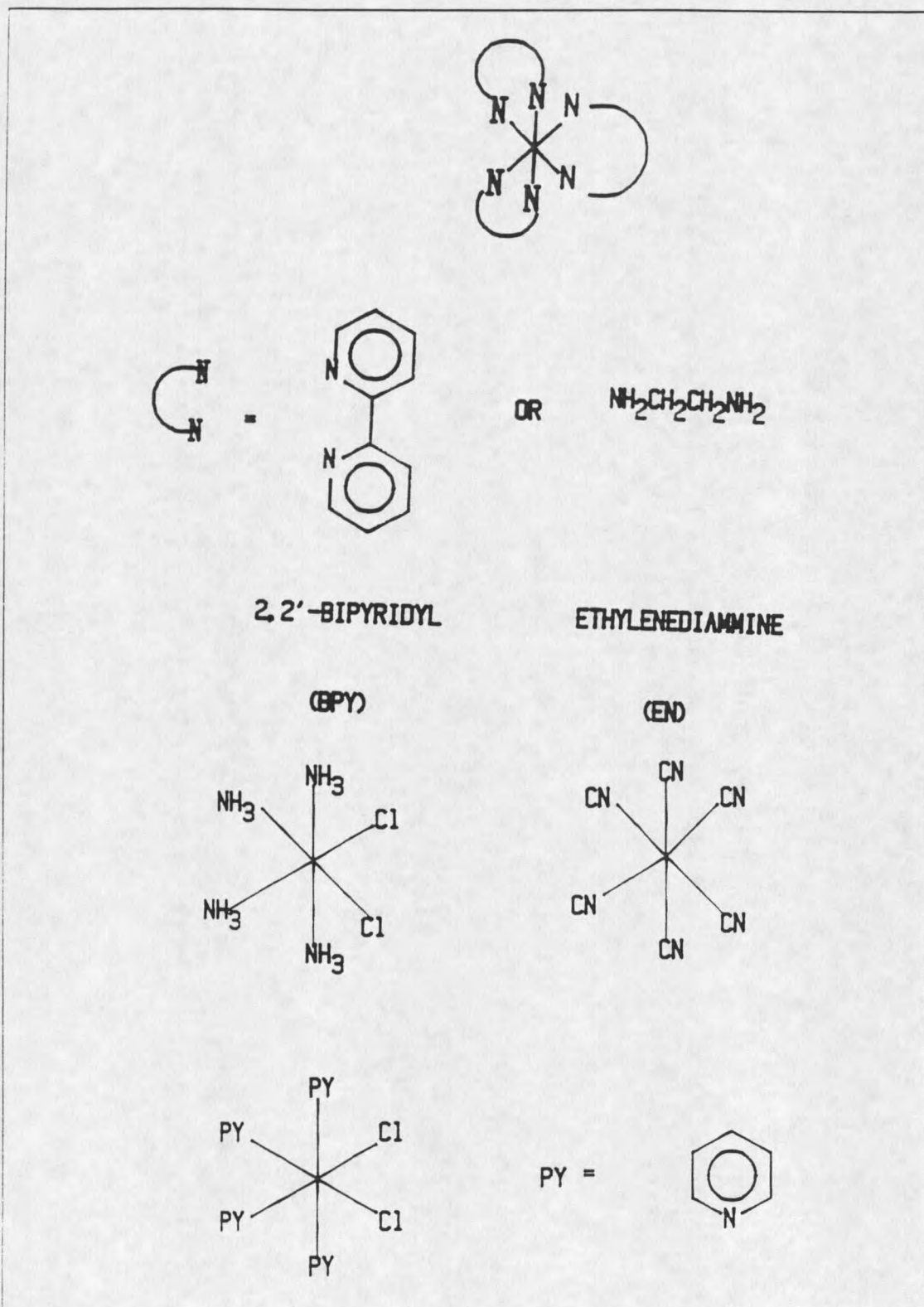


Figure 11: Structures of Cr(III) compounds.

### Biological Assays

The metal complexes were all tested for biological activity using the Ames Salmonella reversion assay. While the Salmonella reversion assay is not a quantitative assay, it does give good qualitative data on whether a compound is mutagenic and the relative differences between the different compounds. It does not, however, take into account the possible effects of cytotoxicity. These cytotoxic effects can be taken into account by assaying the strains used in the Salmonella reversion assay for cell viability. The number of viable cells can then be combined with the reversion data to give a mutant frequency. This mutant frequency, while still not truly quantitative, removes another possible variable for the differences seen among the mutagenic species.

The relative reversion frequency of the original Cr(III) compounds were determined using the Ames strains TA102 and TA2638. Figures 12 and 13 show the relative response for the mutagenic Cr(III) complexes in TA102 and TA2638 respectively. In both *S. typhimurium* strains, the order of reversion frequency is  $[\text{Cr}(\text{phen})_2\text{Cl}_2]^{+1} > [\text{Cr}(\text{phen})_2(\text{H}_2\text{O})_2]^{+3} > [\text{Cr}(\text{bpy})_2\text{Cl}_2]^{+1} > [\text{Cr}(\text{bpy})_2(\text{H}_2\text{O})_2]^{+3} > [\text{Cr}(\text{bpy})_3]^{+3}$ . The revertants/nanomole for these complexes range from 17.5-8.2 in TA102 and 2.3-1.1 in TA2638, Table I. The relative reversion frequencies for the Cr(III) complexes are 2-5 fold over background in TA102 and 3-7 fold over background in TA2638, Table I.

To ensure that the differences observed in activity for these compounds is not due to a differential toxicity, a mutation frequency for the mutagenic complexes

was performed. The results, figures 16 and 17, run in Ames strains TA102 and TA2638 show the same relative response as seen in the Salmonella reversion assay. This increases the confidence of assigning the differences observed to increased biological activity and not as an artifact of the assay system.

The nonmutagenic Cr(III) compounds,  $\text{Cr(en)}_3$ ,  $\text{Cr(en)}_2\text{Cl}_2$ ,  $\text{Cr(py)}_4\text{Cl}_2$ ,  $\text{Cr(NH}_3)_4\text{Cl}_2$ , and  $\text{Cr(CN)}_6$  have shown no significant reversion in either strain in the same concentration range as that of the mutagenic complexes, figures 14 and 15. As well, the ligands themselves are nonmutagenic in Ames strains TA102 and TA2638, figure 18 and 19, or in a previous study using Ames strains TA92, TA100 and TA92.<sup>95</sup>

Table I: Relative reversion rates of original Cr(III) complexes.

<u>Complex</u>	<u>Revertants/Nanomole</u>		<u>Fold Over Background</u>	
	<u>TA102</u>	<u>TA2638</u>	<u>TA102</u>	<u>TA2638</u>
$\text{Cr(phen)}_2\text{Cl}_2$	17.5	2.3	5	6.9
$\text{Cr(phen)}_2(\text{OH})_2$	15.5	2.2	4.4	6.8
$\text{Cr(bpy)}_2\text{Cl}_2$	12	1.8	3.4	5.5
$\text{Cr(bpy)}_2(\text{OH})_2$	9.6	1.3	2.5	3.8
$\text{Cr(bpy)}_3$	8.2	1.1	2.3	3.3

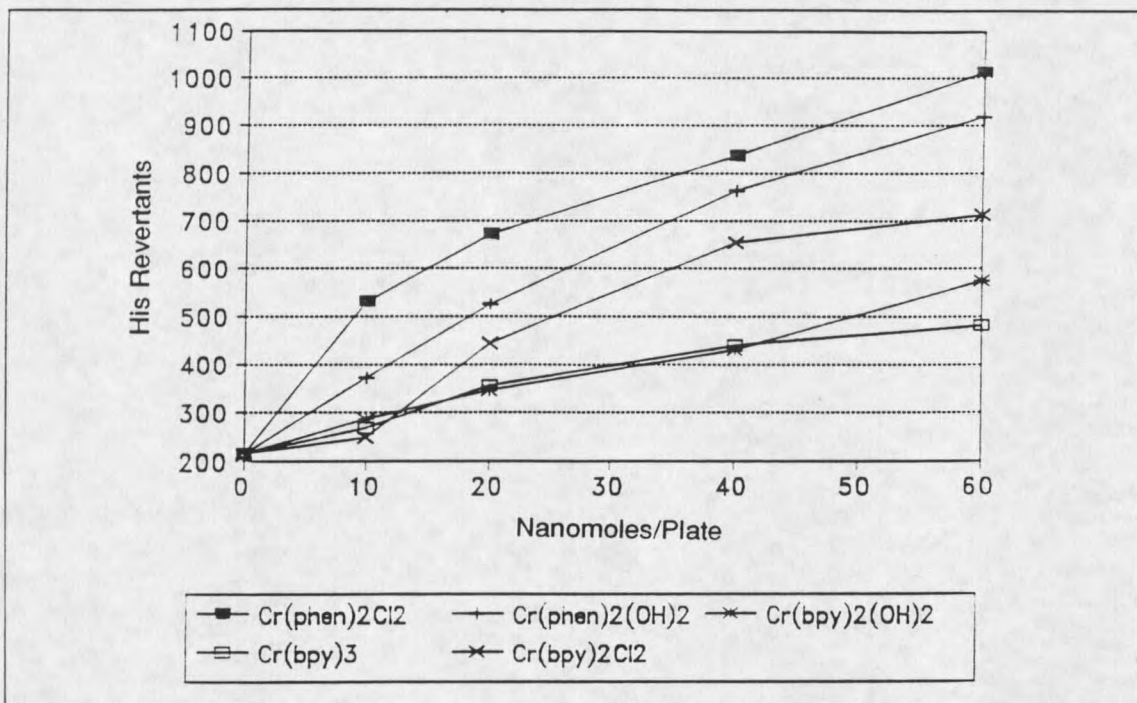


Figure 12: Salmonella reversion assay of original mutagenic complexes in TA102.

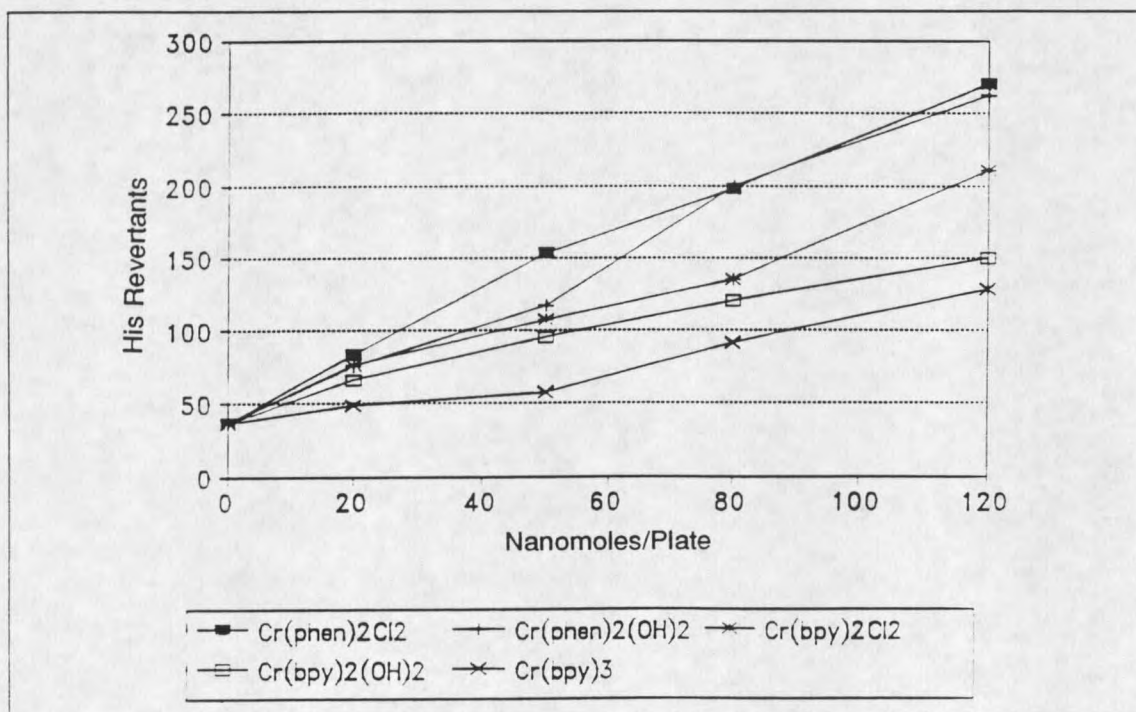


Figure 13: Salmonella reversion assay of original mutagenic complexes in TA2638.

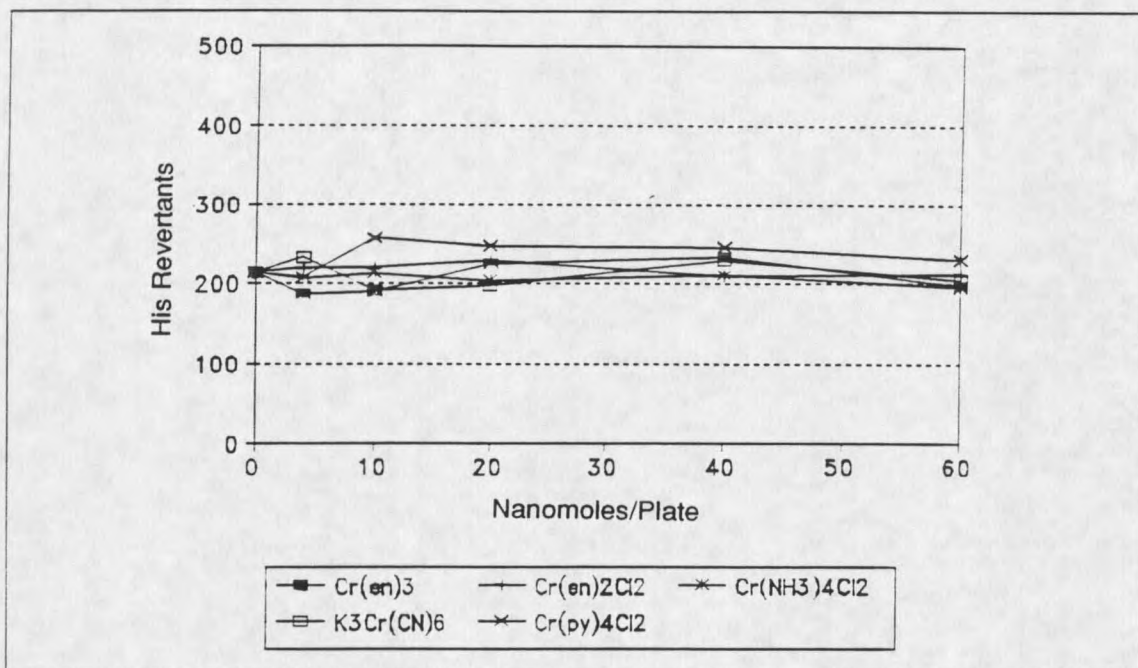


Figure 14: Salmonella reversion assay of nonmutagenic Cr(III) complexes in TA102.

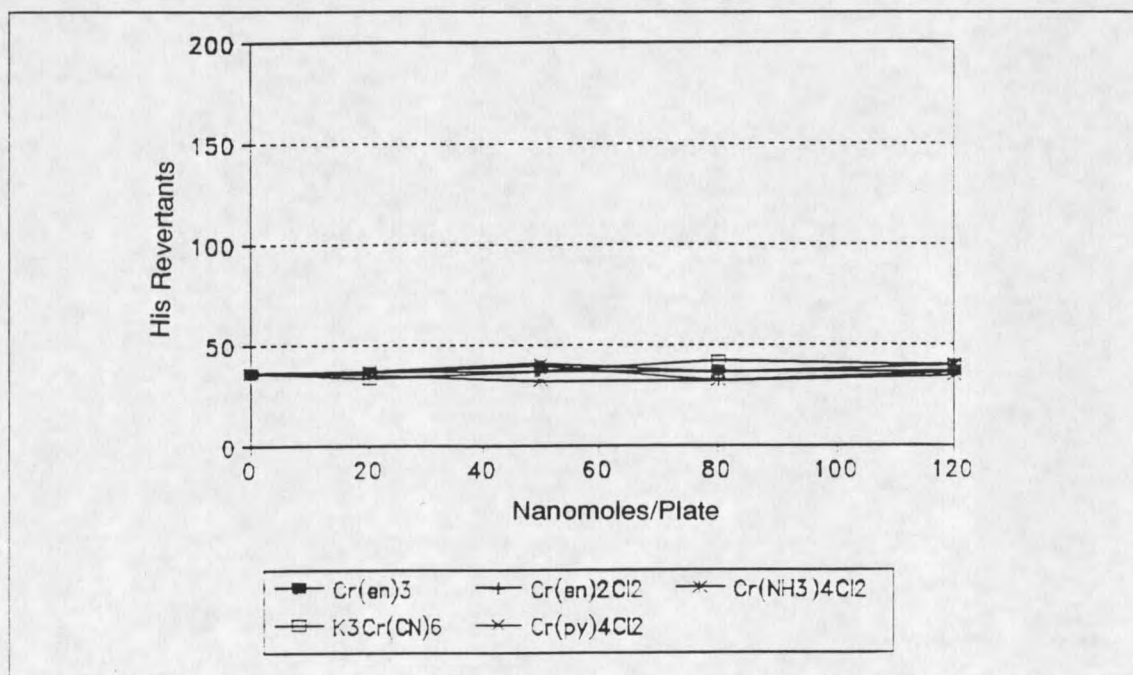


Figure 15: Salmonella reversion assay of nonmutagenic Cr(III) complexes in TA2638.

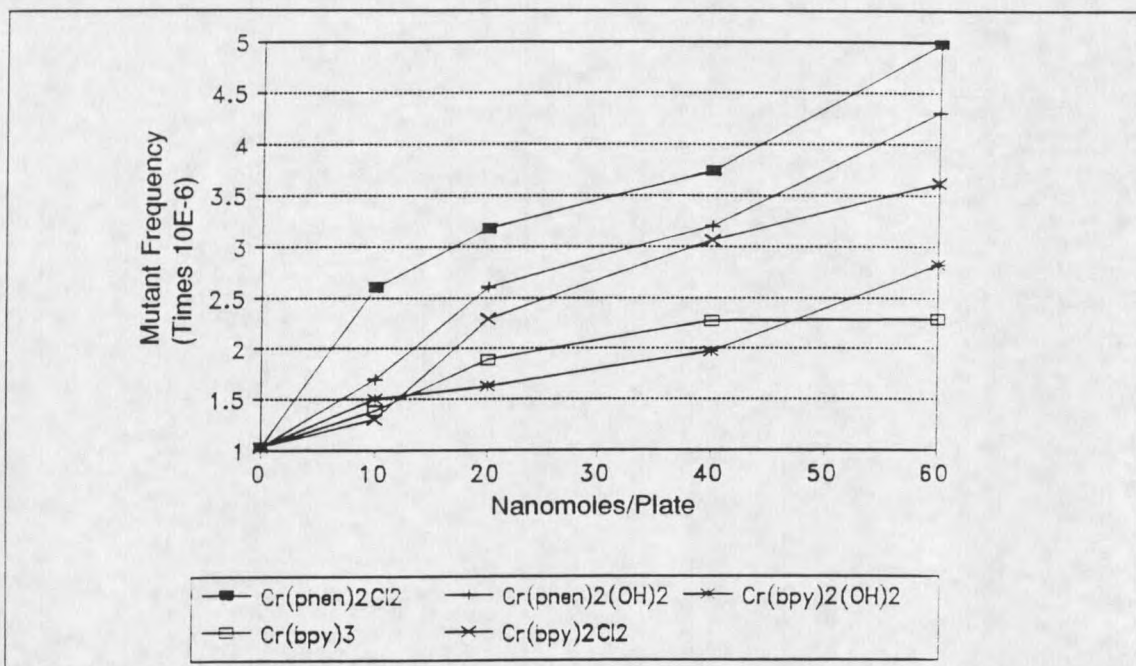


Figure 16: Mutation frequency of original Cr(III) complexes in TA102.

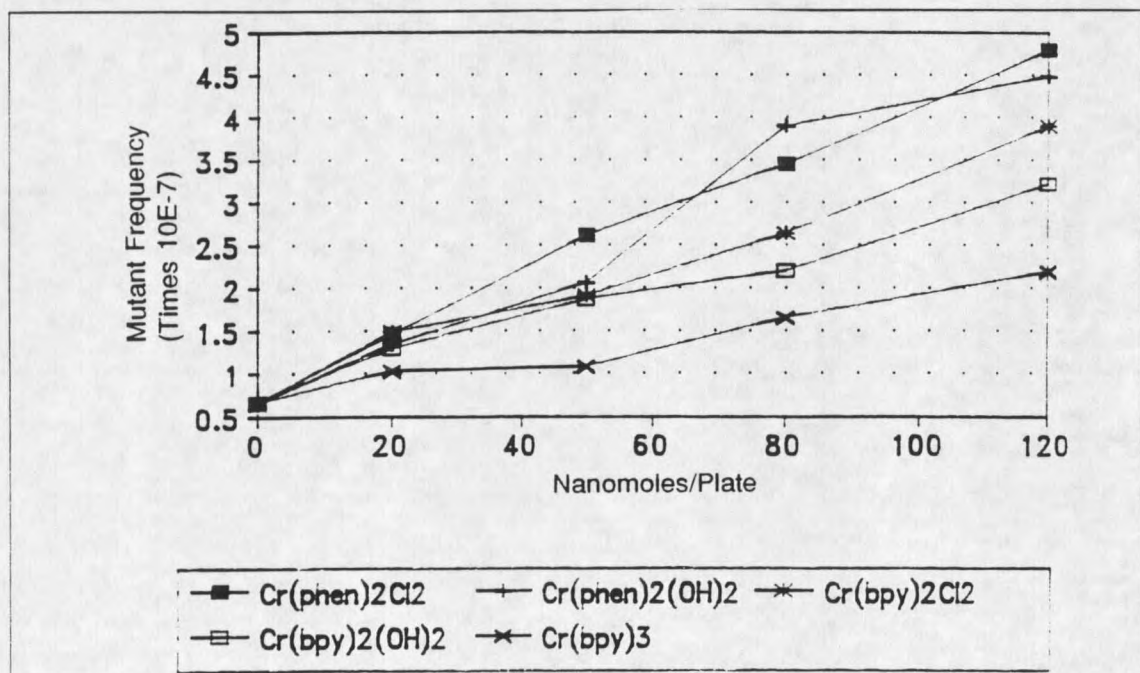


Figure 17: Mutation frequency of original Cr(III) complexes in TA2638.

Several conclusions can be drawn from the narrow range of ligand types that confer activity upon the original Cr(III) species. The bis-bidentate aromatic amine ligands in some way act to confer the metal complex with the physical characteristics necessary to be biologically active. Only two of these bis-bidentate ligands are necessary to bestow their structure/activity relationship. This activity does not appear to be a function of the ligands themselves, but of the whole metal-ligand complex. The exact manner in which these ligands direct this activity, however, cannot be determined from these few complexes although the ability to revert these two strains suggests an oxidative mechanism.

The Salmonella reversion assay for several of these same complexes in a different *S. typhimurium* strain, TA100, was carried out to determine if there is a specificity of damage to the AT base pairs at the site of the His<sup>-</sup> mutation. TA100, unlike TA102 and TA2638, has GC base pairs at the site of the His<sup>-</sup> mutation.<sup>96</sup> This strain has been shown to be more specific towards DNA adduct formation such as those seen with *cis*-platinum. The relative reversion frequency in this strain is seen in figure 20.

The much lower reversion frequency in this strain, essentially zero at this concentration, can be related to the genetics of this organism as well as the specificity of the mutational target site. The TA100 strain is not nearly as sensitive to oxidative mutagens as the TA102 and TA2638 strains. These data then are consistent with the mutagenic Cr(III) complexes having a mechanism of DNA damage that involves an oxygen radical. As well, the genetic differences between

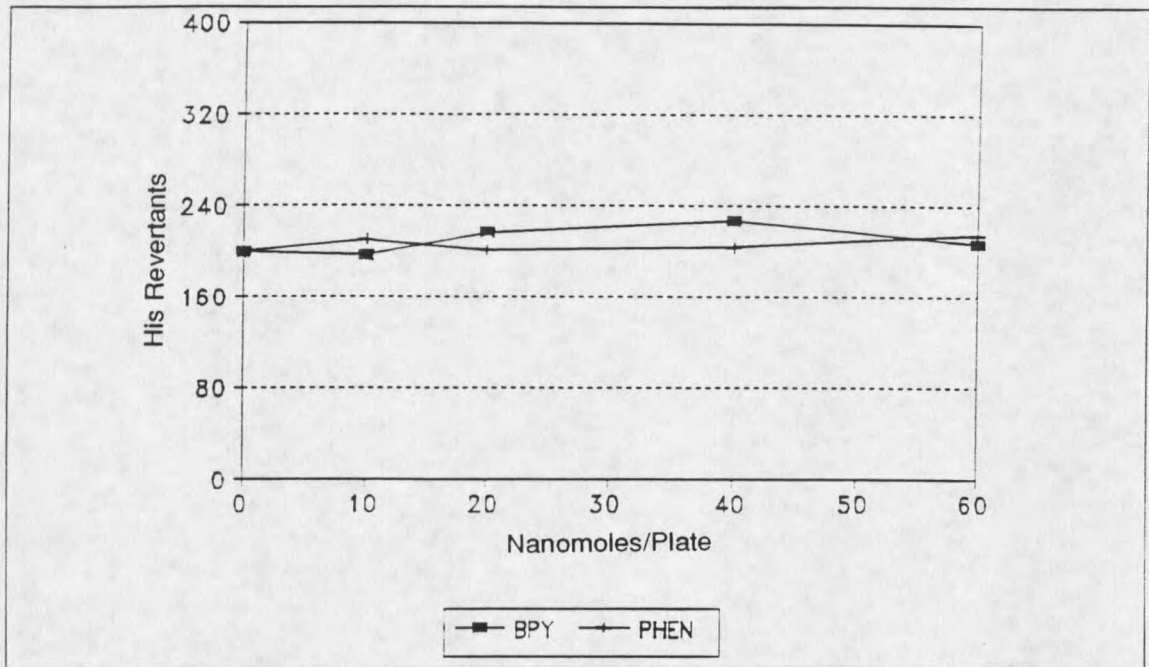


Figure 18: Salmonella reversion assay of bipyridyl and phenanthroline ligands in TA102.

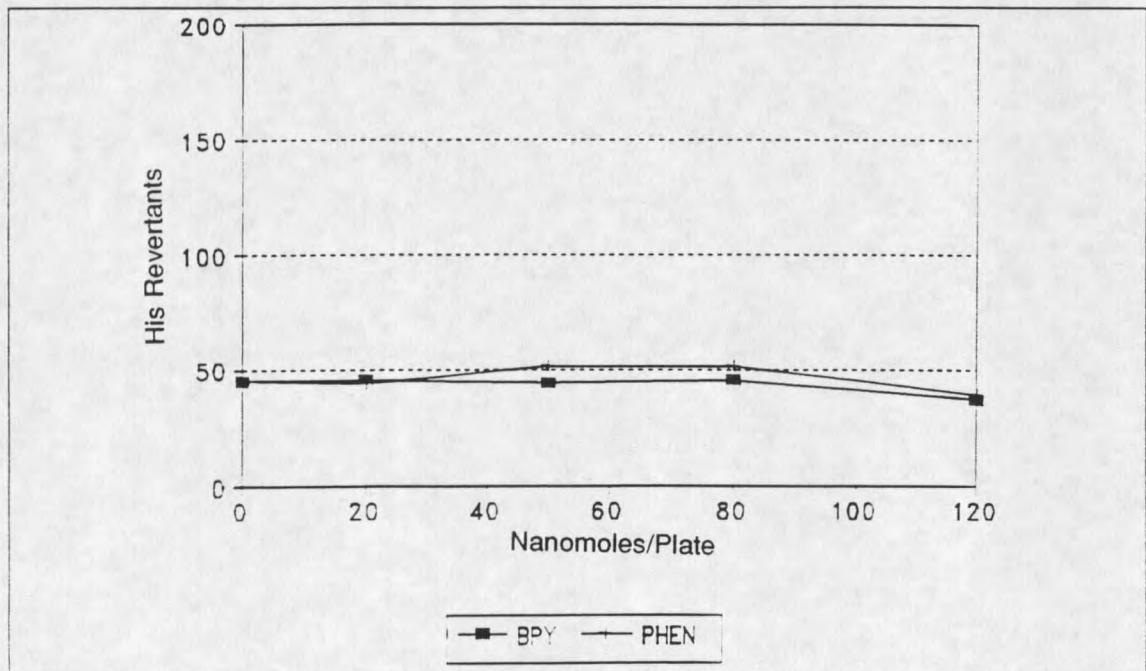
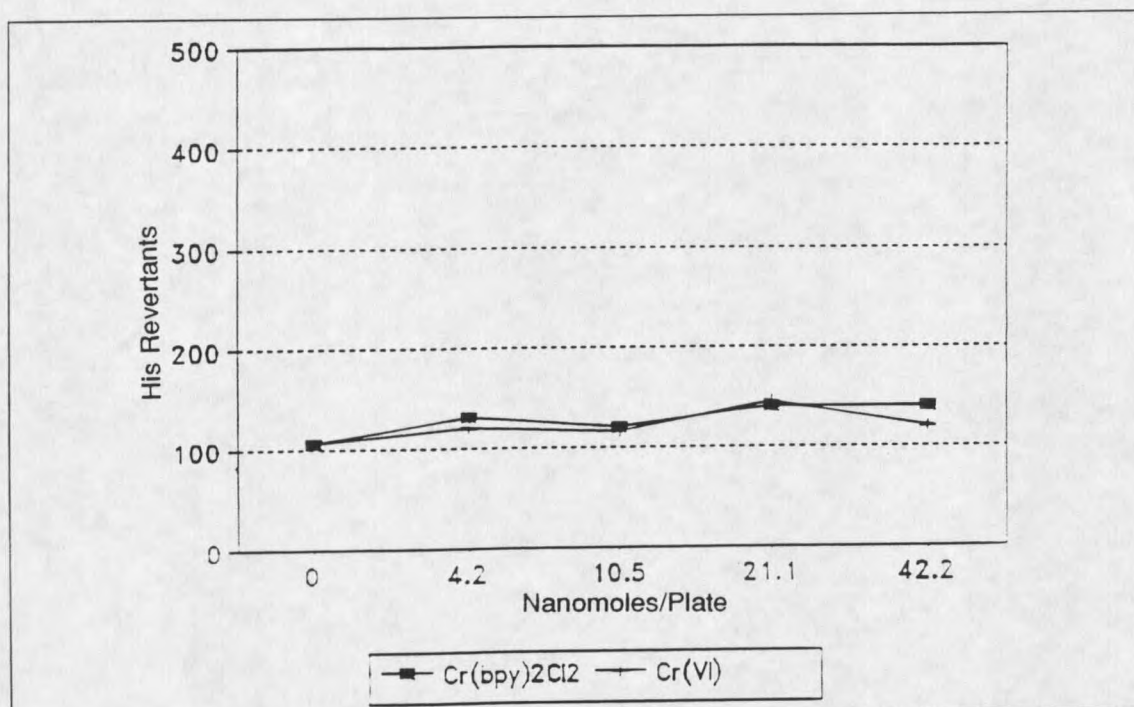


Figure 19: Salmonella reversion assay of bipyridyl and phenanthroline ligands in TA2638.



**Figure 20:** Salmonella reversion assay of Cr(VI) and a representative Cr(III) complex in TA100.

these strains imply that the Cr(III) complexes are acting as typical clastogens, in that they demonstrate radiomimetic tendencies.

The possibility of an oxidative mechanism of damage for the Cr(III) complexes has led us to develop an anaerobic assay for the assessment of oxygen dependence on biological activity. Figures 21, 22, 23, 24 and 25 show the results of typical anaerobic assays relative to their aerobic responses. In all cases that were measured, the mutagenic Cr(III) species showed an absolute dependence on oxygen for the induction of mutagenesis. This finding is consistent with the previous data implicating an oxygen radical mechanism of damage for these complexes. The negative control in this case was Cr(VI) which has been

shown previously to have a possible mechanism of action involving oxygen radicals.<sup>33</sup> The results for Cr(VI), however are not as clear cut as that of the Cr(III). There remains a small amount of mutagenic induction in the absence of oxygen. Even incubation in the presence of *oxyrase*, an oxygen consuming membrane fraction of *E. coli*, a certain amount of mutagenic response was observed. This phenomenon suggests that Cr(VI) may have a secondary mechanism of damage unrelated to the production of oxygen radicals or it may be that Cr(VI) is simply quite effective at using the small amount of available molecular oxygen present. The positive control in this case was MNNG, an alkylating agent, whose mechanism of action should not be dependent on the presence or absence of oxygen. The results show that MNNG is nearly equally efficient at reverting these Salmonella strains independent of the environment.

While this type of measurement is only qualitative in nature, we believe that it represents a rapid method for determination if a putative mutagen may have an oxygen radical mechanism of DNA damage.

An anaerobic assay was also developed using a modification of the SOS response to determine whether Cr(III) had a similar dependence on oxygen for the induction of DNA damage. The results for a representative Cr(III) complex is shown in figure 26. Much like the anaerobic Salmonella reversion assay, the SOS response assay demonstrated a dependence on oxygen for the induction of biological activity. Mitomycin C, in this same assay, showed very little difference in activity between the aerobic and anaerobic assays (data not shown). Paraquat,

although not showing an induction of the SOS response in either aerobic or anaerobic conditions, did show a marked decrease in toxicity under anaerobic conditions. This, we believe, is consistent with what would be expected for an oxygen radical mechanism of damage. These data support the previous work with the anaerobic Salmonella reversion assay.

This assay, although somewhat unwieldy due to the anaerobic conditions required, has the potential to be used for a quick determination of an oxygen radical mechanism of damage for putative mutagens.

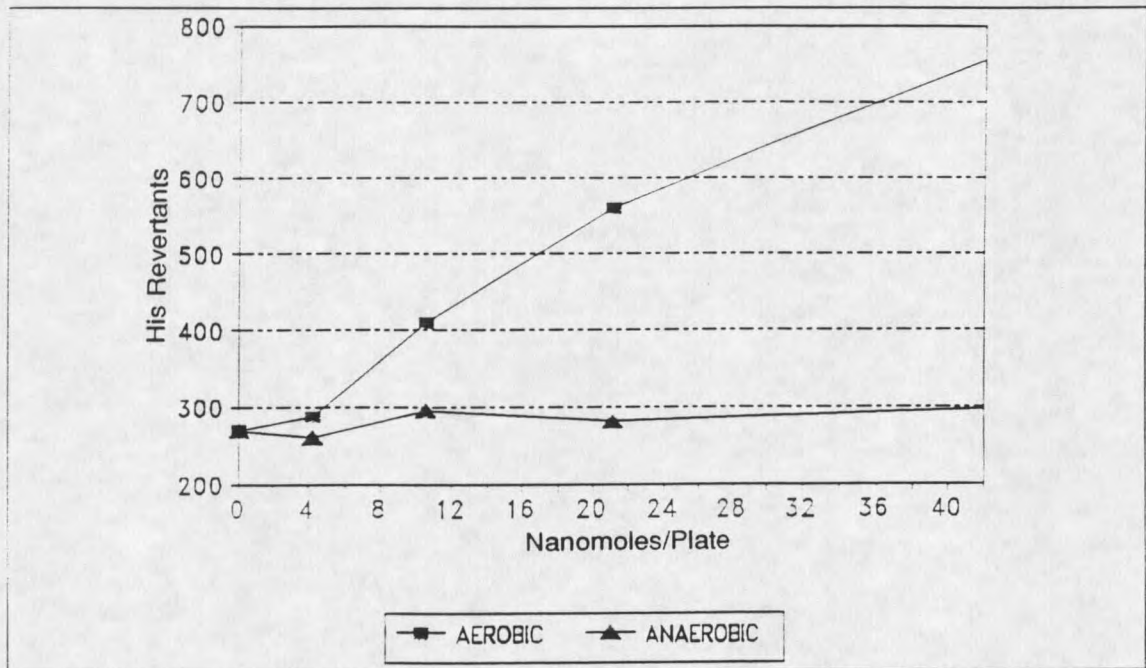


Figure 21: Salmonella reversion assay of Cr(VI) and Cr(III) both aerobic and anaerobic in TA102.

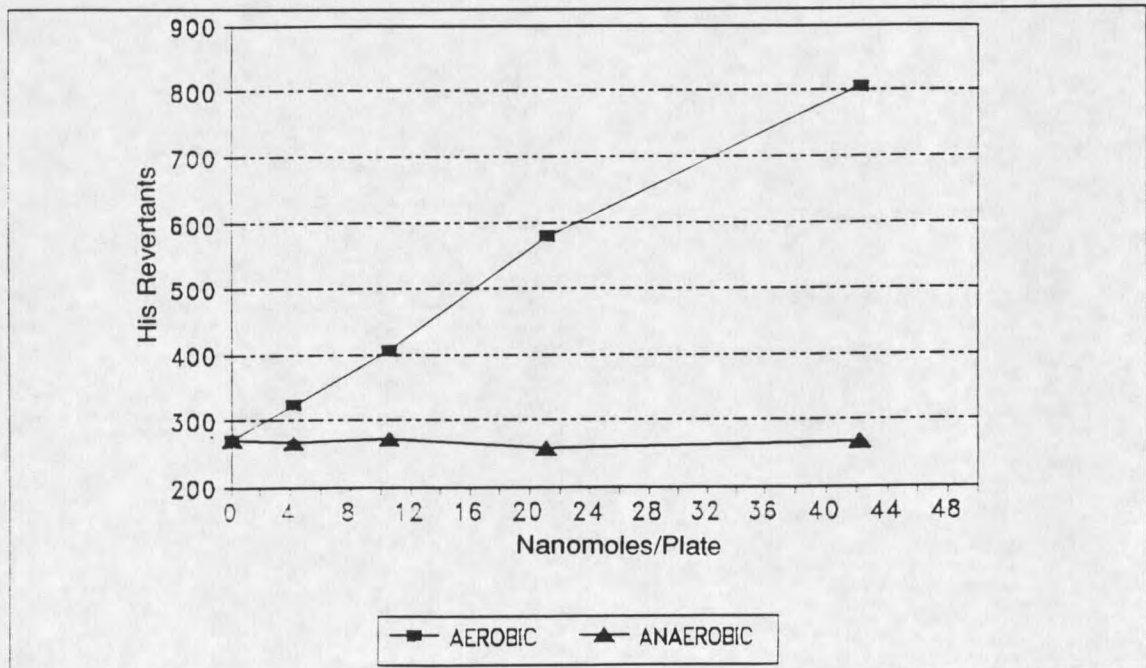


Figure 22: Salmonella reversion assay of a representative Cr(III) complex both aerobic and anaerobic in TA102.

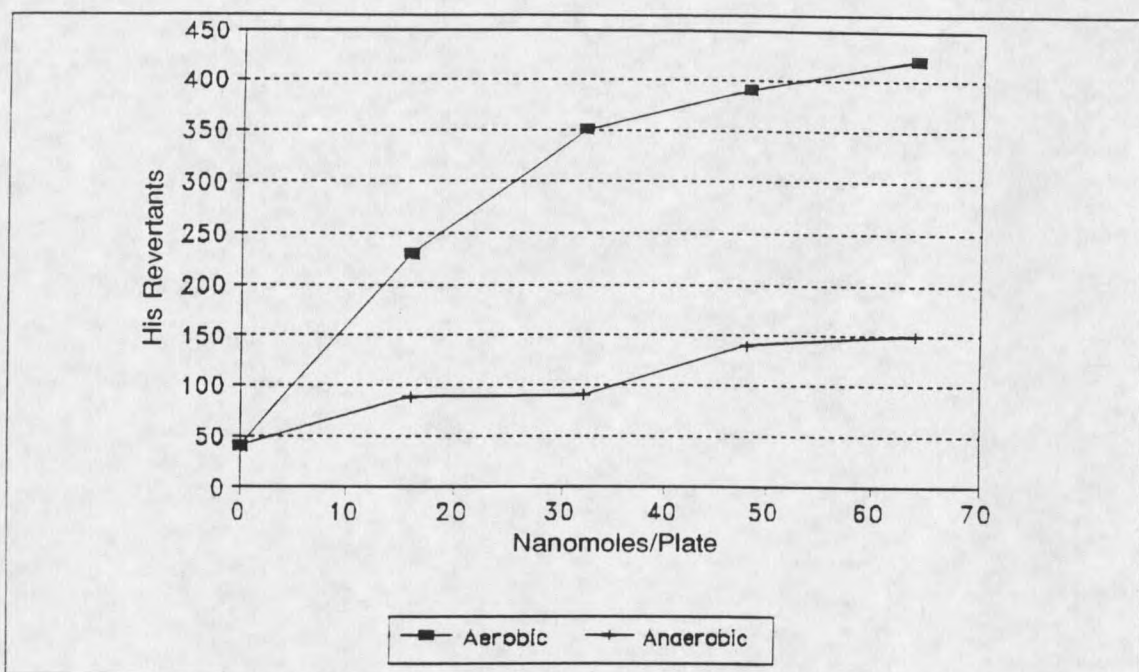


Figure 23: Salmonella reversion assay of Cr(VI) both aerobic and anaerobic in TA2638.

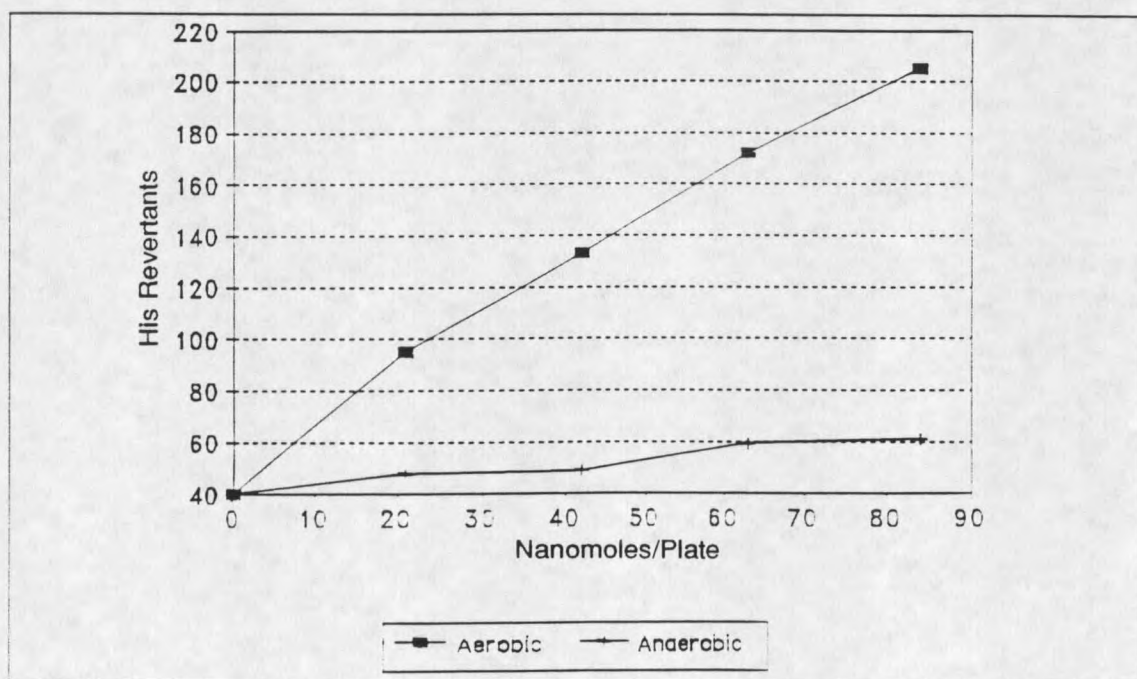


Figure 24: Salmonella reversion assay of a representative Cr(III) complex both aerobic and anaerobic in TA2638.

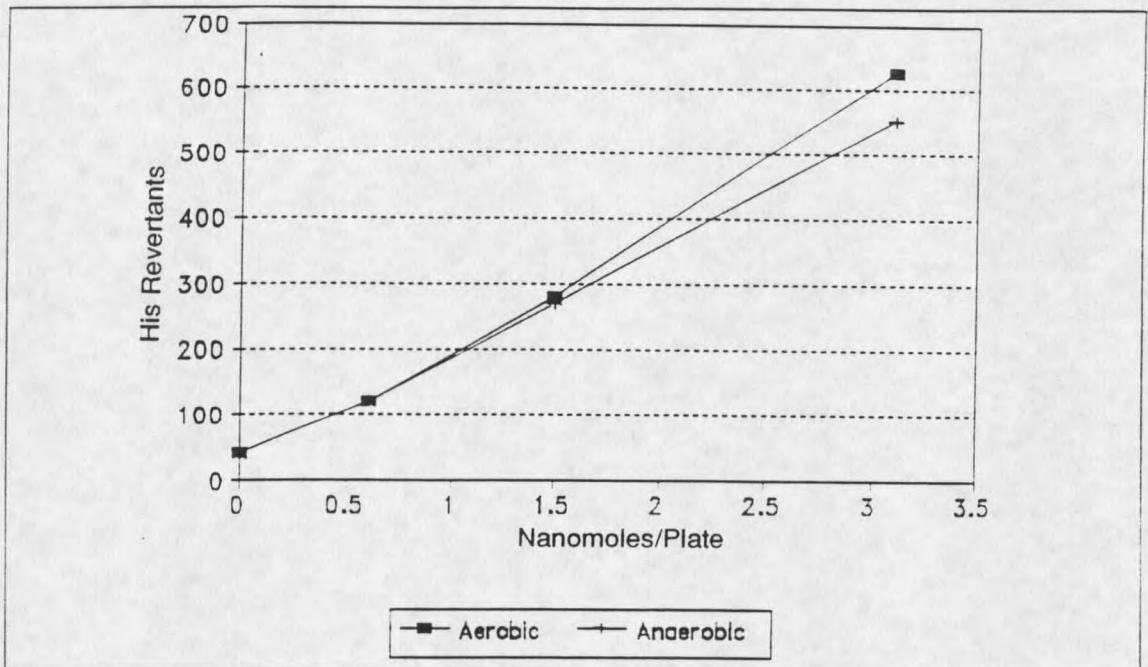


Figure 25: Salmonella reversion assay of MNNG both aerobic and anaerobic in TA2638.

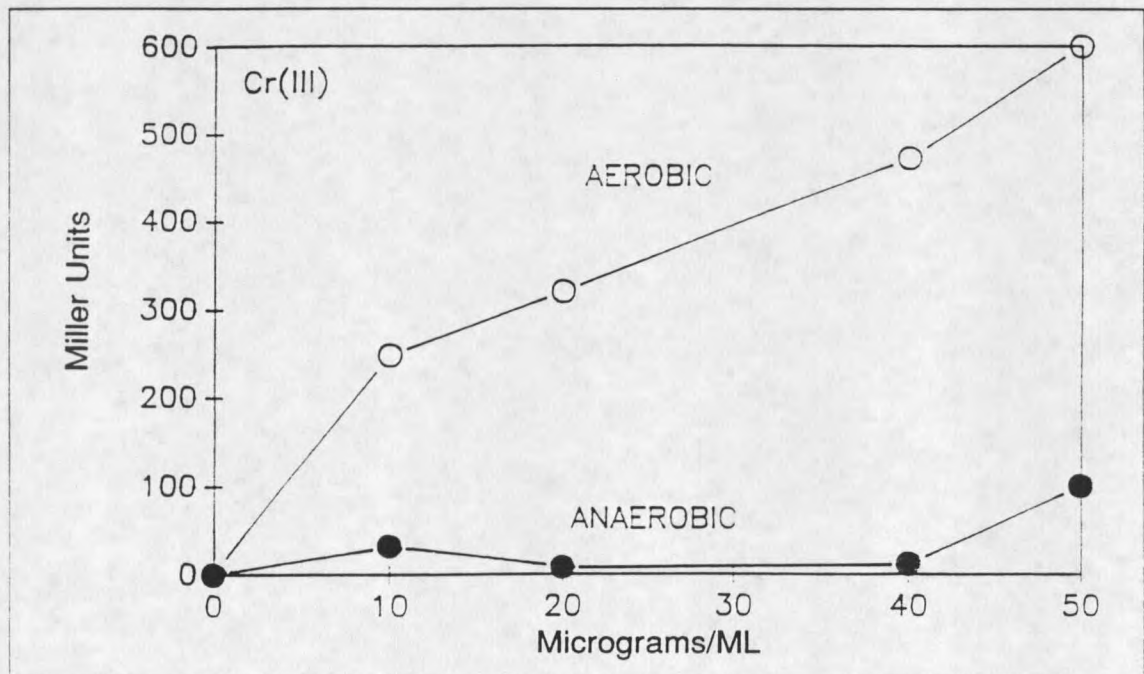


Figure 26: SOS response of a representative Cr(III) complex both aerobic and anaerobic with GE-94.

Because of the obvious ligand dependence on biological activity in the Cr(III) complexes, a series of compounds have been synthesized and tested to determine what effects certain structural changes may exert on the mutagenic complexes. The structural themes tested are changes in the *cis* halogen ligands and substituent effects of substituted bipyridyls.

The changes in the *cis* halogen ligands were measured using the same bis bidentate bipyridyl complex, shown to be mutagenic previously, but with the inner sphere halogen ligands varied between fluorine, chlorine, bromine and iodine. The relative response for these four complexes is illustrated in figures 27 and 28. The revertants/nanomole and fold over background are given in Table II. The results suggest that there is an effective increase in biological activity progressing from fluorine to iodine. While there is very little difference between the bromine and iodine complexes, this may be accounted for by the lower solubility of the iodine complex in the bioassay buffer. These results show a pattern similar to what would be expected if there was a ligand field effect from the spectrochemical series. The effect, however, seems to be reverse of what would be expected since iodine is the least  $\pi$  bonding of all the halogens. This increase in activity for the iodine species is consistent with the predicted model of Tanaka et al., that will be discussed in greater detail in the cyclic voltammetry section.

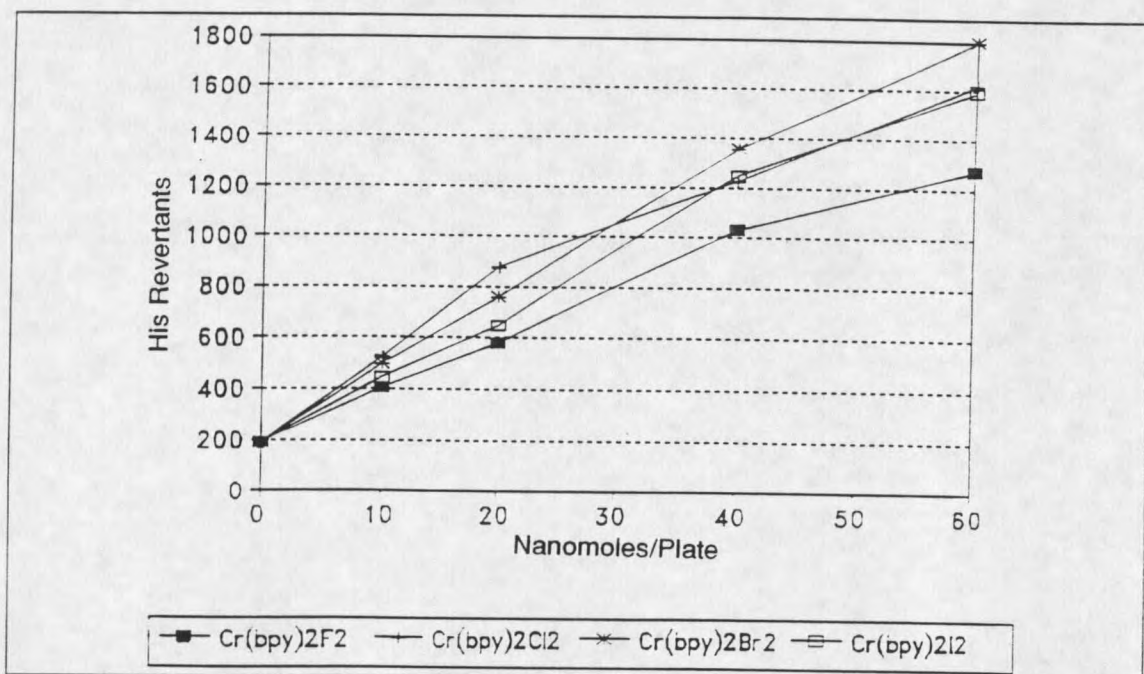


Figure 27: Salmonella reversion assay of the different halogenated complexes of  $\text{Cr}(\text{bpy})_2\text{X}_2$  in TA102.

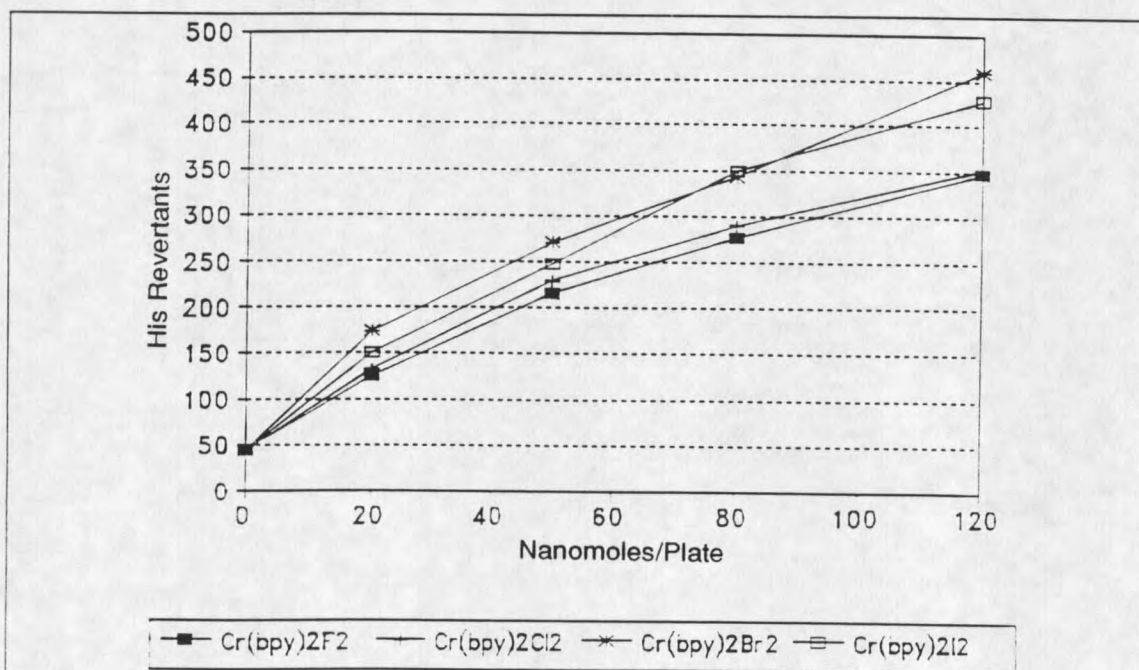


Figure 28: Salmonella reversion assay of the different halogenated complexes of  $\text{Cr}(\text{bpy})_2\text{X}_2$  in TA2638.

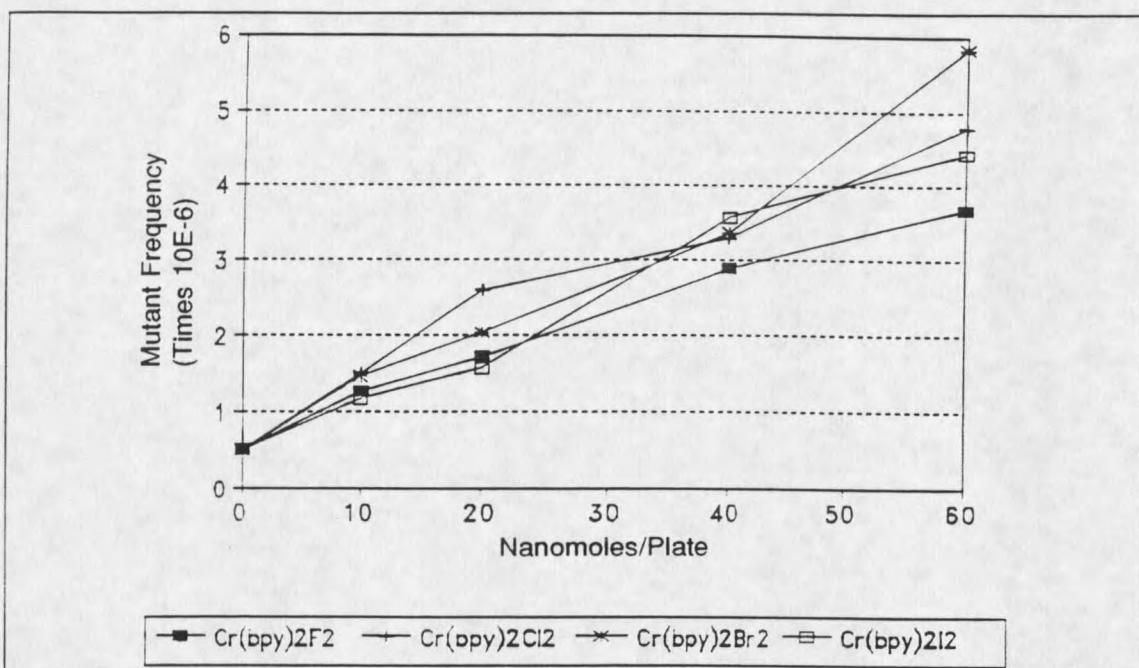


Figure 29: Mutation frequency of different halogenated complexes of  $\text{Cr}(\text{bpy})_2\text{X}_2$  in TA102.

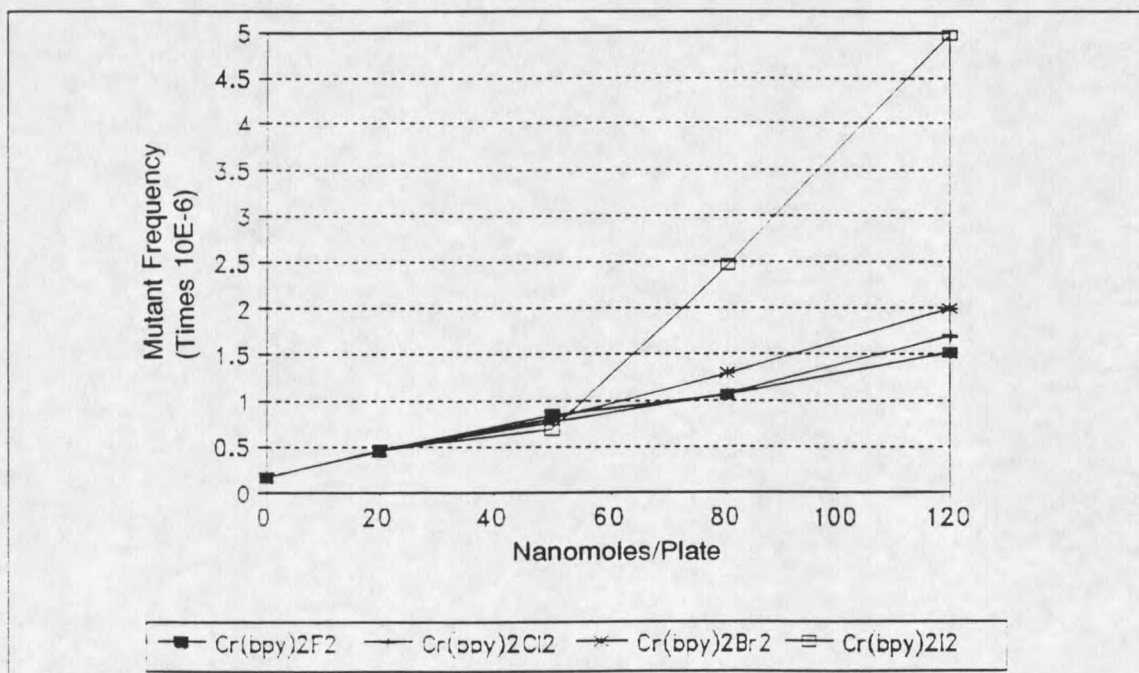


Figure 30: Mutation frequency of different halogenated complexes of  $\text{Cr}(\text{bpy})_2\text{X}_2$  in TA2638.

**Table II** Reversion rate of halogenated bipyridyl complexes.

<u>Complex</u>	<u>Revertants/Nanomole</u>		<u>Fold Over Background</u>	
	<u>TA102</u>	<u>TA2638</u>	<u>TA102</u>	<u>TA2638</u>
Cr(bpy) <sub>2</sub> F <sub>2</sub>	21.3	2.9	6.4	7.6
Cr(bpy) <sub>2</sub> Cl <sub>2</sub>	25.3	2.9	8	7.8
Cr(bpy) <sub>2</sub> Br <sub>2</sub>	30	3.8	9	10.2
Cr(bpy) <sub>2</sub> I <sub>2</sub>	26.7	3.5	8	9.6

Once again, the mutation frequency for these complexes was performed to determine if the relative reversion rate was dependent upon toxicity or was a true measure of biological activity, figures 29 and 30. Even though the diiodo species shows a somewhat lower mutation rate in the Salmonella reversion assay, the greater toxicity of this complex demonstrates that the actual biological response is greater than that of the dibromo species. This changes the relative reversion order for these complexes to that which would be predicted. These data, as shown essentially confirm what is seen with the Salmonella reversion assay with the exception of the diiodo species. In the halogenated complexes, most notably in TA2638, the difference between the diiodo and dibromo complexes are made more obvious. The relative reversion rate, however, remains essentially the same,

this being  $I > Br > Cl > F$ .

A series of substituted bis bidentate bipyridyl complexes with *cis* chloride halogen ligands were synthesized, as described previously, and tested for biological activity, figures 31 and 32. The revertants/nanomole and fold over background are given in Table III. Four bipyridyl complexes, two with electron withdrawing substituents and two with electron donating substituents were tested. The substituents were disubstituted at the 4 and 4' position of the bipyridyl and consisted of methyl and dimethylamino groups for the electron donating compounds and carboxy and methylester groups for the electron withdrawing compounds. The results of the Salmonella reversion assays are quite revealing, if somewhat confusing. As one would expect for a redox cycling complex, the electron donating substituents of the bipyridyl complexes both show activity. An unexpected result was that the bipyridyl complexes with electron withdrawing substituents show no significant biological activity in this same concentration range. An even more unexpected result was that neither of the two active, electron-donating bipyridyl complexes had an activity as great as that of the unsubstituted bipyridyl complex. The predicted model for redox cycling would say that the closer to the electronic state of Cr(II) that you could achieve, the easier this complex should be able to cycle between the two oxidation states and thus the activity should be increased, i.e. the transition state barrier should be lower. Since the electron donating substituents should increase the electron density seen by the chromium metal, it was believed that this should lower this transition state barrier.

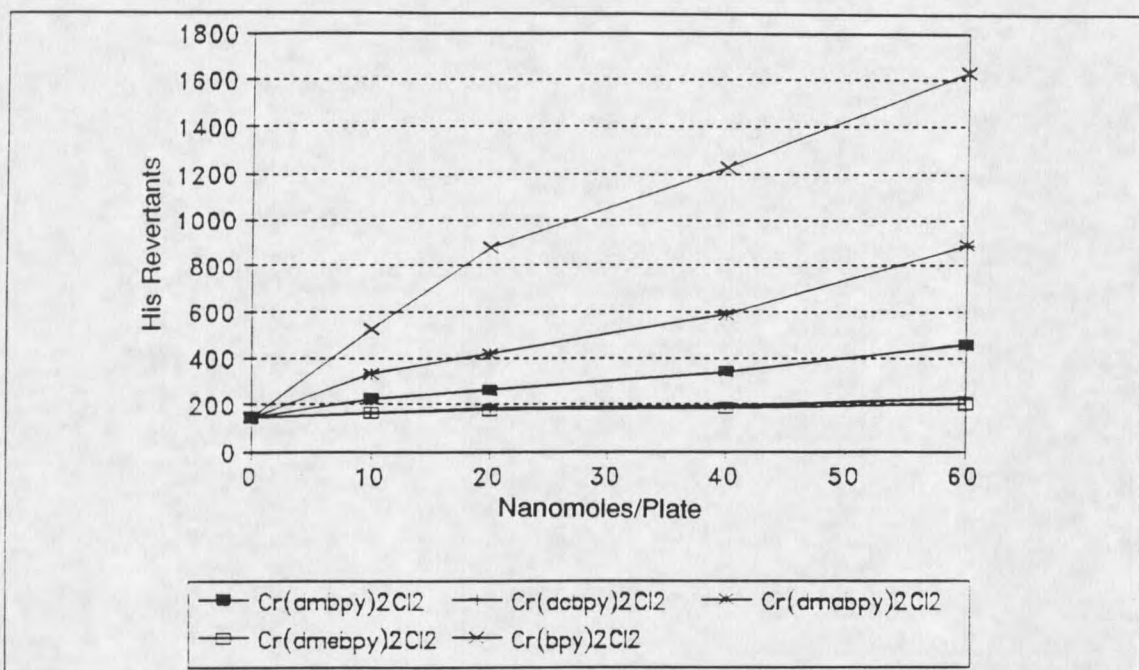


Figure 31: Salmonella reversion assay of substituted bipyridyl complexes of Cr(III) in TA102.

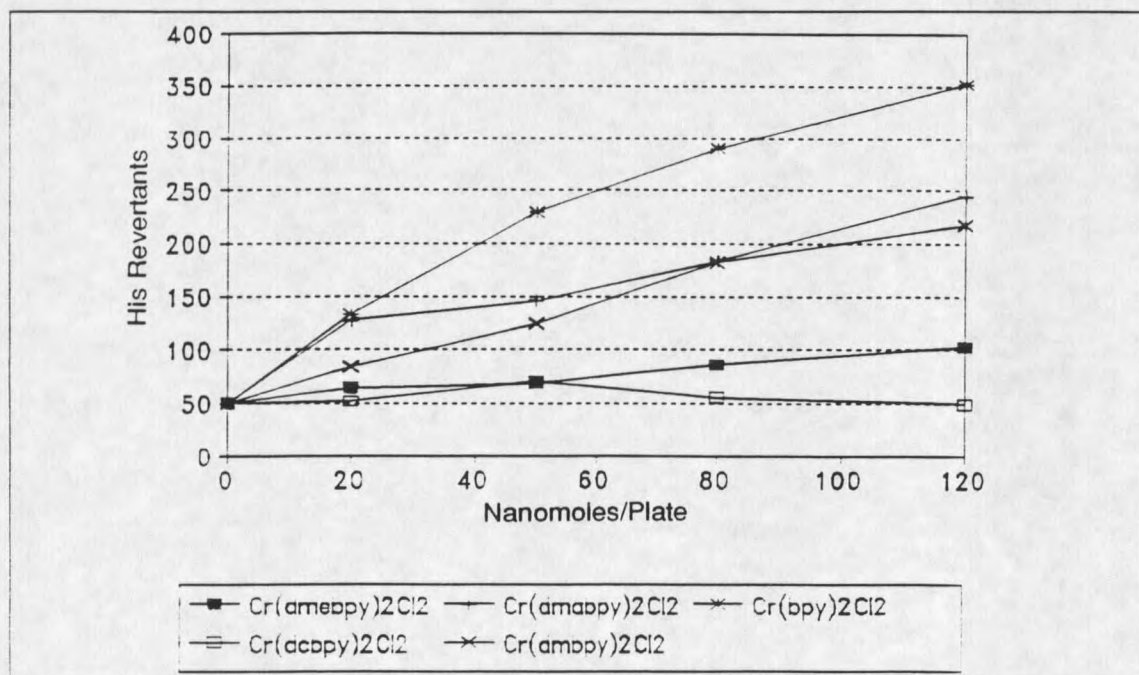


Figure 32: Salmonella reversion assay of substituted bipyridyl complexes of Cr(III) in TA2638.

This, however, is not what is observed. Among the substituted bipyridyls themselves, it does appear to hold true since the reversion order decreases as the electron donating capability decreases,  $-\text{N}(\text{CH}_3)_2 > -\text{CH}_3 > -\text{COOH} > -\text{COOCH}_3$ . The complex that contradicts this model is the unsubstituted bipyridyl compound. This contradiction, however, may be purely superficial since electron donation has been predicted to have little effect on the chromium metal center as postulated previously by Herzog.<sup>90</sup> If this is true, there must be some effect that would account for the lack of activity seen for the electron withdrawing substituents. Other variables, such as membrane permeability and DNA interactions may account for some of these differences. The simplest theory to account for this could be that ligand electronic effects have very little to do with the actual activity and that it is purely the geometric constraints imposed by these rigid bidentate ligands that control the activity.

If geometric constraints account for the activity, another problem arises when explaining the results of the differential reversion frequency in the halogenated bipyridyl complexes. The differences seen are explained by the splitting of the octahedral geometry by differences in the spectrochemical series. While it can be argued that the lack of the predicted effect in the substituted bipyridyls precludes an electronic argument, the cis halogen ligands may have a different type of orbital overlap that controls the activity. Instead of a  $\pi$ -orbital overlap, the halogens may influence the activity through a  $\sigma$ -overlap. This would account for the different effects seen for the halogenated complexes. This, then

raises the further question of what exactly is the role of the bis-bidentate aromatic amine ligands. As discussed previously, it may be that these ligands simply serve for structural rigidity to forbid large distortions of the geometry that would result in irreversible redox kinetics. Or, it may be a rare combination of electronic and structural contributions whose optimum resides with the unsubstituted bipyridyl complexes. Further discussion of this point will be carried out in the section on cyclic voltammetry.

To assure that the response observed in the Salmonella reversion assay was not due to differential cytotoxicity, mutant frequencies were carried out on the different substituted bipyridyl complexes, figures 33 and 34. The mutant frequency is the number of viable mutant colonies per number of cells. This assay, as described previously, assures that a highly toxic compound, that may have a significant mutagenic potential, is not giving spuriously low colony counts resulting from killing of the bacteria. In the substituted bipyridyls, no changes in the relative reversion rate over the Salmonella reversion assay are seen.

Not all complexes that give a positive biological response in prokaryotic systems show the same response in eukaryotic systems. The different physiology and morphology between prokaryotes and eukaryotes can give ambiguous and conflicting results. For example, the anti-fungal compound Dexon is mutagenic in bacteria and yeast but is inactive in mammalian cells due to the presence of an azoreductase enzyme which effectively degrades it to a biologically inert form.<sup>97</sup> Morphological changes such as different membranes and transport systems

between the two cell types have the potential to preclude intracellular access to DNA. These factors make extrapolating between what is observed in prokaryotic systems into eukaryotic systems hazardous at best. The only true test for crossing over of the systems is to run a eukaryotic mutagenesis assay.

Two of the complexes shown to be mutagenic in Salmonella,  $[\text{Cr}(\text{phen})_2\text{Cl}_2]^{+1}$  and  $[\text{Cr}(\text{bpy})_2\text{Cl}_2]^{+1}$ , have been tested against two mammalian cell lines for both mutagenesis and toxicity. These cell lines are the human TK6 cell line (thymidine kinase) and the CH (Chinese Hamster) cell line V79. The results of these tests are given in Table IV. Using Cr(VI) as the control, it was shown that the Cr(III) complexes have an approximately equivalent level of mutagenicity as Cr(VI) in these same cell lines. However, the toxicity appears to be even greater than that of the Cr(VI) compound used. One of the interesting aspects of

**Table III** Relative reversion rates of substituted bipyridyls.

<u>Complex</u>	<u>Revertants/Nanomole</u>		<u>Fold Over Background</u>	
	<u>TA102</u>	<u>TA2638</u>	<u>TA102</u>	<u>TA2638</u>
$\text{Cr}(\text{dmbpy})_2\text{Cl}_2$	7.5	1.8	2.5	4.4
$\text{Cr}(\text{dcbpy})_2\text{Cl}_2$	3.5	0.42	1.2	1
$\text{Cr}(\text{dmabpy})_2\text{Cl}_2$	15	2.1	5	5
$\text{Cr}(\text{dmebpy})_2\text{Cl}_2$	3.5	0.83	1.2	2

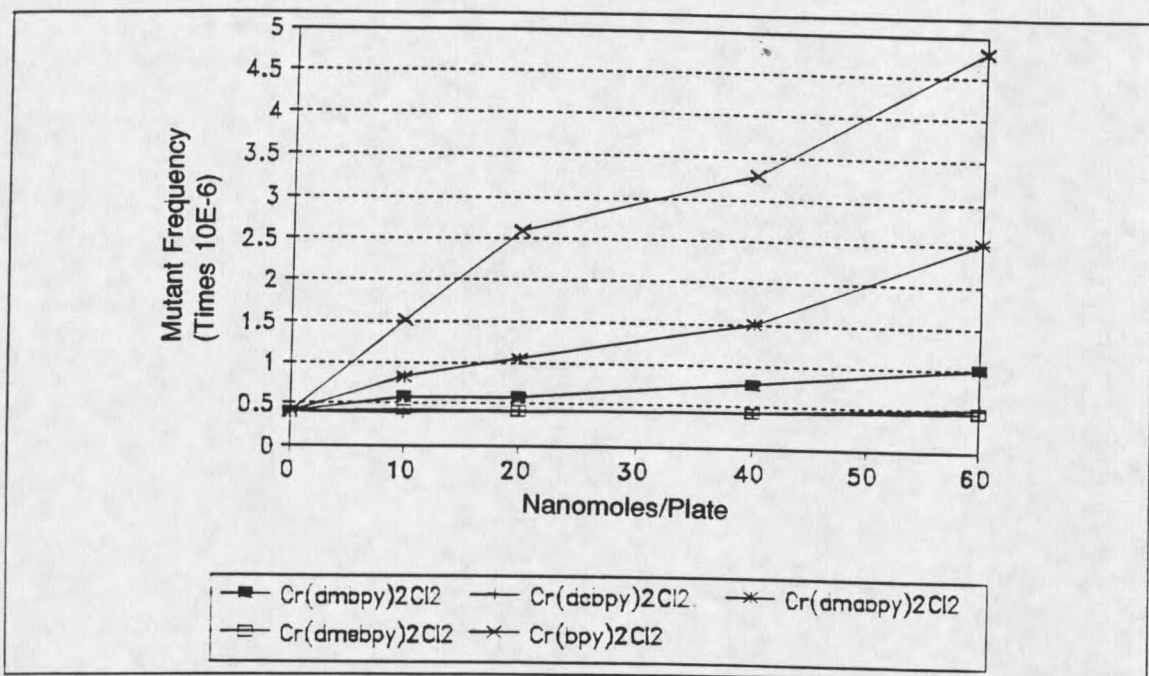


Figure 33: Mutation frequency of substituted bipyridyl complexes of Cr(III) in TA102.

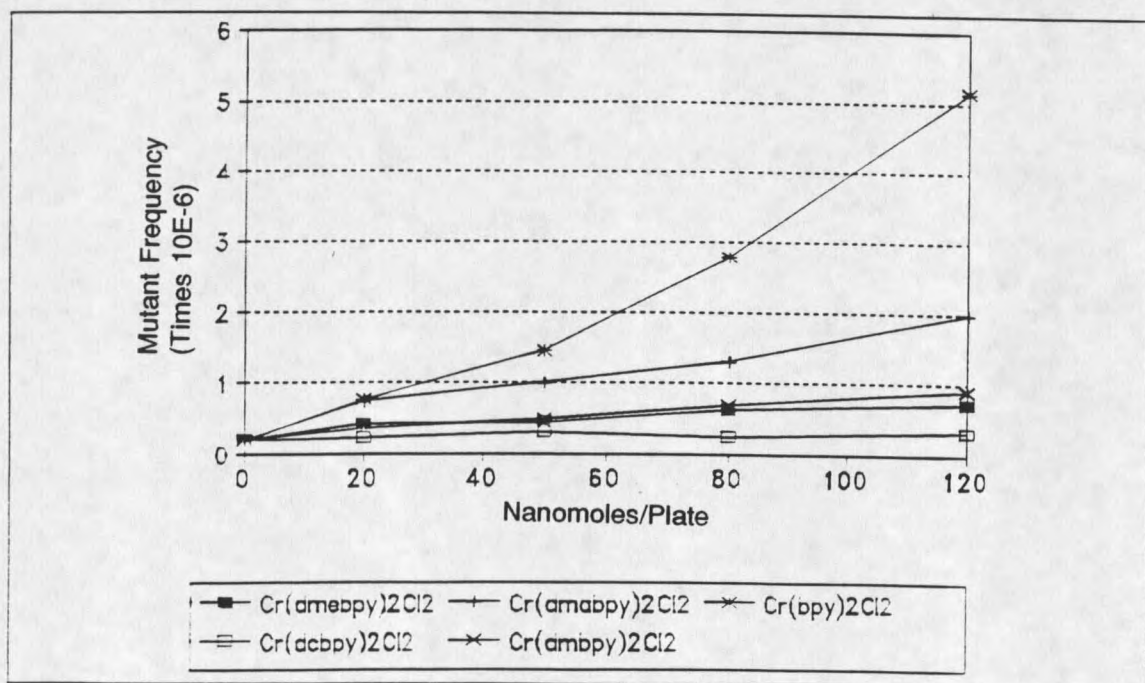


Figure 34: Mutation frequency of substituted bipyridyl complexes of Cr(III) in TA2638.

this data is the differential activity between the two Cr(III) species. One of the complexes,  $\text{Cr}(\text{bpy})_2\text{Cl}_2$ , shows significantly more activity towards one of the cell lines than the other. When compared to the prokaryotic *Salmonella* strains, you see that the reversion order is reversed for these two complexes. In the *Salmonella* reversion assay, the  $\text{Cr}(\text{phen})_2\text{Cl}_2$  species has a greater activity. In the eukaryotic system, and especially in the CH V-79 cells, the  $\text{Cr}(\text{bpy})_2\text{Cl}_2$  species demonstrates a greater activity. This specificity towards one or the other cell lines is interesting but the exact significance is speculative. It may be that there is a DNA damaging specificity between these two complexes relating to different cell types. The differences seen between the two mammalian cell lines may be explained on a genetic basis since two different genetic targets are being assayed. The human TK6 cell line assays for damage to the thymidine kinase gene. This gene codes for a protein that is in the salvage pathway for deoxyribonucleotide synthesis. The justification for use of this gene as a mutational target, is that the level of protein synthesis is high in rapidly dividing cells such as cancer cells. The V79 CH cell line has the HGPRT locus as the mutational target. This target site is the gene that codes for the hypoxanthine-guanine phosphoribosyltransferase protein. This protein, as well, is a salvage pathway enzyme that is essential for purine metabolism. A major difference between these two genes is that the CH HGPRT gene is a haploid sex-linked gene located on the X chromosome while the thymidine kinase is a diploid somatic gene. It is this difference between the two mutational sites that may explain the differences observed.

In the human TK6 cell line the activity of the two complexes are approximately equivalent but in the CH V-79 cell line, the  $\text{Cr}(\text{bpy})_2\text{Cl}_2$  complex shows nearly twice the activity. This could be due to the specificity of interaction between the two complexes. Specifically, since the CH V-79 mutational site is on a single strand, any compound that interacts with DNA could direct that radical production in one direction or another to either increase or decrease the mutation rate on that strand. A compound which interacts in a much less specific manner, should distribute the mutation rate equally between both complimentary strands of DNA. In the TK6 cell line, both strands of DNA contain the gene coding for this protein. Thus, if you have two compounds of roughly equivalent activity but with one having site specificity and the other a more general interaction, the mutation rate should be roughly equivalent. This theory is supported by work which will be discussed in greater detail in the metal-DNA interaction section of this thesis.

Table IV: Mammalian Toxicity and mutagenesis of selected chromium compounds.

<u>Complex</u>	<u>Human TK6</u>			<u>CH V-79</u>		
	<u>[<math>\mu</math>M]</u>	<u>%Surv</u>	<u>Mut. Freq.</u>	<u>[<math>\mu</math>M]</u>	<u>%Surv</u>	<u>Mut Freq.</u>
Cr(VI)	0.1	85	8E-06	50	65	7.9E-06
	0.5	83		100	48	5.5E-06
	2	50		150	39	9.1E-06
	10	2.7		200	41	1.5E-05
	50	0				
Cr(bpy) <sub>2</sub> Cl <sub>2</sub>	2	137	3.8E-06	250	50	4.8E-05
	5	87		500	40	
	10	88		1000	30	
	20	67		1500	25	
	40	0		2000	25	
Cr(phen) <sub>2</sub> Cl <sub>2</sub>	1.8	83	3.5E-06	500	70	2.9E-05
	3.8	77		1000	45	
	9	66		2000	40	
	18	0				
	36	0				

### Membrane Permeability

Results of the membrane permeability study on a series of mutagenic and nonmutagenic compounds in a eukaryotic cell system (Chinese Hamster Lung Fibroblasts) demonstrate that, unlike previously suggested, the aromatic amine ligands do not enhance transport across the cell membrane, figure 35. In fact, all nonmutagenic Cr(III) complexes, with the exception of CrCl<sub>3</sub>·6H<sub>2</sub>O, used in this study have shown enhanced transport over the mutagenic Cr(III) complexes, figure 36. In certain cases, Cr(NH<sub>3</sub>)<sub>4</sub>Cl<sub>2</sub>, the nonmutagenic complexes had a 100-fold increase in membrane permeability over the mutagenic complexes. CrCl<sub>3</sub>·6H<sub>2</sub>O,

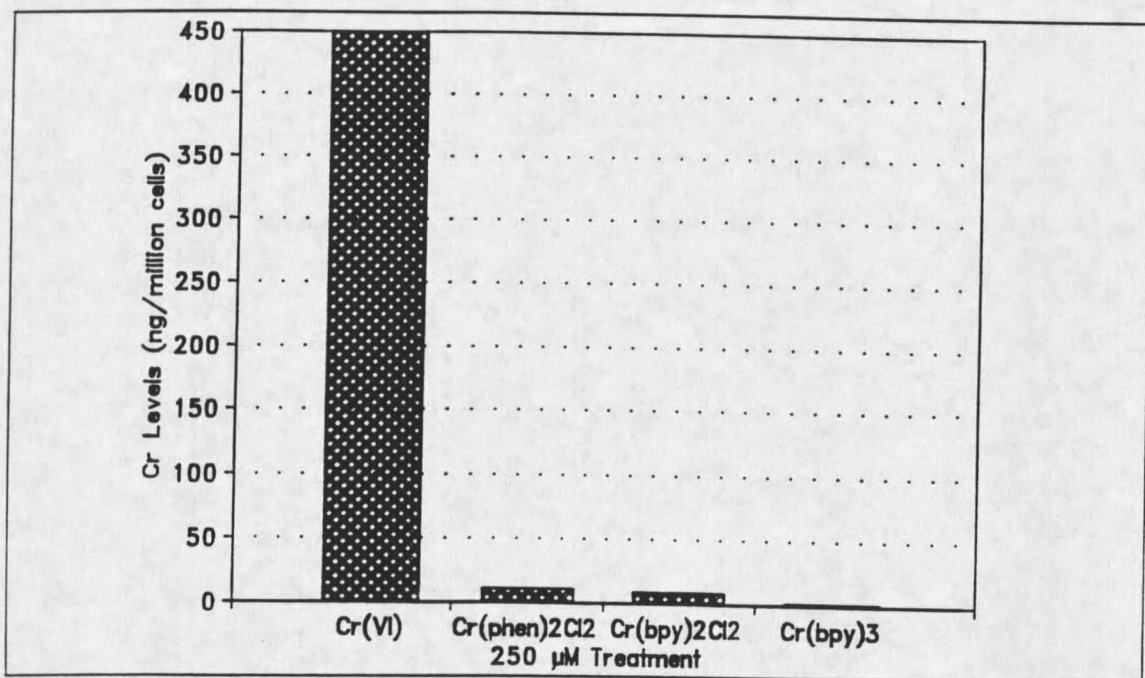


Figure 35: Membrane permeability of mutagenic chromium compounds in mammalian cells.

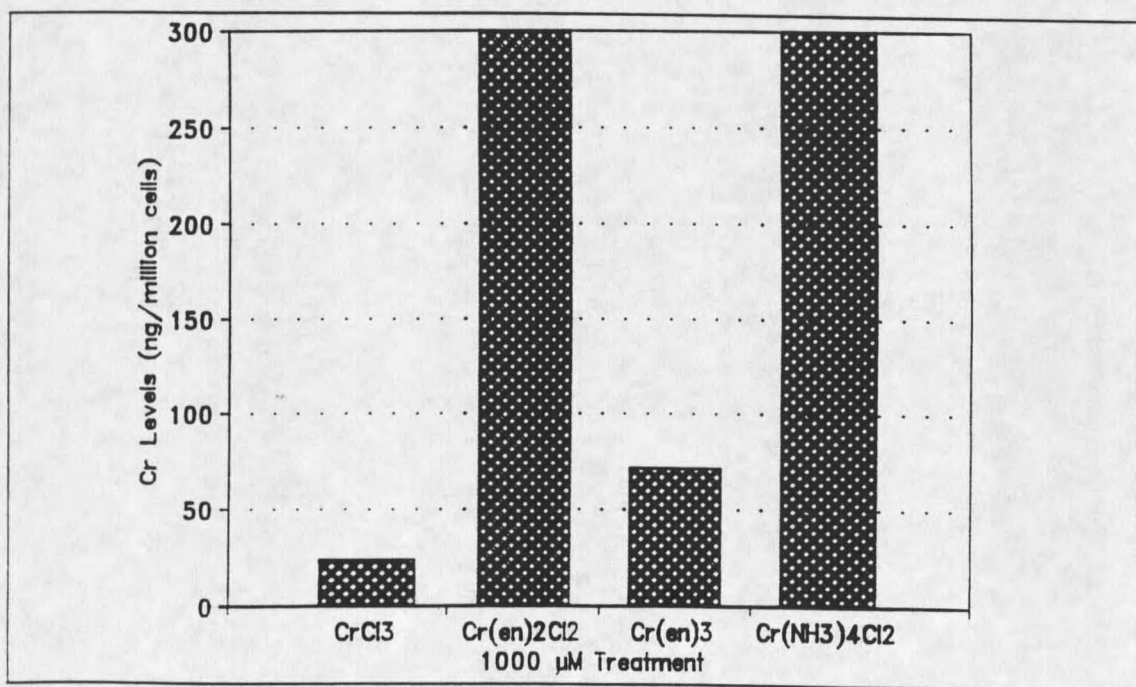


Figure 36: Membrane permeability of nonmutagenic Cr(III) complexes in mammalian cells.

a nonmutagenic complex that is the classic example for poor cellular uptake in the selective uptake/reduction model of Cr(VI) mutagenesis, shows a level of uptake similar to that of the mutagenic species, while Cr(VI) shows a level that is even slightly lower than that of the nonmutagenic Cr(III) complex with the greatest uptake. It has been postulated that the charge on a complex influences the ability to cross the plasma membrane. In this study, there appears to be little correlation of membrane permeability with the charge on the complex. Both the +3 and +1 charged complexes demonstrated an ability to cross the plasma membrane. The exact method by which these complexes get across the membrane, active or passive transport, cannot be determined from this study. Some correlation with membrane permeability may exist for the polarity of the ligand and cellular uptake. The more hydrophobic ligands, phenanthroline and bipyridyl, show the lowest degree of membrane permeability while the most polar,  $\text{NH}_3$ , shows the greatest degree of permeability.

Whether or not this same type of cellular uptake is occurring in the prokaryotic *Salmonella* strains is unknown. However, the similarity of activity between the Cr(III) species measured in the prokaryotic and eukaryotic systems versus that of the Cr(VI) species suggests that this may be true. Further phenomenological evidence for poor uptake of the mutagenic complexes is shown in figure 37. This figure demonstrates that when an 8.0% solution of DMSO (dimethylsulfoxide) in water is added to solubilize the Cr(III) metal complex, the result is increased mutagenicity in the *Salmonella* reversion assay. DMSO is

known for its ability to influence cellular uptake and thus, the significant increase in mutation seen with this assay correlates directly with the membrane permeability data in the eukaryotic system.

These data support a model for specific ligand/chromium interactions that directly influence the biological activity of these compounds and not a mechanism based solely on cellular uptake. This does not mean that membrane permeability has no influence on biological activity. Obviously, if a putative mutagen cannot cross the cellular membrane it cannot damage the DNA. A differential ability to cross this membrane may account for many of the differences observed between the mutagenic species, but it is obviously not a limiting factor in the induction of mutagenesis by these complexes.

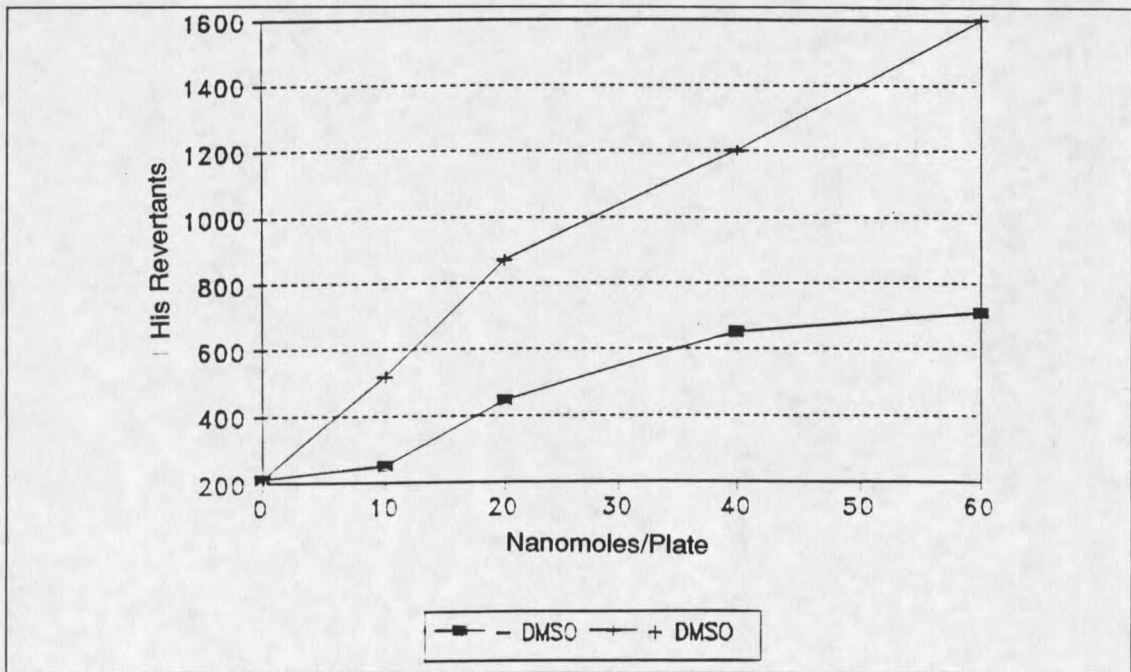


Figure 37: DMSO induced uptake in relation to mutation rate.

### Cyclic Voltammetry

Cyclic voltammetry was employed to investigate the redox kinetics of the chromium complexes. To invoke an oxygen radical mechanism of DNA damage for the mutagenic complexes, requires that these complexes must be able to function as cyclical electron donors. This in turn implies that these complexes must have a reversible redox couple to allow them to cycle between two "stable" oxidation states. Information obtained from the cyclic voltammeter allows you to compare and contrast both the reduction potentials of the complexes as well as the reversibility of the redox couples.

Cyclic voltammetry and polarography of chromium(III) complexes have been investigated in a number of previous studies. Specifically, the complexes of Cr(III) with 2,2'-bipyridyl have been investigated because of their reversibility in aqueous solvents.<sup>98-101</sup> This is in contrast to most Cr(III) complexes that have shown irreversible redox kinetics under aqueous conditions.<sup>102-103</sup>

Comparison of reduction potentials, reversibility and structural changes which accompany redox reactions can be made between the compounds using cyclic voltammetry. The fate of a compound can be determined by generating a new redox species on the forward (negative) scan and exploring the redox couple and chemical stability on the reverse (positive) scan. Chemical reversibility occurs when the electronic and geometric structure of the reactant and the product are similar. This similarity can be brought about by the solvent or by the nature of the ligand. Figure 38 shows a single scan cyclic voltammogram for the known oxygen

radical generator paraquat. Determination of a formal reduction potential is typically made by taking the average of the forward (reduction) and return (oxidation) waves. This approximation, however, is only accurate for reversible systems. A reversible system is defined as a reaction that is fast enough to maintain the concentrations of the reduced and oxidized forms of the analyte in equilibrium at the electrode surface. The separation between the two peak potentials,  $\Delta E_p$ , (where  $\Delta E_p = E_{pc} - E_{pa}$ ), in a reversible electron transfer process should be close to  $58/n$  mV, where  $n$  is the number of electrons transferred. However, many systems will display reversibility when the voltage is scanned slowly but at increasing scan rates,  $\Delta E_p$  will be greater than  $58/n$ . Reversibility can then be viewed as a matter of degree depending on a variety of factors that are both compound and environment specific. Determination of the half-wave potential ( $E_{1/2}$ ), which roughly corresponds to the formal electrode potential ( $E^\circ$ ), can be made off the cyclic voltammogram by reading the potential where the current is half the value of the peak current  $i_{pc}$ . This is the half-peak potential,  $E_{p/2}$ , that is related to the  $E_{1/2}$  by the following equation (9).

$$E_{p/2} = E_{1/2} \pm 28.0/n \text{ mV (sign is positive for a reduction)} \quad (9)$$

Chemically irreversible reactions are those that yield products that cannot electrochemically regenerate the original reactant. The lack of a return peak and the changing cathodic peak potential,  $E_{pc}$ , with scan rate precludes an accurate reduction potential calculation using the above method. The relationship between

reversibility and shifts in the reduction potential can be represented using a reaction coordinate diagram, figure 39. The reduction potential  $E_{1/2}$  is dependent on the amount of energy needed in the system to bring the electronic state of the oxidized compound to the same electronic state of the reduced compound. There still exists, however, a barrier relating to fluctuations in the nuclear geometry of the complex that are controlled by the Franck-Condon principle. The Franck-Condon principle states that nuclear motions are slow in comparison to electron motion and at all times during a reaction, the rearrangements of the atomic geometry control the electronic state of the molecules. The height of this barrier, and the possibility of a competing reaction for the reduced species is what controls the reversibility of the reaction.

Chromium(III) is considered an inert metal complex. This classification is due to the  $d^3$  orbitals that result in a 12dq ligand field stabilization energy. A reduction, to the  $d^4$  complex of Cr(II), is subject to severe Jahn-Teller distortions. A Jahn-Teller distortion arises when you have nonuniformly filled  $t_{2g}$  or  $e_g^*$  orbitals. In a  $d^4$  complex, regardless of whether it is high spin or low spin, you will see this Jahn-Teller distortion. In Cr(II), the Jahn-Teller distortion tends to force the geometry towards that of the tetrahedral Cu(II) ion. Because this distortion must overcome the crystal field stabilization of the octahedral Cr(III), slow redox chemistry is expected for these complexes. A Cr(III)-ligand complex that results in distortion of the octahedral complex towards that of the Cr(II) complex should thus need less energy to reach the Cr(III)/Cr(II) transition state and the reduction

potential should be more positive.

A less distorted octahedral complex would need more energy applied to the system to overcome this octahedral stabilization energy. A consequence of having to put a large amount of energy into the system can be seen by observing the energy versus reaction coordinate diagram in figure 39. The second transition state hump correlates with a highly energetic, labile Cr(II) molecule interacting with the solvent. In the case of many Cr(II) species, reduced in aqueous solvent, it is apparent that this labile Cr(II) species has the ability to reduce water to  $H^+$  and  $OH^-$  to catalyze the oxidation back to Cr(III). A consequence of this reoxidation, at least in some species, is the formation of insoluble oxide polymers that are unable to participate further in redox reactions.

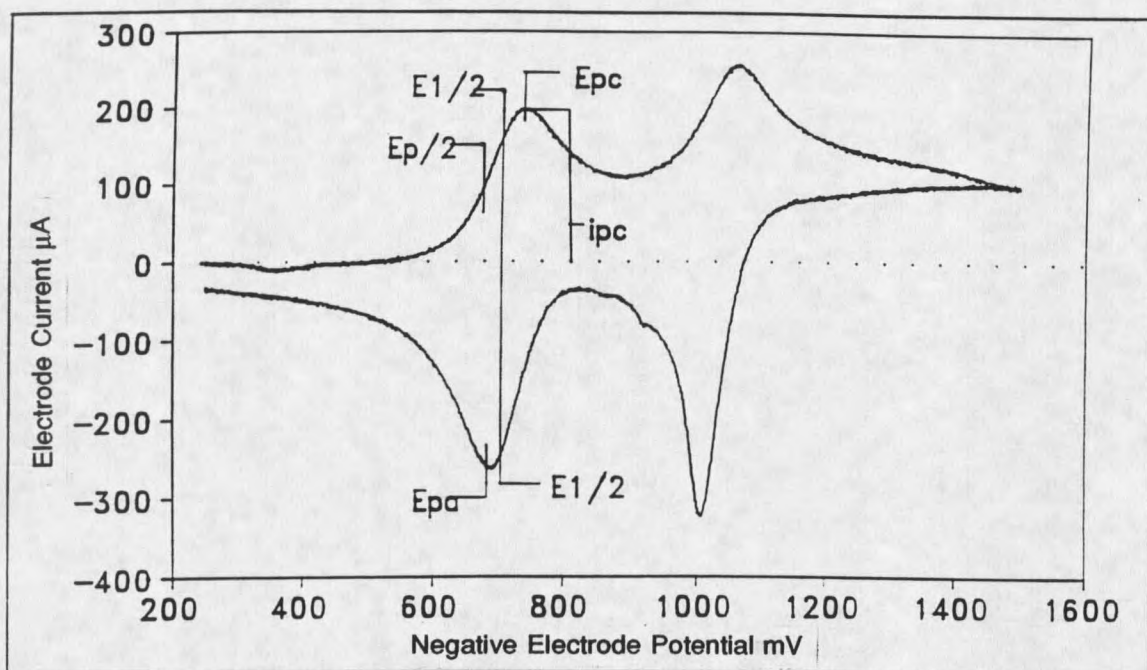


Figure 38: Single scan cyclic voltammogram of paraquat showing potential and current parameters.

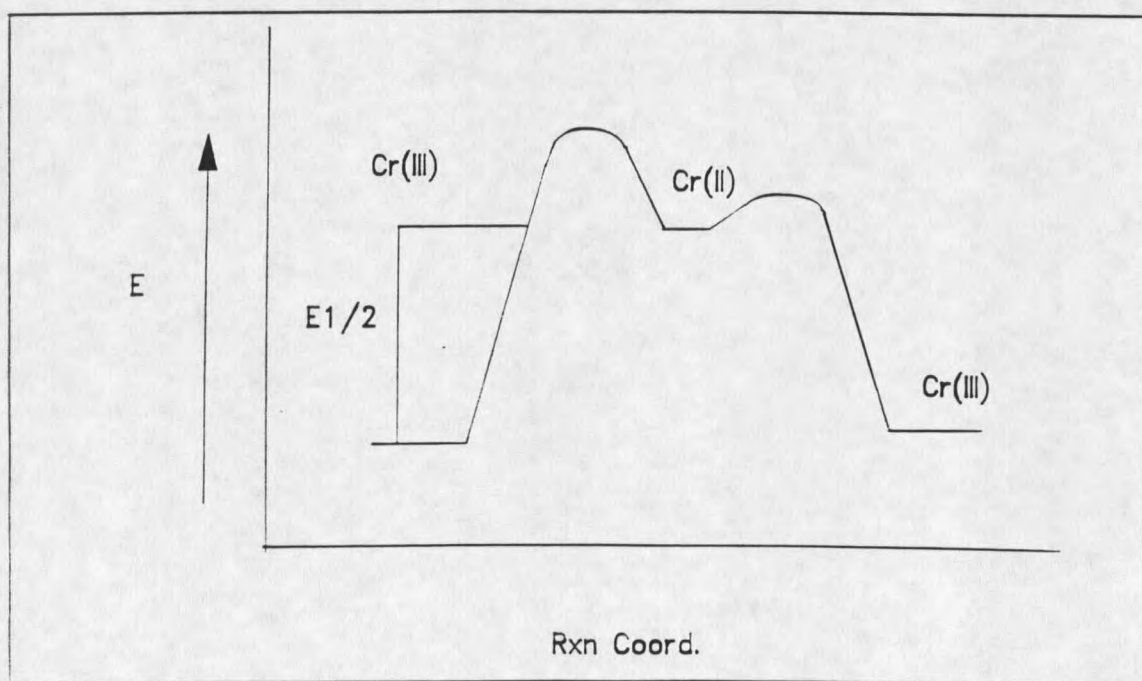


Figure 39: Reaction coordinate versus energy diagram for reversible and irreversible electrochemical reactions.

In this study, cyclic voltammetry was employed to determine if there is a difference in the redox kinetics between the mutagenic and nonmutagenic complexes and how this difference could account for the disparity in biological activity. The model developed from the biological activity data implicates an oxygen radical in the mechanism of damage. To invoke an oxygen radical mechanism of damage for the mutagenic and not the nonmutagenic species, there must be a difference in the redox kinetics between the mutagenic and nonmutagenic Cr(III) species. This difference in redox kinetics should be: 1) positive shifts of the reduction potential into the range of intracellular reductants and 2) reversibility of the Cr(III)/Cr(II) redox couple.

Figures 40, 41, 42, 43 and 44 show the cyclic voltammograms of the original mutagenic species,  $\text{Cr}(\text{phen})_2\text{Cl}_2$ ,  $\text{Cr}(\text{phen})_2(\text{H}_2\text{O})_2$ ,  $\text{Cr}(\text{bpy})_2\text{Cl}_2$ ,  $\text{Cr}(\text{bpy})_2(\text{H}_2\text{O})_2$  and  $\text{Cr}(\text{bpy})_3$ . Cyclic voltammograms for the nonmutagenic complexes,  $\text{Cr}(\text{en})_3$ ,  $\text{Cr}(\text{en})_2\text{Cl}_2$ ,  $\text{Cr}(\text{NH}_3)_4\text{Cl}_2$ ,  $\text{Cr}(\text{py})_4\text{Cl}_2$  and  $\text{Cr}(\text{CN})_6$  are shown in figures 45, 46, 47, 48 and 49. The contrast between the two types of voltammograms shown here, mutagenic versus nonmutagenic, are quite dramatic. In every case, the mutagenic complexes demonstrate both a shift in reduction potential to more positive potentials as well as a degree of reversibility that could be associated with an ability to serve as cyclical electron donors in a Fenton-like reaction. The nonmutagenic complexes on the other hand show either classical chemical irreversibility as seen with  $\text{Cr}(\text{en})_2\text{Cl}_2$ ,  $\text{Cr}(\text{py})_4\text{Cl}_2$  and  $\text{Cr}(\text{NH}_3)_4\text{Cl}_2$  species

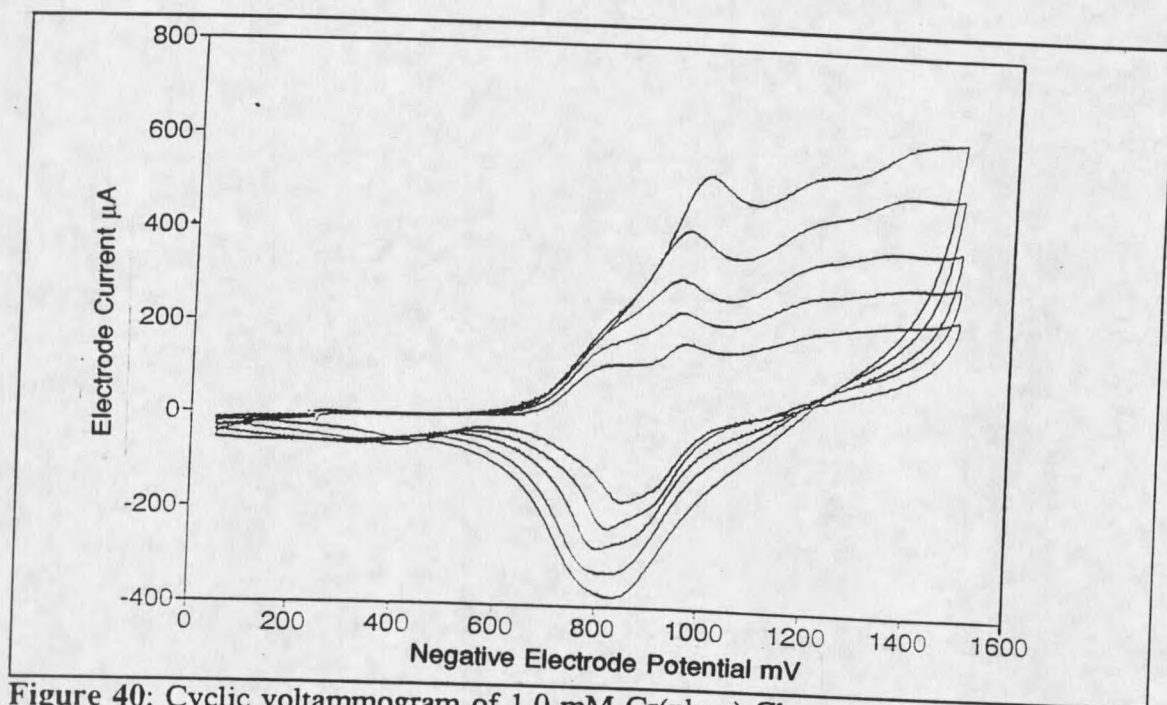


Figure 40: Cyclic voltammogram of 1.0 mM Cr(phen)<sub>2</sub>Cl<sub>2</sub>.

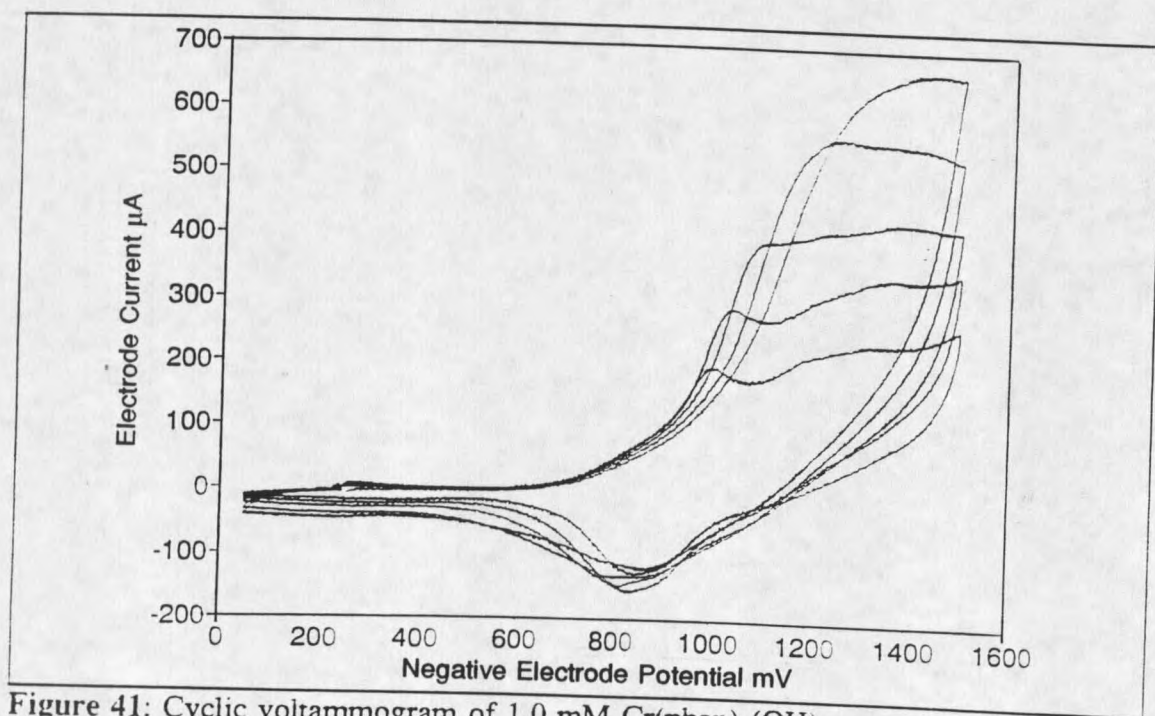


Figure 41: Cyclic voltammogram of 1.0 mM Cr(phen)<sub>2</sub>(OH)<sub>2</sub>.

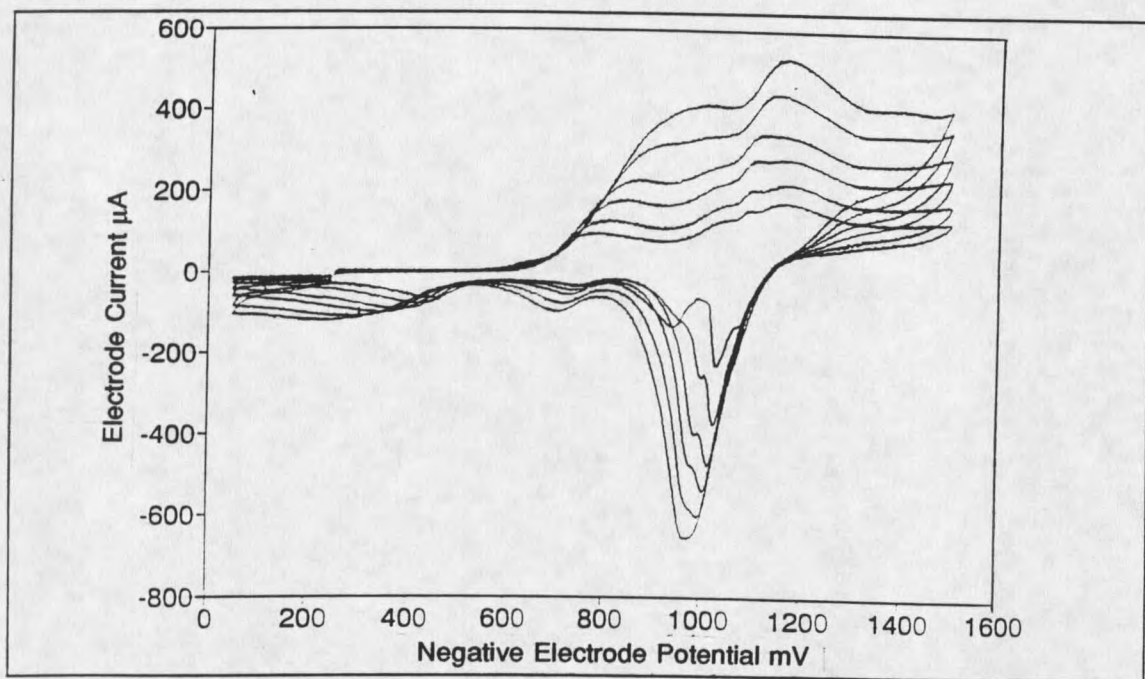


Figure 42: Cyclic voltammogram of 1.0 mM  $\text{Cr}(\text{bpy})_2\text{Cl}_2$ .

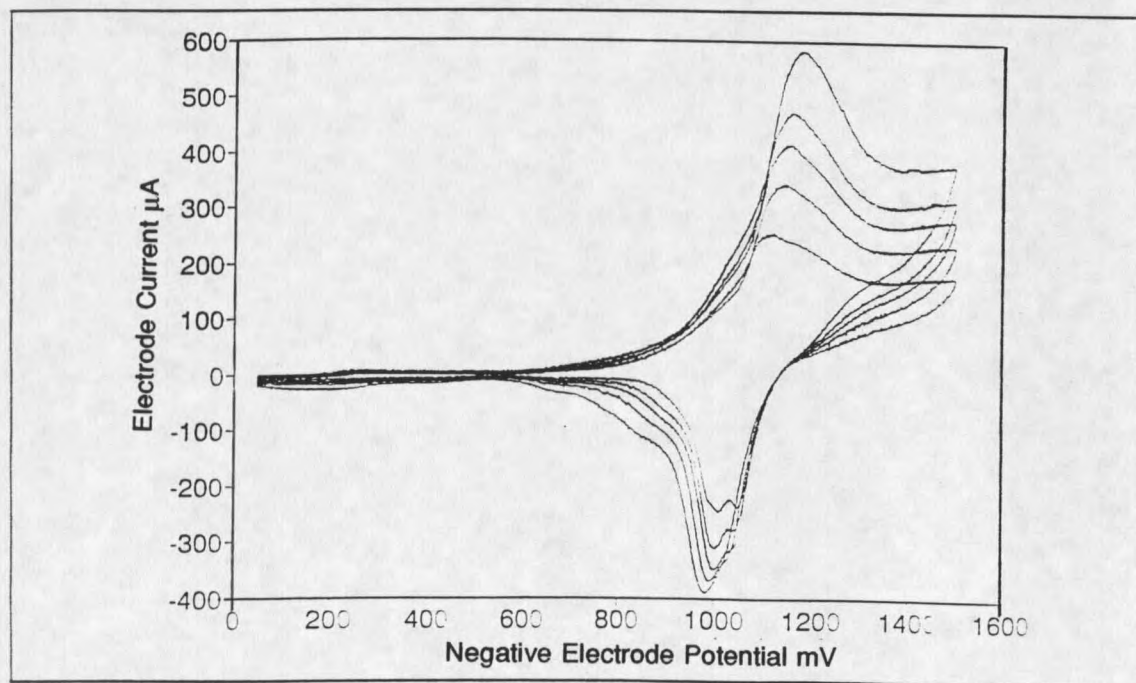


Figure 43: Cyclic voltammogram of 1.0 mM  $\text{Cr}(\text{bpy})_2(\text{OH})_2$ .

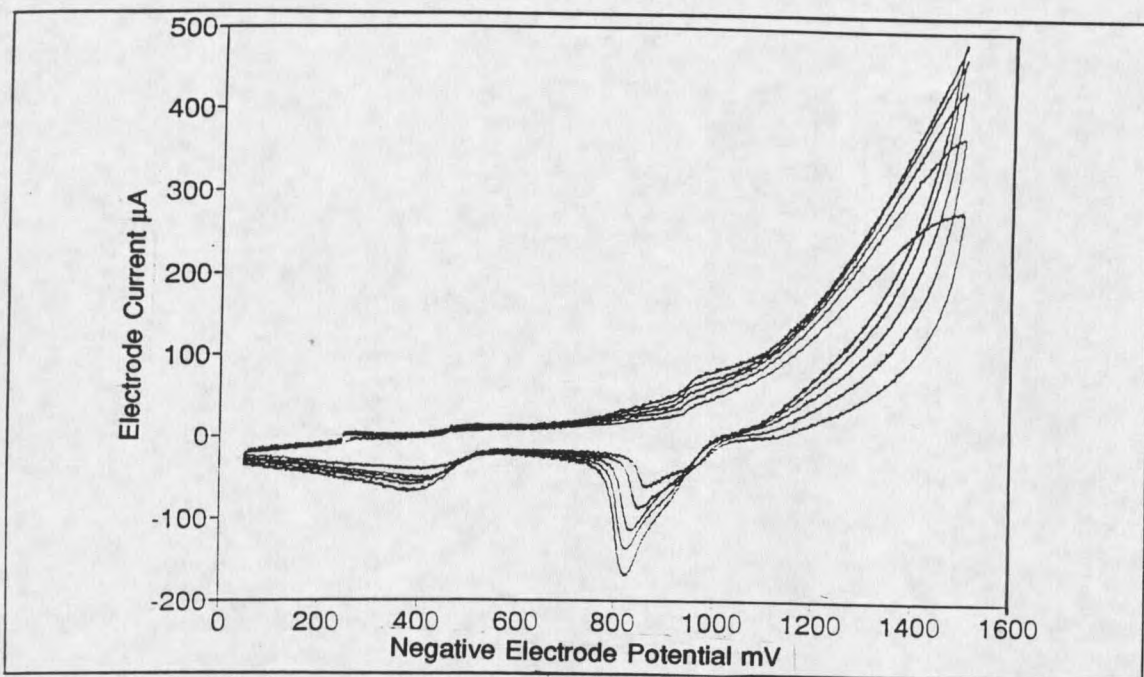


Figure 44: Cyclic voltammogram of 1.0 mM Cr(bpy)<sub>3</sub>.

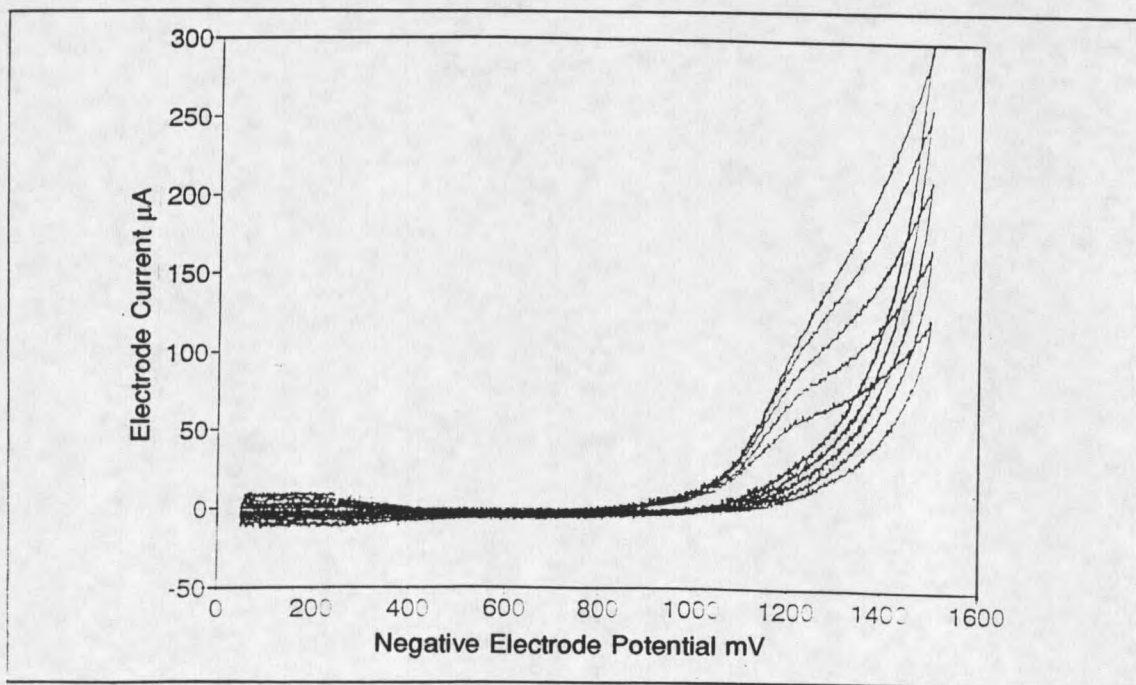


Figure 45: Cyclic voltammogram of 1.0 mM Cr(en)<sub>2</sub>Cl<sub>2</sub>.

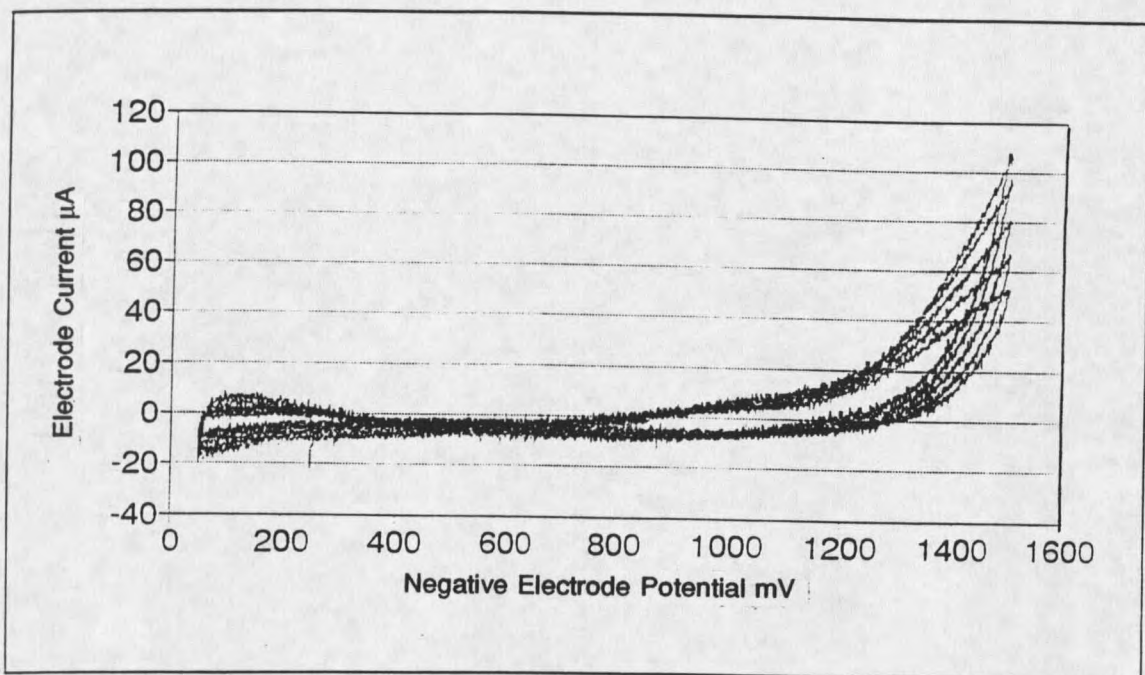


Figure 46: Cyclic voltammogram of 1.0 mM  $\text{Cr}(\text{en})_3$ .

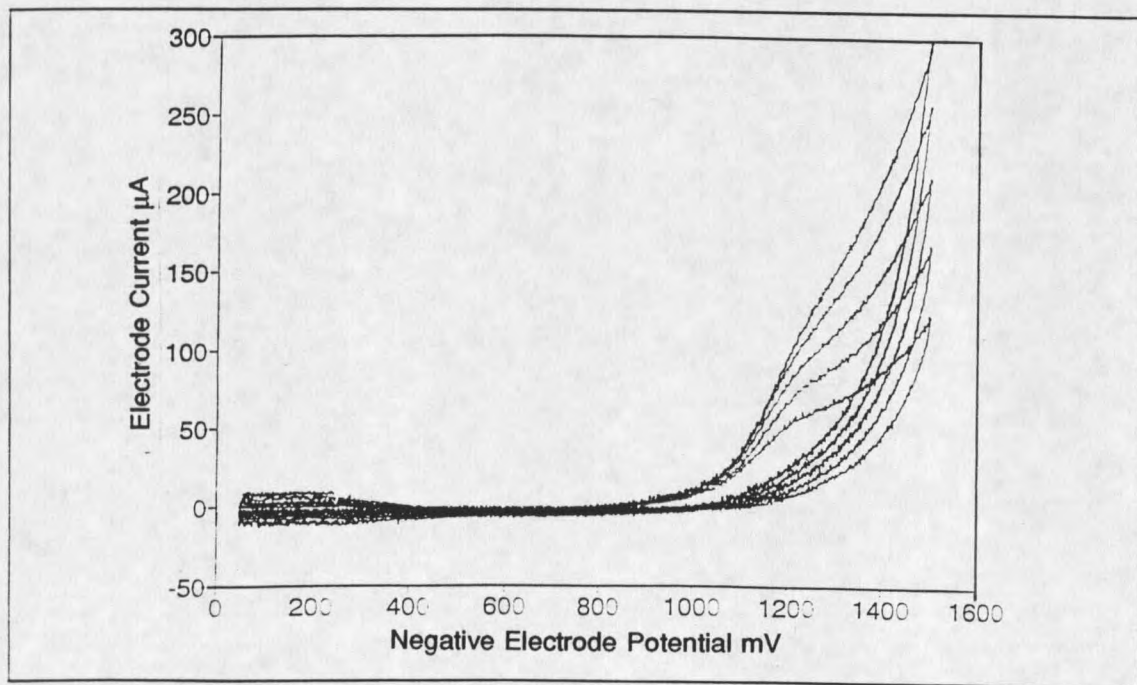


Figure 47: Cyclic voltammogram of 1.0 mM  $\text{Cr}(\text{NH}_3)_4\text{Cl}_2$ .

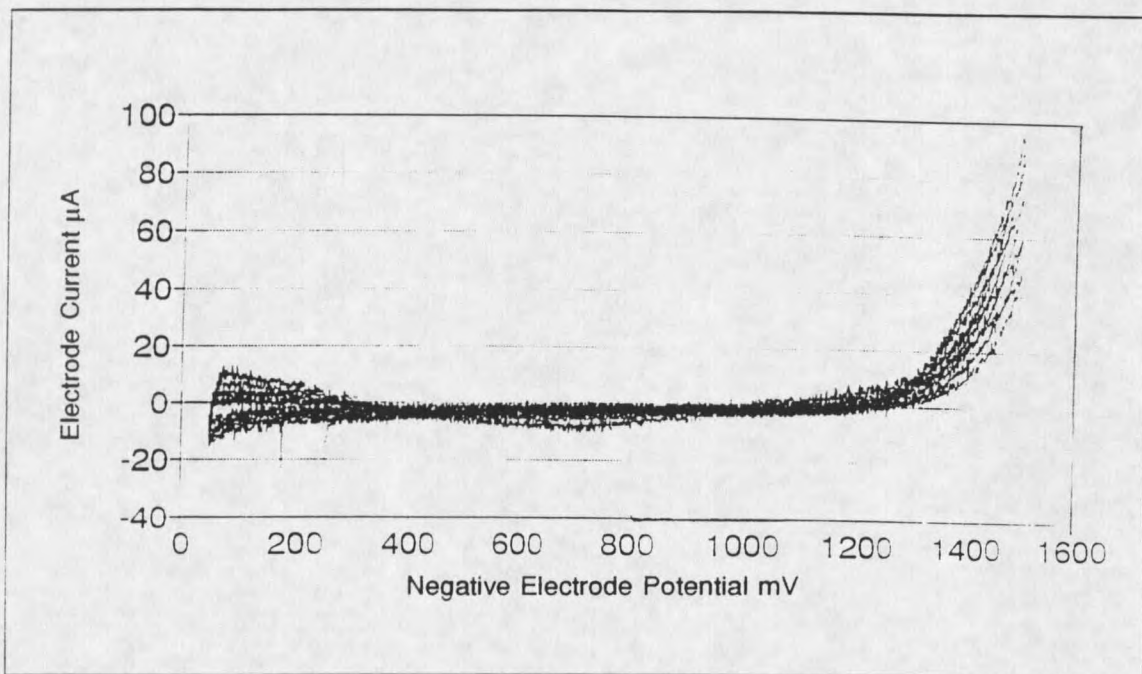


Figure 48: Cyclic voltammogram of 1.0 mM  $\text{Cr}(\text{CN})_6$ .

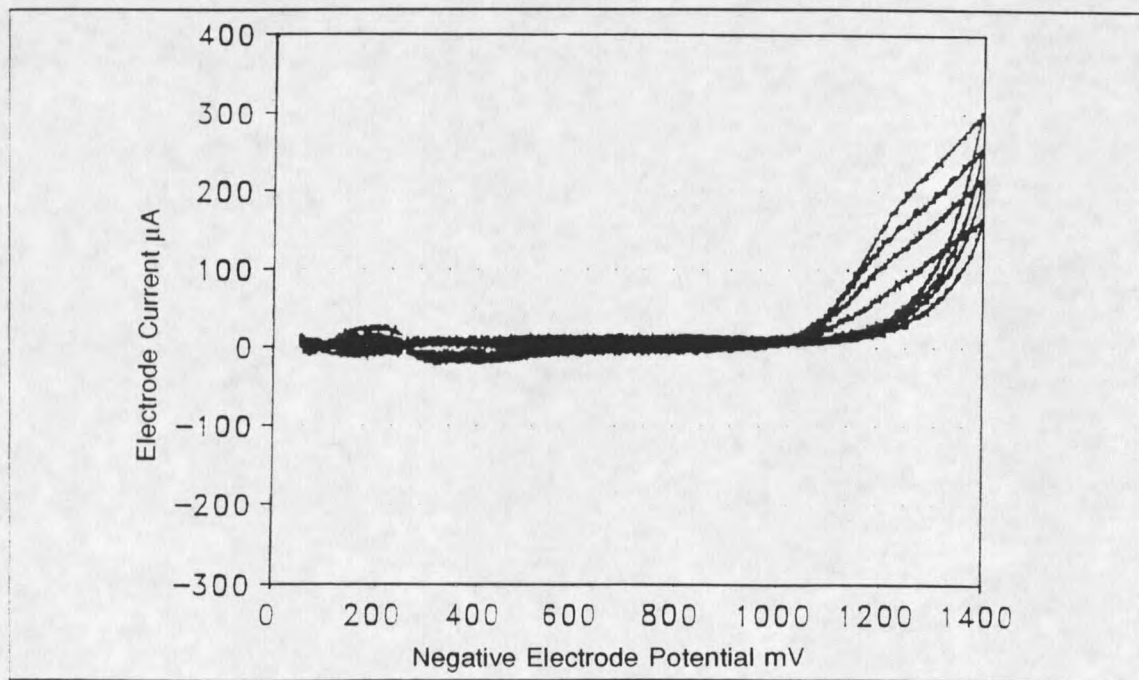


Figure 49: Cyclic voltammogram of 1.0 mM  $\text{Cr}(\text{py})_4\text{Cl}_2$ .

or, in the case of  $\text{Cr(en)}_3$  and  $\text{Cr(CN)}_6$ , fail to show any redox chemistry in this potential range prior to the catalytic generation of hydrogen at the electrode surface. This irreversible reaction is explained in the reaction coordinate energy diagram shown in figure 36. As described previously, to bring the electronic state of the nonmutagenic complexes to the same energy level as their corresponding  $\text{Cr(II)}$  complex prior to the electron transfer, more energy needs to be added to the system than with the mutagenic species. When reduction does occur, the highly energetic  $\text{Cr(II)}$  species formed under these conditions can undergo a catalytic chemical reaction with water to reform the  $\text{Cr(III)}$  species with the concomitant production of hydrogen at the electrode surface. Thus, there is no  $\text{Cr(II)}$  present on the return sweep of the CV. The reaction that the nonmutagenic species are undergoing in the cyclic voltammeter is given below (10).



This is an EC type of mechanism, but one that leads to an irreversible electrode reaction, in contrast to that of the mutagenic complexes, where the EC mechanism leads to a reversible electrode reaction (11). As well, this reaction explains both the irreversibility and the generation of hydrogen at the electrode surface.

The ligands themselves have been assayed in the cyclic voltammeter and have shown no redox chemistry occurring at these same potentials, figures 50 and 51. The ligands do not even show catalytic generation of hydrogen at the

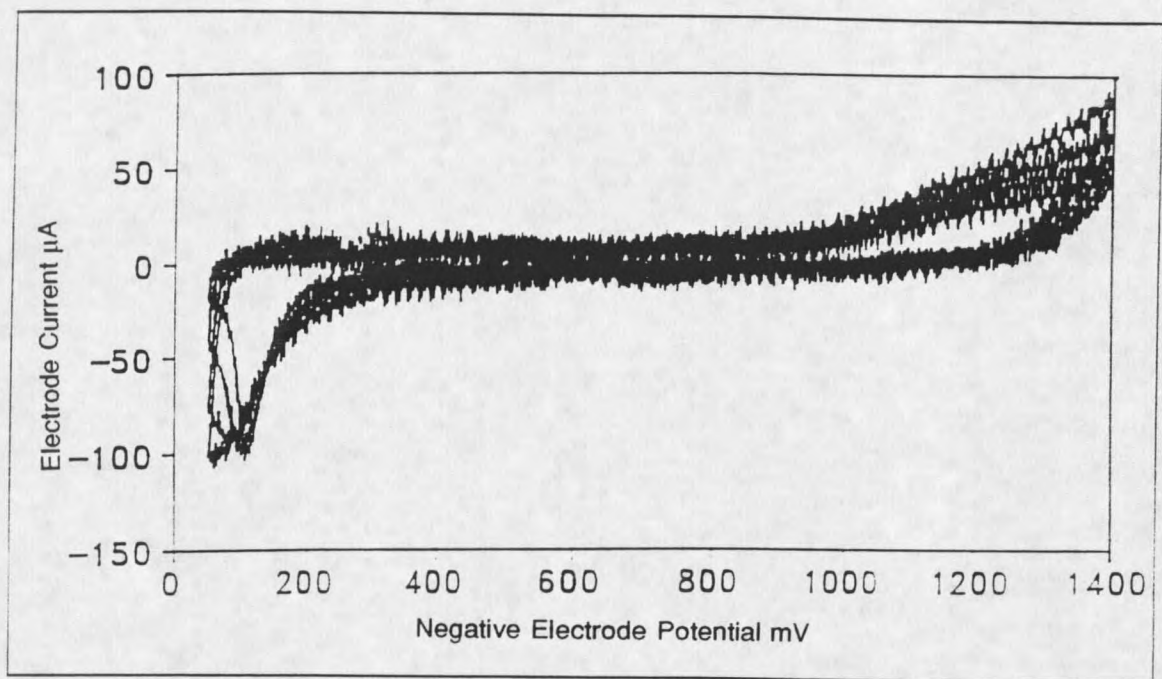


Figure 50: Cyclic voltammogram of 1.0 mM phenanthroline ligand.

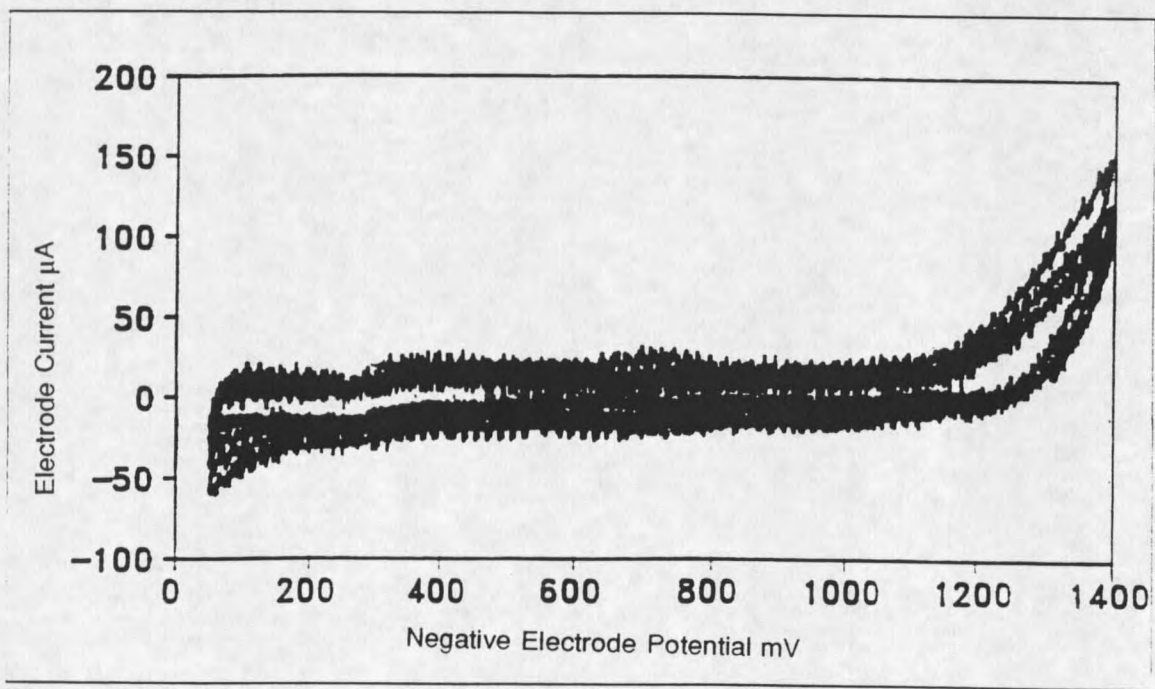
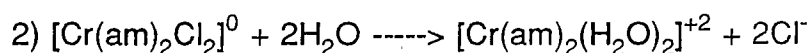
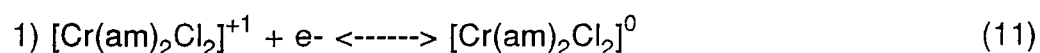


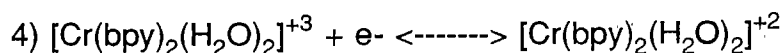
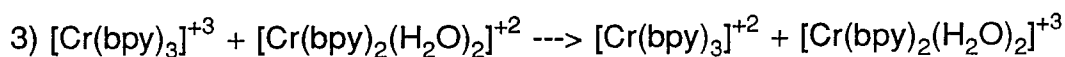
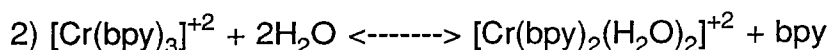
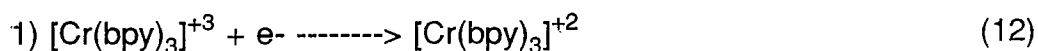
Figure 51: Cyclic voltammogram of 1.0 mM bipyridyl ligand.

electrode surface. This, we believe, supports the model that reduction is occurring at the metal center versus reduction at the ligand itself as seen with certain iron complexes. As well, this supports the work of others that show that reduction of chromium complexes occur at the metal center due to limited interactions of the metal-ligand orbitals.<sup>90</sup> This then implies that the Cr(III) species must go through an inner sphere electron transfer upon redox cycling which is supported by previous work on electron transfer in chromium species.<sup>104</sup>

Analysis of the bis-bidentate dichloro mutagenic species shows that reduction occurs in three steps which become ill-defined at faster sweep rates. The half-wave potentials for the Cr(III)/Cr(II) couple of these complexes are given in Table V. Comparison of these waves with 1.0 mM cadmium chloride solution shows that each reduction wave roughly corresponds to the transfer of one electron. The pattern of the voltammograms, while complicated, are indicative of an EC mechanism where the first reduction is followed by a chemical reaction relating to solvolytic ligand exchange of the chloride halogens for water. Further reduction can result in the loss of a phenanthroline or bipyridyl ligand that can allow formation of the tris-bidentate amine complex on the return sweep. It is likely, however, that the only physiologically significant redox couple is in the range of the Cr(III)/Cr(II) couples. In both the bis-phenanthroline dichloro and bis-bipyridyl dichloro case, the polarographic behavior suggest the following reactions (am= bpy or phen) (11).



With the tris-bipyridyl complex, the reaction is quite similar but the first reduction results in the loss of a bipyridyl ligand accompanied by a catalytic electron transfer process, again producing the bis-bipyridyl diaquo complex. This is shown in the following reaction scheme (12).



The oxidation in step 2 is reversible in the presence of free bipyridyl ligand and can result in the reformation of the tris complex but the kinetics favor the bis-bipyridyl diaquo complex. This is especially true if the ligand is not present in saturating amounts. The  $\text{pK}_a$ 's of the diaquo complexes have been measured giving  $\text{pK}_{a1}$  of 3.5, 3.4 and  $\text{pK}_{a2}$  of 6.1, 6.0 for  $[\text{Cr}(\text{bpy})_2(\text{H}_2\text{O})_2]^{+3}$  and  $[\text{Cr}(\text{phen})_2(\text{H}_2\text{O})_2]^{+3}$  respectively. These results are similar to that obtained previously.<sup>105</sup> Thus, the complex present at intracellular pH is presumably the

dihydroxy species of the bipyridyl and phenanthroline complexes. The cyclic voltammograms of these species show a degree of reversibility similar to the dichloro species and thus could be the ultimate cyclical electron donors in a Fenton-like reaction. Electron transfer occurring through a hydroxy inner sphere ligand of Cr(II) has been shown previously and tends to support this assignment.<sup>104</sup> While it appears that kinetically, the dihydroxy species of either the phenanthroline or bipyridyl complex would be the ultimate species formed from the intracellular reduction of these complexes, it would be rash to say that this is the ultimate DNA damaging species that is formed intracellularly since both forms have some degree of reversibility in the cyclic voltammeter. It is safe to say that both forms possess the redox properties that would be consistent with our model of oxygen radical generation.

The possible formation of  $\mu$ -hydroxy bridged dimers, either *in vivo* or *in vitro*, must be taken into consideration when invoking the formation of the dihydroxy species. Formation *in vitro* is unlikely because of the basic pH needed for the synthesis of this species.<sup>106</sup> The acid dissociation constant of the  $\mu$ -hydroxy bridged dimers is much higher than that observed with even aged solutions of the dihydroxy complexes. While this appears to rule out the presence of these species *in vitro*, we cannot rule out the occurrence *in vivo*. The concentration that would be present intracellularly and cellular pH, however, would seem to make this unlikely.

The work of Maki et al describes a relationship between splitting of the

octahedral symmetry of hexacoordinate complexes and positive shifts of the redox potential.<sup>107</sup> The further apart the ligands are in the spectrochemical series, the greater will be the splitting of the octahedral symmetry and the result will be a shift to more positive reduction potentials. If the redox cycling theory for the mechanism of action for these Cr(III) complexes is correct, there should be a correlation between positive shifts of this reduction potential with increased biological activity. This theory appears to hold true for the differences seen between the tris-bipyridylchromium(III) complex and the bis-bipyridyldichlorochromium(III) cases shown above. The first reduction of the tris-bipyridyl complex, which should have no splitting of the octahedral complex (because all ligands are equivalent), has a half-wave potential for the Cr(III)/Cr(II) redox couple of -0.93 V while the bis-bipyridyl complex, which is split by the *cis* chloride halogens, has a half-wave potential for the Cr(III)/Cr(II) redox couple of -0.76 V. This is reflected in their biological activity and is consistent with the bis-bipyridyl complex being more active. Negative shifts in reduction potentials between the dichloro and dihydroxy species of both the bis-bipyridyl and bis-phenanthroline complexes demonstrate this same phenomenon of biological activity coupled to reduction potential.

Using the theory developed from the bioassays and cyclic voltammetry of the original complexes, it was proposed that substituting different halogens at the *cis* position should show shifts in the reduction potential dependent on their placement in the spectrochemical series in relation to the observed biological

activity. Figures 52, 42, 53 and 54 show the separate voltammograms for the bis-bipyridyldihalogenchromium(III) complexes. Table VI gives the half-wave potentials for the Cr(III)/Cr(II) redox couple for these species. From the previous biological data for these complexes we know that the activity increases as you go down the periodic table of halogens. This increase in activity matches their relative positions in the spectrochemical series. The cyclic voltammograms show that the reduction potential shifts to more positive potentials as you increase the symmetry splitting. These data, appear to match the model predicted from the previous set of complexes.

The first reduction wave on the diiodo cyclic voltammogram is a 2e-reduction of a mercuric iodide formed on the surface of the electrode, figure 54. This is due to the electrolyte used in the assay and should not be confused with

**Table V:** Half-wave potentials of the Cr(III)/Cr(II) redox couple for the original Cr(III) complexes.

<u>Complex</u>	<u><math>E_{1/2}</math>(V)</u>	<u><math>n</math></u>
Cr(phen) <sub>2</sub> Cl <sub>2</sub>	-0.73	1
Cr(phen) <sub>2</sub> (OH) <sub>2</sub>	-0.96	1
Cr(bpy) <sub>2</sub> Cl <sub>2</sub>	-0.76	1
Cr(bpy) <sub>2</sub> (OH) <sub>2</sub>	-1.1	1
Cr(bpy) <sub>3</sub>	-0.93	1

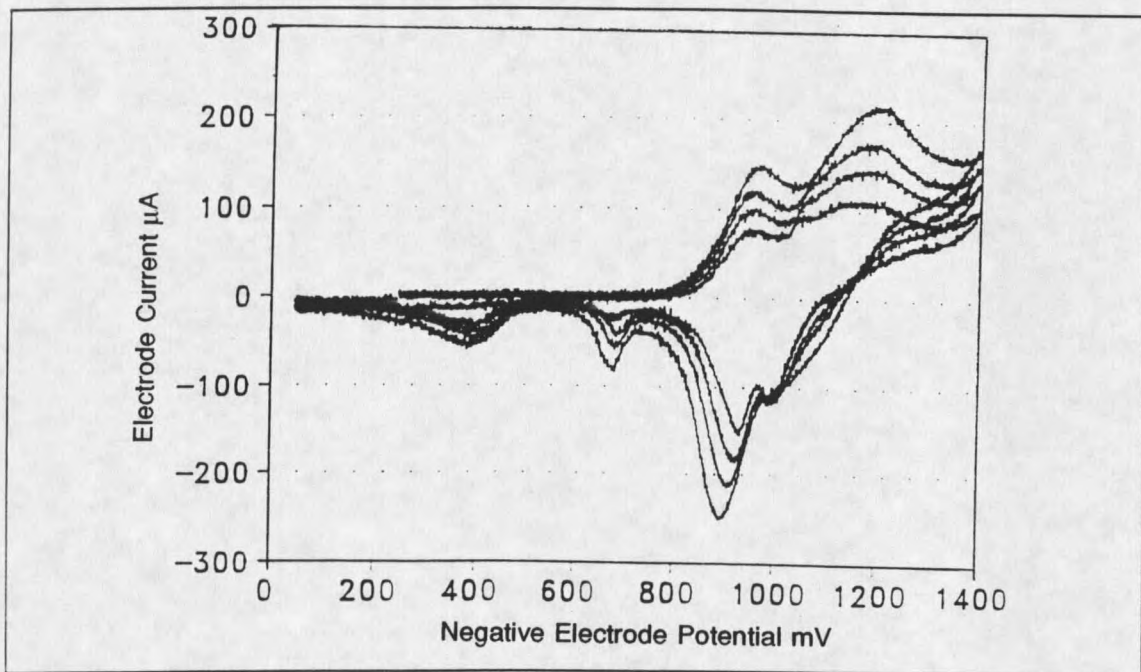


Figure 52: Cyclic voltammogram of 1.0 mM Cr(bpy)<sub>2</sub>F<sub>2</sub>.

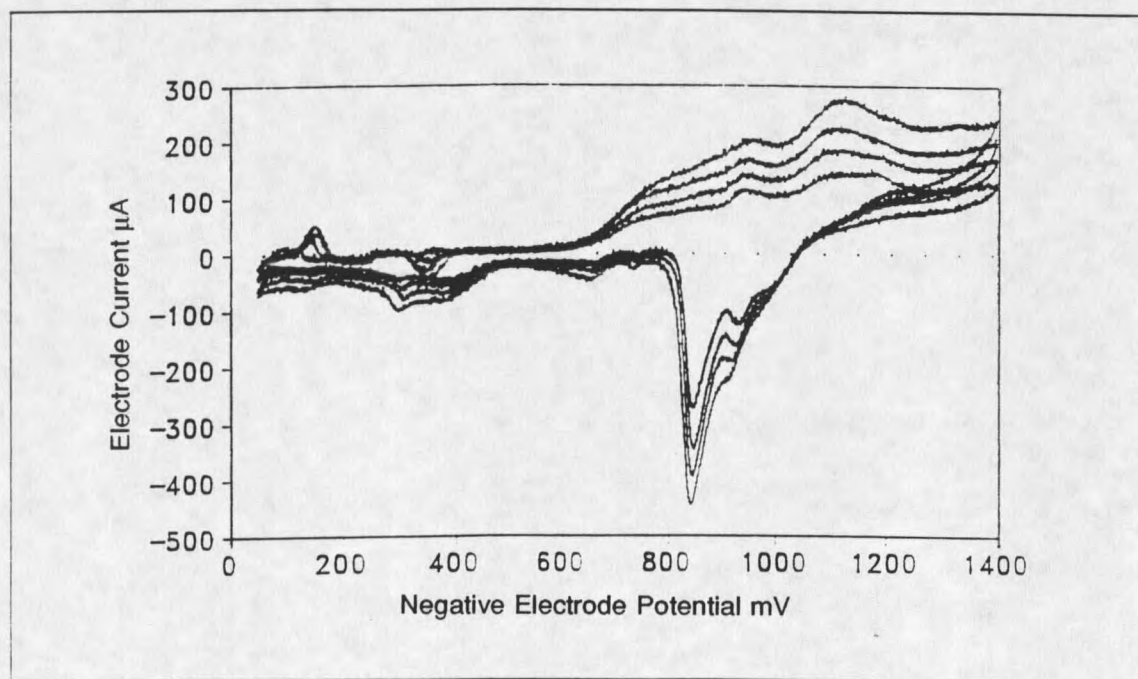


Figure 53: Cyclic voltammogram of 1.0 mM Cr(bpy)<sub>2</sub>Br<sub>2</sub>.

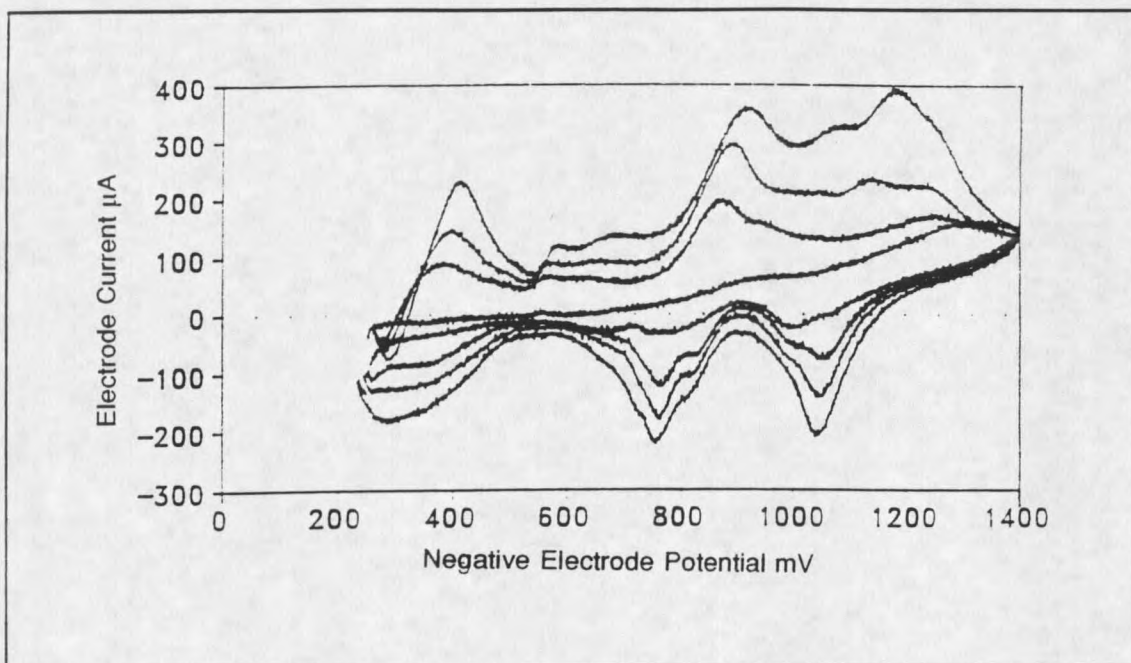


Figure 54: Cyclic voltammogram of 1.0 mM  $\text{Cr}(\text{bpy})_2\text{I}_2$ .

Table VI: Half-wave potentials of the Cr(III)/Cr(II) redox couple for halogenated bipyridyl complexes.

<u>Complex</u>	<u><math>E_{1/2}(\text{V})</math></u>	<u><math>n</math></u>
$\text{Cr}(\text{dmbpy})_2\text{Cl}_2$	-1.16	1
$\text{Cr}(\text{dcbpy})_2\text{Cl}_2$	-----	1
$\text{Cr}(\text{dmabpy})_2\text{Cl}_2$	-1.32	1
$\text{Cr}(\text{dmebpy})_2\text{Cl}_2$	-0.73	1

a metal-ligand reduction. The reduction wave seen at approximately -650 mV is the first true metal-ligand reduction. This spurious wave arises from incomplete background subtraction of the electrolyte caused by the increase in ionic concentration when the metal complex is added. The fluoride, bromide and iodide halogen complexes all show similar redox kinetics and suggests a mechanism comparable to that of the chloro species shown in (11). Qualitatively, it is important to note that these four mutagenic complexes all demonstrate a degree of reversibility and positive shifts of the reduction potential not present in the nonmutagenic complexes. Once again, this is consistent with the predicted model of redox activation of the metal center to generate oxygen radicals.

The work of Vlcek using a series of monosubstituted pentaamine Cr(III) complexes observed a linear relationship between red shifting of the first visible absorption band and the half-wave potential.<sup>94</sup> This same phenomenon is observed for the different halogenated complexes of bis-bipyridyl Cr(III), figure 55. The first visible absorption band in this set of complexes is due to metal-halogen ligand orbital overlap. The red shift to lower energies needed to promote an electron into a higher energy orbital should correspond to the energy difference between the HOMO (highest occupied molecular orbital) and the LUMO (lowest unoccupied molecular orbital). This energy difference between the two orbital levels should have a direct correlation upon the energy required to fill the LUMO with an electron in a reduction. This correlation appears to relate directly to the spectrochemical series. It is apparent that the reduction potential is directly related

to the field strength of the ligand, with the stronger field ligands having more negative reduction potentials. This dependence of the half-wave potential on field strength of the  $X^-$  ligand is believed to be an indication that a prior internal electronic rearrangement  $d_{t_{2g}}^3 \rightarrow d_{t_{2g}}^2 d_{e_g}$  is required for acceptance of an electron from the electrode.<sup>94</sup> As the field strength of  $X$  increases, this electrode process becomes kinetically less favorable due to less splitting of the octahedral symmetry and a more negative potential is required for this electron promotion. Figure 55 shows that indeed there is a linear relationship between the half-wave potential and the absorbance maxima for these compounds. The correlation coefficient for this linear relationship is  $r=0.997$  and the equation of the line is  $y= 78.4x + 613$ . The absorbance maxima of the complexes shifts to higher energy wavelengths and the half-wave potential becomes more negative in the following order;  $I > Br > Cl > F > H_2O$ . The fact that the mutagenesis decreases in this same order suggests that this ligand field splitting, due to the ligand field strength plays a major role in the potentiation of the biological effect. The biological activity, however, does not increase linearly with the half-wave potential, figure 56. Instead, an exponential increase in biological activity with more positive reduction potentials is observed. This effect, however, cannot be substantiated without synthesizing a mutagenic complex with even more positive half-wave potentials than that shown. The fact that Fe-EDTA, which is one of the most efficient oxygen radical producers known, has an even more positive half-wave potential,  $-0.12$  V versus the  $1.0$  M Ag/AgCl reference electrode, is consistent with this theory.

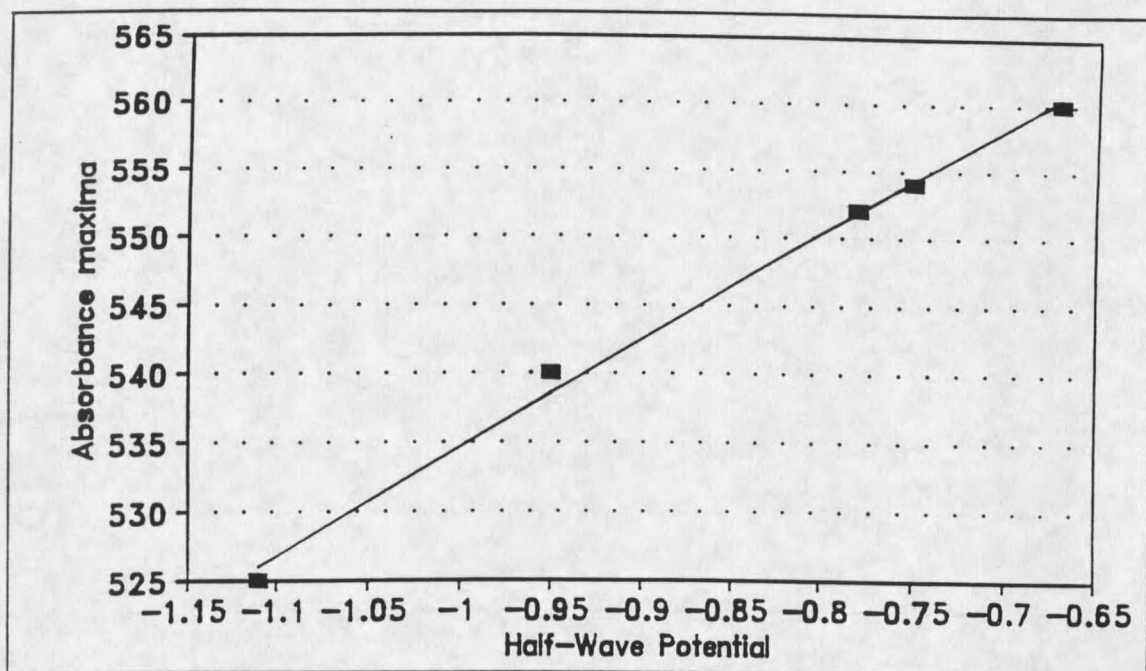


Figure 55: Correlation between absorbance maxima of first visible absorption band and half-wave potential.

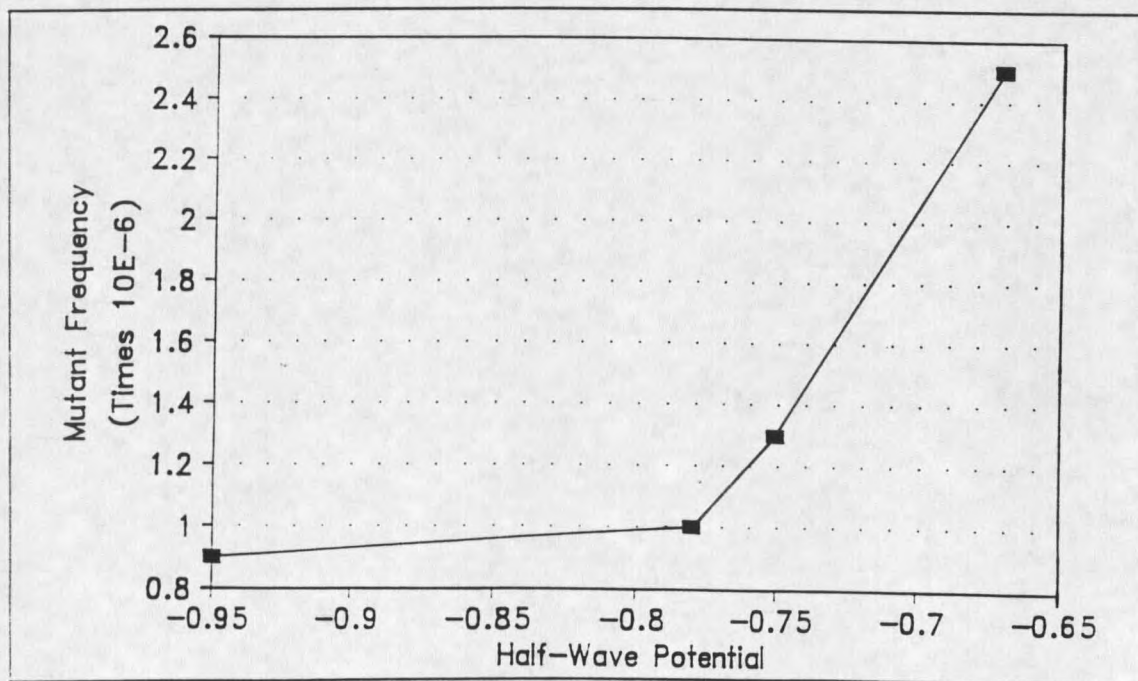


Figure 56: Correlation of half-wave potentials with mutational frequency.

It is certainly possible that this is an artifact of the system but it does have some grounding in theory. However, the broad first absorbance band for these compounds makes finding the absorbance maxima with any large degree of confidence somewhat doubtful and a certain bias could have been placed on the system.

To further expand the model, an obvious second step was to synthesize a series of bipyridyls with different electron donating and withdrawing substituents. It was apparent from the complexes discussed above that we have elucidated some of the key elements that control the mutagenic potential of Cr(III) complexes. While all the ligands have an effect in determining the degree of biological activity, it is the aromatic amine ligands of bipyridyl and phenanthroline which serve to direct the mutagenic activity of these complexes. From the cyclic voltammetry data, it is these ligands that impart an electronic and nuclear geometry that is similar enough to that of the Cr(II) complex to allow more positive reduction potentials as well as reversibility. A case can be made based on the electron density contained in the aromatic rings serving to, at least partially, distort the electronic structure of these Cr(III) complexes towards that of the Cr(II) electronic structure. Thus, it was considered that electron-donating substituents should further increase this electronic distortion towards that of the Cr(II) complexes, while the electron-withdrawing substituents should serve to distort the electronic structure towards that of the "normal" Cr(III) complexes. Further elaboration of the above model would then predict that the electron-donating substituted bipyridyl complexes

should have a higher biological activity and more positive reduction potentials than that of the unsubstituted bipyridyl complex or the electron-withdrawing substituted bipyridyl complexes which should show more negative reduction potentials and lower biological activity than that of the unsubstituted bipyridyl complex.

Figure 57, 58, 59 and 60 show the results of the cyclic voltammograms of these substituted bipyridyl complexes. The biological data for these complexes has been discussed previously. The half-wave potentials for the Cr(III)/Cr(II) redox couple are given in Table VII. The results of this assay are at best, mixed. Within the substituted bipyridyl complexes themselves, the biological activity data appears to uphold the model. The complexes with the electron-donating groups show increased activity over the complexes with the electron-withdrawing groups. The cyclic voltammograms of the electron donating groups show a degree of reversibility that would be predicted by the model and is consistent with redox cycling. The electron withdrawing groups do not show the redox characteristics expected for the predicted model with the exception of the dimethylester complex. The reversible wave seen for the methyl ester complex does not appear to be a function of the reduction of the metal center. Instead, we believe that this wave is a function of a reduction occurring at the ester on the bipyridyl ligand. Assigning this as such, is difficult because of the low solubility of the ligand itself in our electrolyte system.

Superficially, the model appears to fail with this set of complexes in two ways. First is that the unsubstituted bipyridyl complex shows both the greatest

biological activity and more positive shifts of the reduction potential than either of the electron-donating complexes. The model, derived earlier, would predict that this complex should be intermediate in both activity and shifts in the reduction potential. While these data uphold the basic model correlating reversibility and positive shifts of the reduction potential with biological activity, it tends to cloud the issue on what underlying physical phenomena is responsible for the activation of these aromatic amine complexes of Cr(III).

**Table VII:** Half-wave potentials of the Cr(III)/Cr(II) redox couple of the substituted bipyridyl complexes.

---

<u>Complex</u>	<u><math>E_{1/2}</math>(V)</u>	<u><math>n</math></u>
Cr(bpy) <sub>2</sub> F <sub>2</sub>	-0.95	1
Cr(bpy) <sub>2</sub> Cl <sub>2</sub>	-0.76	1
Cr(bpy) <sub>2</sub> Br <sub>2</sub>	-0.74	1
Cr(bpy) <sub>2</sub> I <sub>2</sub>	-0.67	1

---

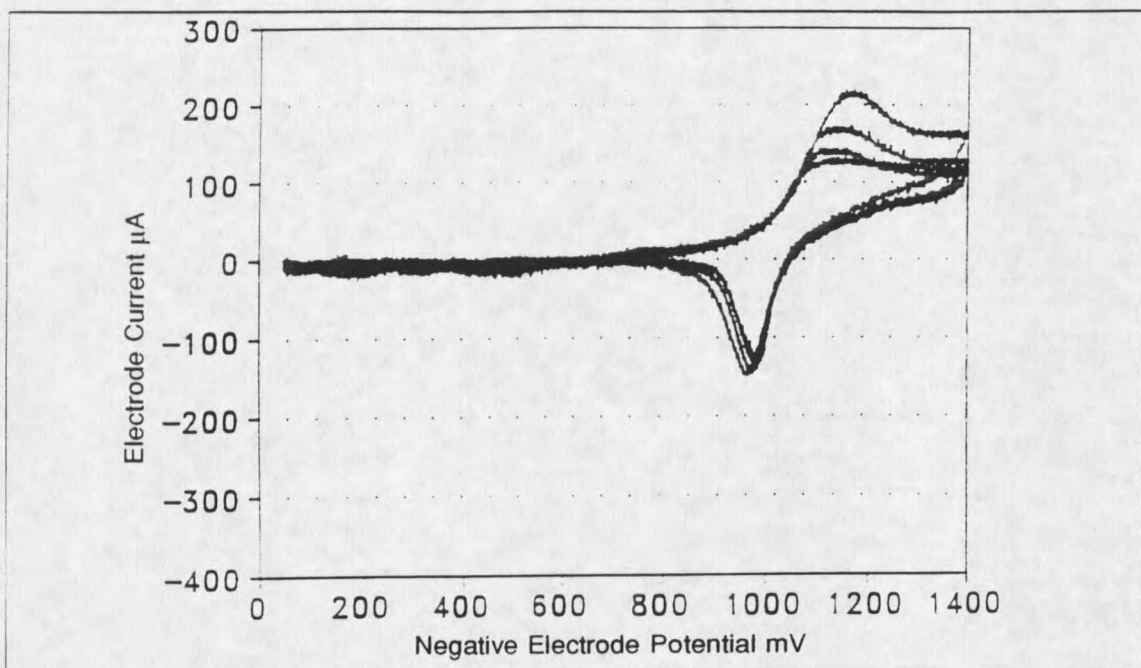


Figure 57: Cyclic voltammogram of 1.0 mM Cr(dmbpy)<sub>2</sub>Cl<sub>2</sub>.

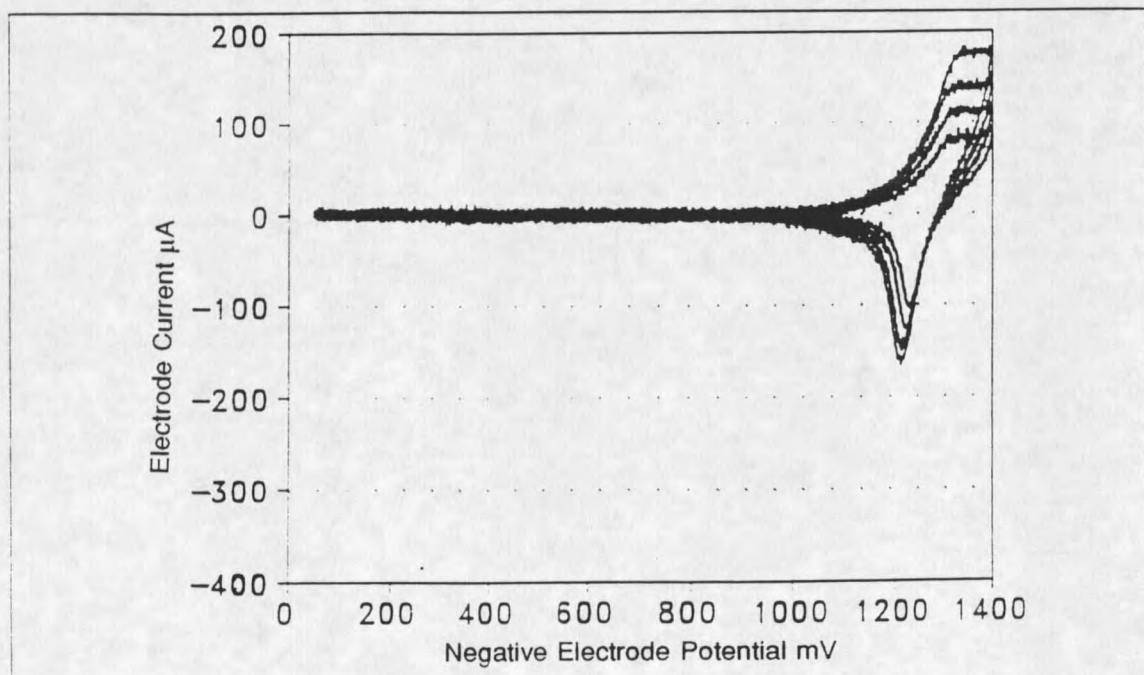


Figure 58: Cyclic voltammogram of 1.0 mM Cr(dmabpy)<sub>2</sub>Cl<sub>2</sub>.

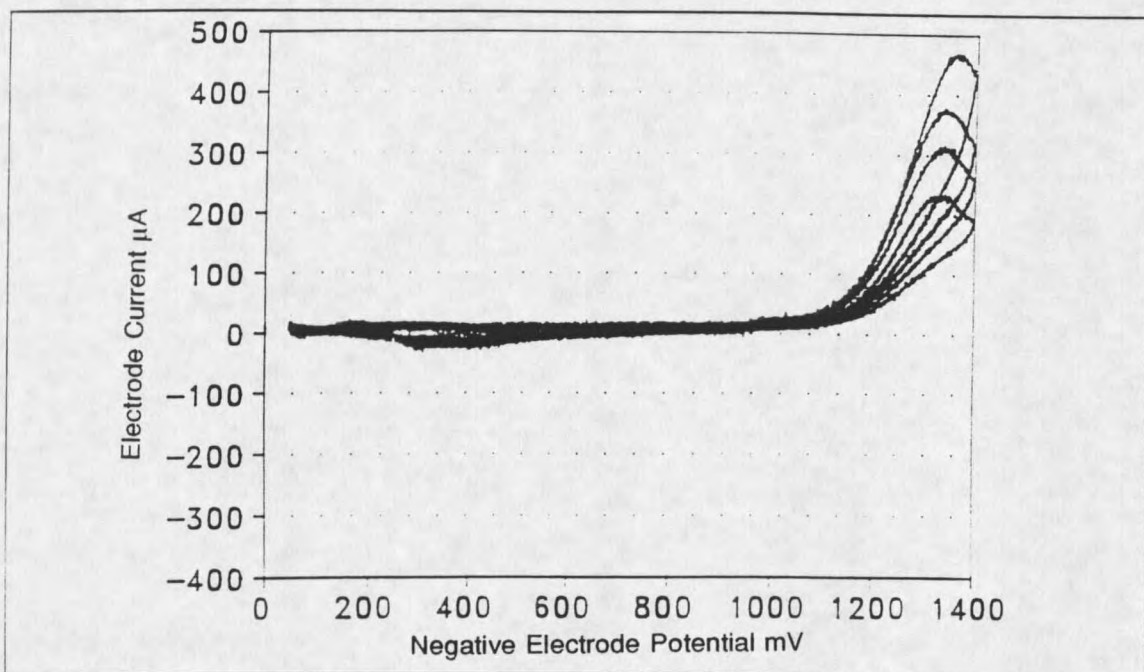


Figure 59: Cyclic voltammogram of 1.0 mM Cr(dcbpy)<sub>2</sub>Cl<sub>2</sub>.

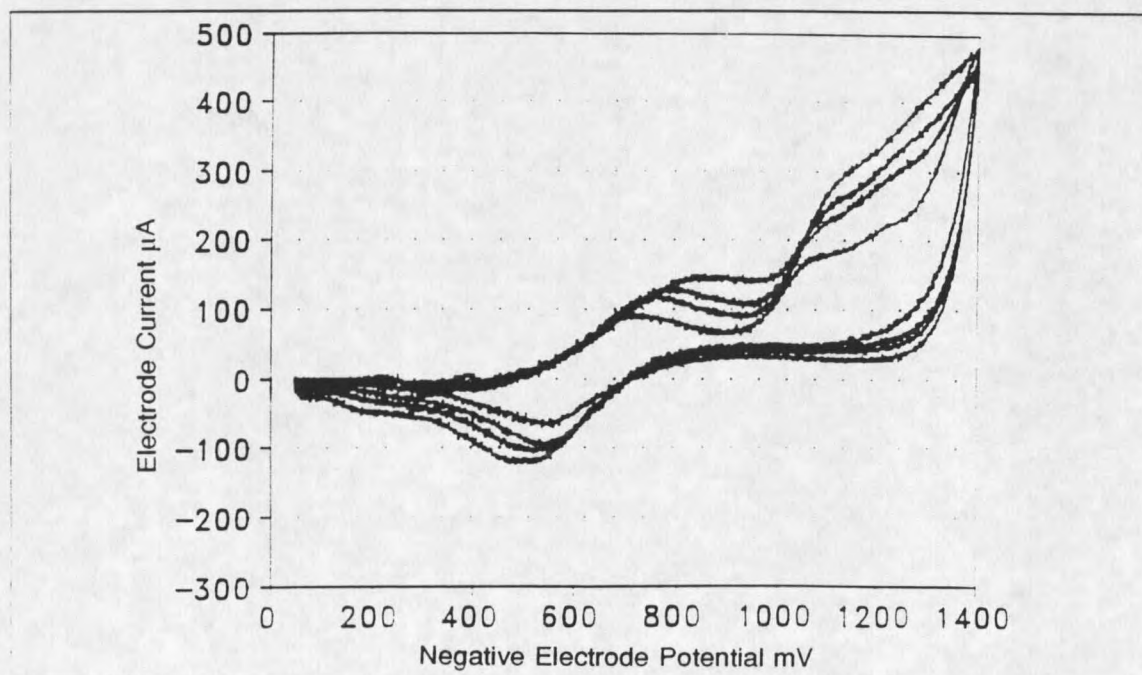


Figure 60: Cyclic voltammogram of 1.0 mM Cr(dmebpy)<sub>2</sub>Cl<sub>2</sub>.

### Plasmid Relaxation Studies

Electrophoretic studies on purified plasmid DNA were carried out to detect the specific type of DNA damage that would be associated with a redox cycling mechanism of oxygen radical generation. Oxygen radicals, and in particular, the hydroxyl radical are known to induce strand cleavage in DNA. This strand cleavage leads to conformational changes in the DNA that can be observed using electrophoresis.<sup>108</sup> Supercoiled DNA (Form I), when cleaved at a single strand, can unwind to form the relaxed (Form II) conformation. If two radicals cleave separate strands of the DNA, then a double strand break forms and results in the linear conformation (Form III). Mobility in electrophoresis is based on a volume and charge basis. Strand cleavage should not significantly alter the charge on the DNA but any conformational changes will drastically alter the volume that the DNA occupies in the gel. Thus, any changes resulting from radical induced cleavage will show up as different bands of DNA on the gel following electrophoresis.

Figure 61 shows the electrophoretic DNA pattern of the original set of chromium complexes reacted in the presence of *pUC-18* plasmid DNA. The results are, from left to right: lane 1 = plasmid DNA alone, lane 2 = plasmid DNA + Ascorbate/H<sub>2</sub>O<sub>2</sub>, all other wells, 3-12 contain plasmid DNA + Ascorbate/H<sub>2</sub>O<sub>2</sub> as well as the specified metal. Lane 3 = Fe-EDTA, lane 4 = Cr(phen)<sub>2</sub>Cl<sub>2</sub>, lane 5 = Cr(phen)<sub>2</sub>(H<sub>2</sub>O)<sub>2</sub>, lane 6 = Cr(bpy)<sub>2</sub>Cl<sub>2</sub>, lane 7 = Cr(bpy)<sub>2</sub>(H<sub>2</sub>O)<sub>2</sub>, lane 8 = Cr(bpy)<sub>3</sub>, lane 9 = Cr(en)<sub>3</sub>, lane 10 = Cr(en)<sub>2</sub>Cl<sub>2</sub>, lane 11 = Cr(NH<sub>3</sub>)<sub>4</sub>Cl<sub>2</sub>, lane 12 = Cr(CN)<sub>6</sub>.

The results of this assay show what would be expected for complexes that can generate oxygen radicals. A small amount of relaxation of DNA is seen with the reductant/oxidant alone, lane 2. This amount of relaxation is also observed in the nonmutagenic complexes, lanes 9-12. The remaining lanes all show significantly more relaxation of the supercoiled DNA than with the control alone. Lane 3 is the Fe-EDTA complex that is a well known hydroxyl radical generator. The supercoiled DNA has nearly completely relaxed to the form II conformation. Lanes 4-8 contain the five original mutagenic Cr(III) complexes. All of the mutagenic Cr(III) complexes show a significant degree of the form II relaxed conformation and lane 4, containing  $\text{Cr}(\text{phen})_2\text{Cl}_2$ , even shows a significant amount of linear, form III DNA. These results are consistent with redox cycling production of oxygen radical, and more specifically the hydroxyl radical.

The reaction of Cr(III) complexes in the presence of DNA without the reductant/oxidant shows very little change in DNA conformation, figure 62. The amount of relaxed DNA is approximately equivalent for all wells and matches closely that seen with the control. The results, from left to right are lane 1 = DNA alone, lane 2 = Fe-EDTA, lane 3 =  $\text{Cr}(\text{phen})_2\text{Cl}_2$ , lane 4 =  $\text{Cr}(\text{phen})_2(\text{OH})_2$ , lane 5 =  $\text{Cr}(\text{bpy})_2\text{Cl}_2$ , lane 6 =  $\text{Cr}(\text{bpy})_2(\text{OH})_2$ , lane 7 =  $\text{Cr}(\text{bpy})_3$ , lane 8 =  $\text{Cr}(\text{en})_3$ , lane 9 =  $\text{Cr}(\text{en})_2\text{Cl}_2$ , lane 10 =  $\text{Cr}(\text{NH}_3)_4\text{Cl}_2$  and lane 11 =  $\text{Cr}(\text{CN})_6$ . This suggests that for these complexes to exert their activity, the presence of an intracellular reductant is essential. Ascorbate, turns out to be a rational choice for this reductant. Ascorbate has been shown to be present intracellularly and has been

implicated as the major intracellular reductant of Cr(VI) in the lungs, liver and kidney of rats.<sup>109</sup>

The different halogenated bipyridyl complexes all show an ability to change the conformation of DNA as suggested with the previous mutagenic complexes. The electrophoretic gel for these complexes is shown in figure 63. While the results are not as clear as in the previous gels, they do reveal two important aspects. The complexes, when in the presence of a reductant show a change in the conformation of the supercoiled plasmid DNA while these same complexes, when assayed without a reductant show only background levels of relaxation. The loss of the supercoiled band may be the result of the nonspecific interaction of the bipyridyl complex to break up the duplex strand of DNA to disallow binding and thus fluorescence of the ethidium bromide stain. We believe, however that the gel does show a conformation change consistent with our model. The results are from left to right: lane 1 = DNA alone, lane 2 = DNA + reductant, lane 3 =  $\text{Cr}(\text{bpy})_2\text{F}_2$  + reductant, lane 4 =  $\text{Cr}(\text{bpy})_2\text{Cl}_2$  + reductant, lane 5 =  $\text{Cr}(\text{bpy})_2\text{Br}_2$ , lane 6 =  $\text{Cr}(\text{bpy})_2\text{I}_2$  + reductant, lane 7 =  $\text{Cr}(\text{bpy})_2\text{F}_2$  no reductant, lane 8 =  $\text{Cr}(\text{bpy})_2\text{Cl}_2$  no reductant, lane 9 =  $\text{Cr}(\text{bpy})_2\text{Br}_2$  no reductant, lane 10 =  $\text{Cr}(\text{bpy})_2\text{I}_2$  no reductant. The reductant in this case was ascorbate/ $\text{H}_2\text{O}_2$ .

The different substituted bipyridyls complexes of chromium were run in the identical assay. The electrophoretic gel for this set of complexes was ambiguous due to the lower activity of these complexes. The presence of redox active species such as iron, in both the DNA and the buffers, served to produce too

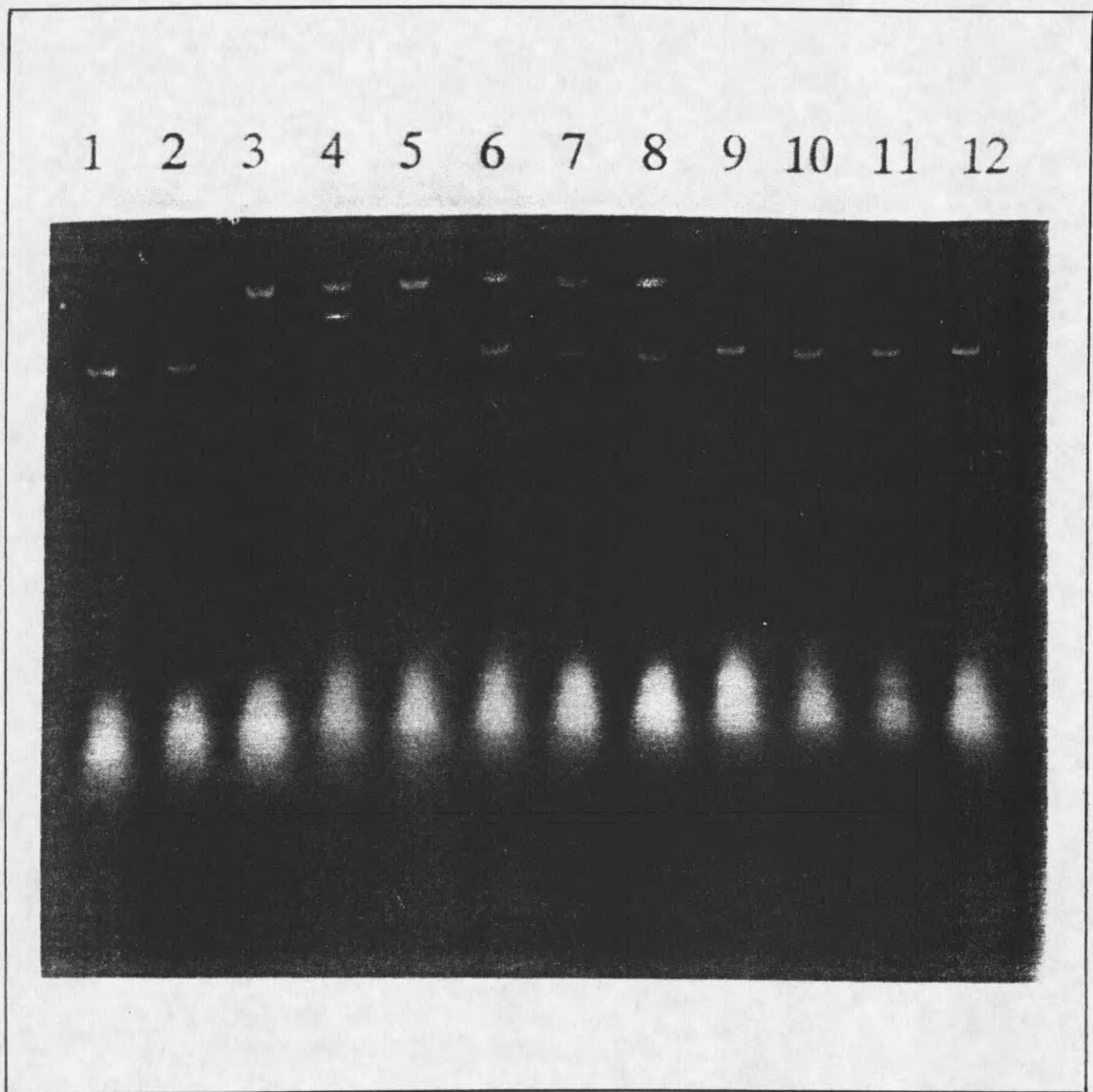


Figure 61: Plasmid relaxation of supercoiled DNA in the presence of mutagenic and nonmutagenic Cr(III) complexes with a reductant.

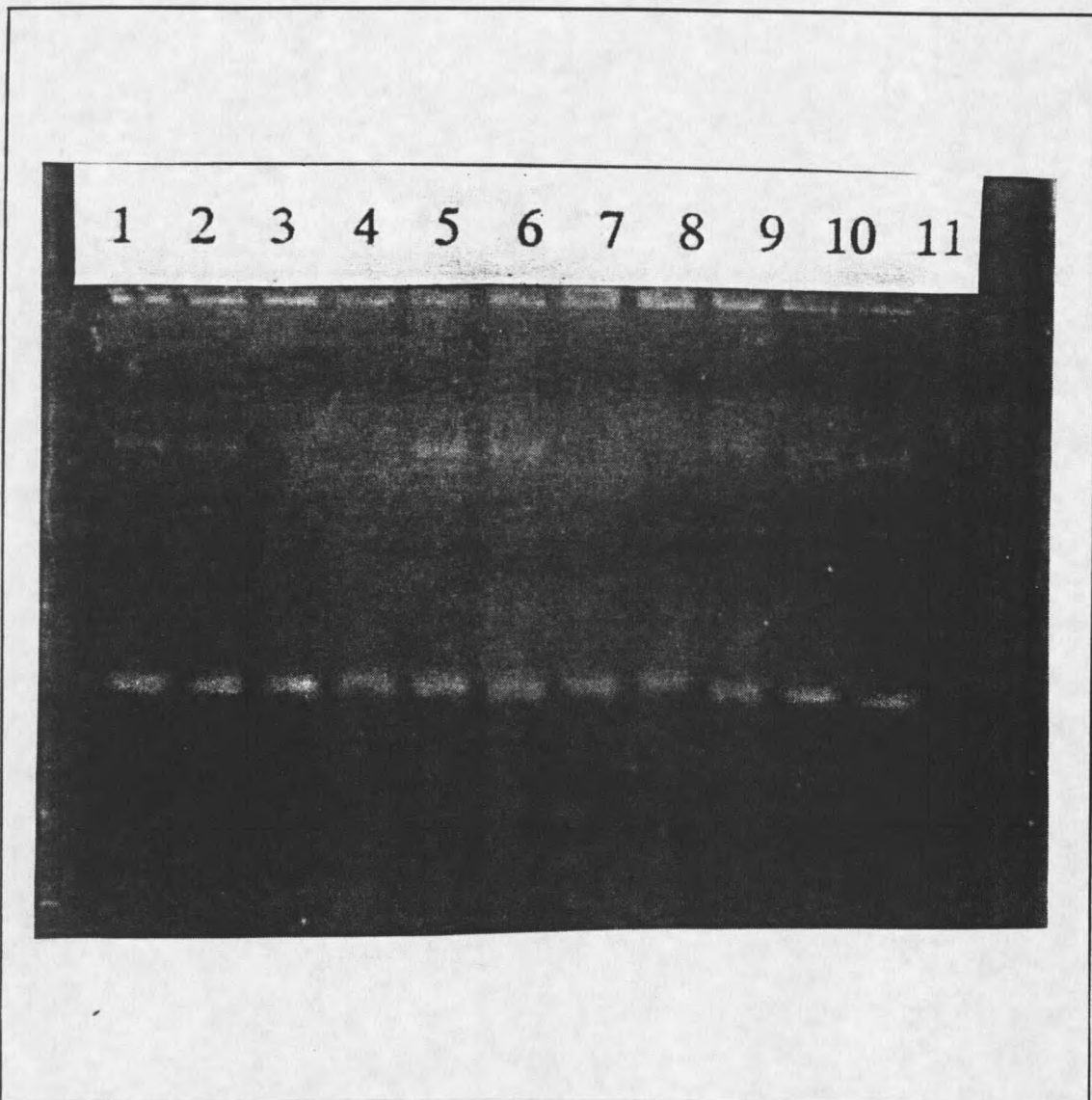


Figure 62: Plasmid relaxation of supercoiled DNA in the presence of mutagenic and nonmutagenic Cr(III) complexes without a reductant.

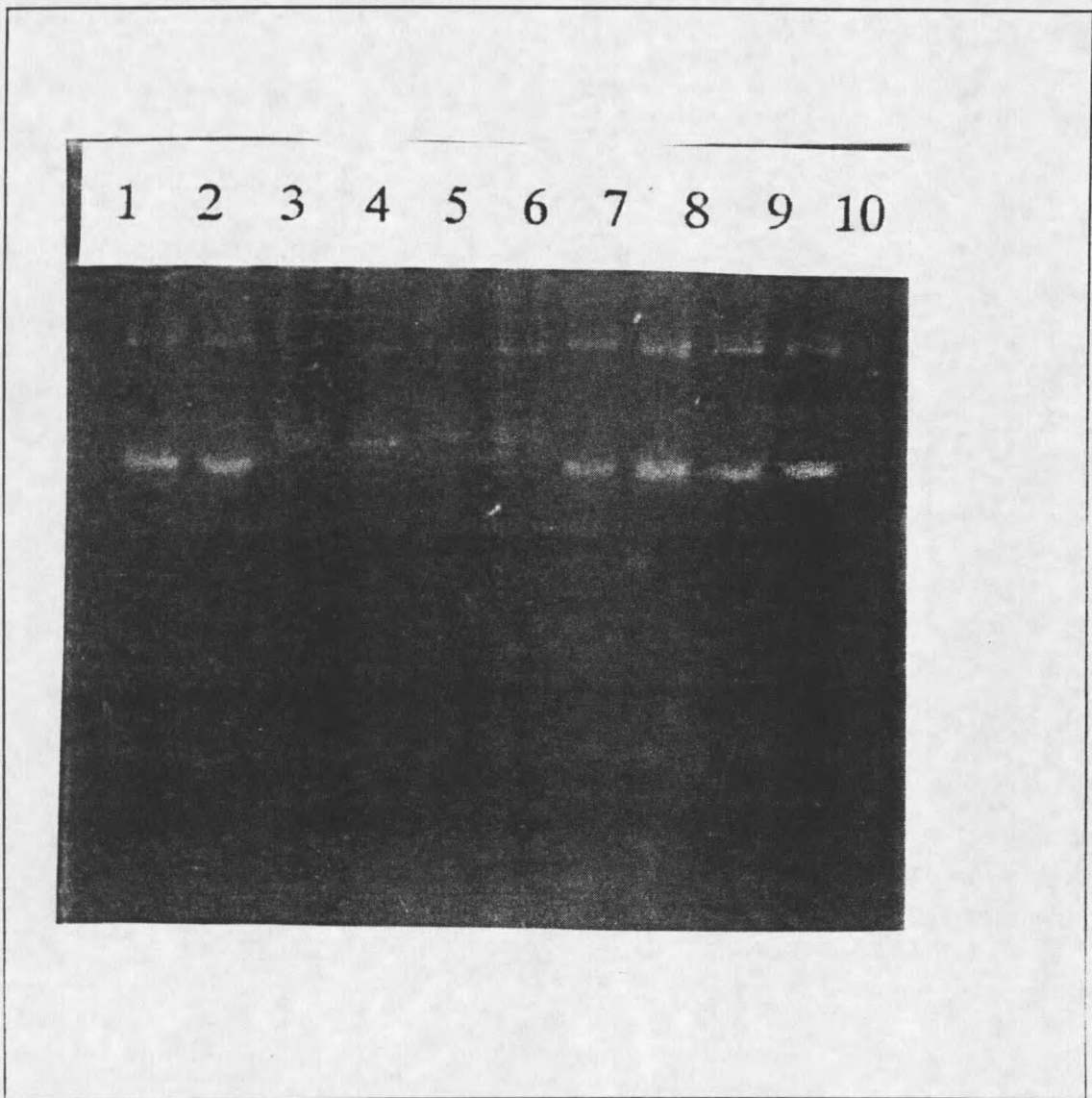


Figure 63: Plasmid relaxation of supercoiled DNA in the presence of the different halogenated complexes of bipyridyl with and without a reductant.

much background relaxation of the supercoiled DNA prior to significant relaxation owing to the chromium species.

### Interactions Of Cr(III) Complexes With DNA

The interactions that the mutagenic Cr(III) complexes have with DNA are an important aspect of assessing the total mechanism of damage. Certain DNA-metal interactions have the potential to be mutagenic in and of themselves. This is aptly demonstrated in the case of *cis*-platinum. Some interactions, however, are probably not responsible for the damage themselves, but allow for the spatial centering of the metal complex at the surface of DNA necessary to allow a reactive intermediate to damage DNA. These types of non-damaging spatial interactions can be intercalation, minor groove stacking and coulombic interaction.

Intercalation occurs when the ligand, attached to the metal complex has the right polarity and planarity to allow it to insert, in a coplanar manner, between the aromatic DNA bases. This type of interaction has been observed with tris-bidentate metal complexes of ruthenium, cobalt and rhodium possessing phenanthroline, terpyridyl and bipyridyl ligands.<sup>68-71</sup> Intercalation, for the above complexes, has demonstrated chiral specificity.<sup>68,69</sup> This chiral specificity of binding is not surprising since DNA itself is a chiral molecule. The isomer that has shown preferential intercalation with DNA is the (+) isomer of the metal complex. This does not preclude binding of the (-) isomer but it is not the preferred isomer.

Minor groove stacking refers to the ability of certain metal complexes to be

able to interact with the minor groove of DNA. This interaction is likely to be a form of coulombic attraction, since the minor groove is along the exposed negatively charged phosphate backbone. As well, hydrophobic interactions between the DNA bases and the ligand may play a role in the binding. The tris-bipyridyl complex of Cr(III) has been reported to have this type of interaction.<sup>110</sup> It is reported, that this type of interaction is also somewhat chiral specific but in this case, it is the (-) isomer that shows preferential binding. Once again, this does not preclude interaction of the (+) isomer, it is just preferred for the (-) isomer.

Coulombic attraction is simply the attraction of two oppositely charged species for each other. This type of interaction can occur between any positively charged complex and the negatively charged phosphate backbone of DNA. This type of interaction is rather vague in definition and should not show any chiral specificity but may be charge dependent.

### Electrophoretic Mobility

Electrophoretic mobility can also be used to detect the influence of intercalating agents on the amount of negative and positive supercoiling. When a species intercalates between the base pairs of DNA, it has the potential to change the winding angle of the supercoiled DNA.<sup>68</sup> While there is some dependence on the type of supercoil that the DNA has, either positive or negative supercoils, the overall effect is the same. This effect is an unwinding of the supercoil towards the relaxed form as the metal-ligand intercalating complex

concentration increases and the binding sites become saturated. At a certain concentration, the effect is reversed and the DNA is rewound in the opposite direction towards the reverse supercoiled form. One drawback of this assay is that it lacks sensitivity and an intercalating complex that will not appreciably alter the winding angle will not show this type of interaction. The metal-ligand complex must also be able to form a transient intercalated complex with the DNA in the presence of an electric field. Thus, the response described is only seen for good intercalators that have a high affinity for this type of interaction and will show a large perturbation in the winding angle of the supercoils.

Figure 64 shows the results of an electrophoretic mobility assay using the basic bis-bidentate and tris-bidentate aromatic amine ligands. As one would expect, the phenanthroline complex with the higher degree of planarity associated with the three ring system shows a classical winding and unwinding of the supercoiled DNA with increasing concentrations. The bis-bidentate bipyridyl complex of Cr(III) and the tris-bidentate complex of Cr(III) show no response in this assay. This leads to the suggestion that neither of these two complexes are good intercalators. This may be a function of the two aromatic ring system that is not as planar as that of the phenanthroline complex. The tris-bidentate bipyridyl complex of Cr(III) would not be expected to show any intercalation since it has been reported previously to be a minor groove binder and not an intercalator. This work cannot be interpreted against intercalation for the bipyridyl complexes, but it is probable that they are not as efficient as the phenanthroline complex.

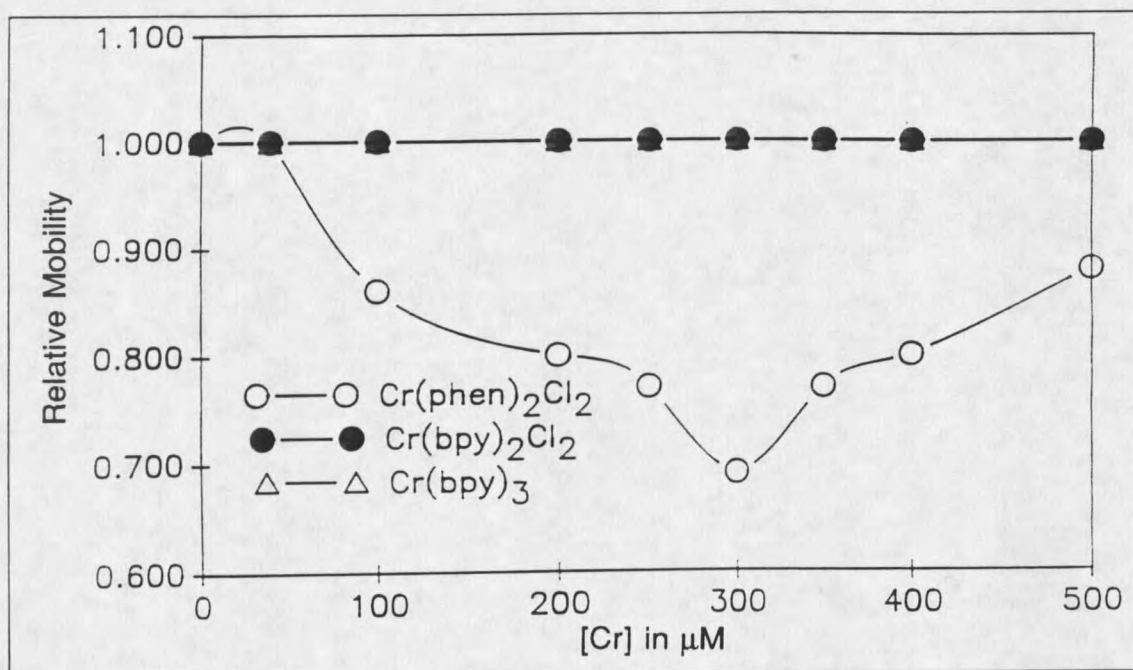


Figure 64: Electrophoretic mobility of supercoiled DNA in the presence of a metal gradient of select Cr(III) compounds.

### Equilibrium Dialysis And Polarimetry

If indeed, there is a chiral specificity of interaction with DNA, we should be able to measure this using a combination of equilibrium dialysis of the metal complex versus DNA and subsequent polarimetry. Using a dialysis membrane with a molecular weight cutoff large enough to allow the metal to pass through but not the DNA, we can measure the enrichment of the nonpreferentially bound isomer of the metal complex. For effective measurements of this type, the racemization between the two isomers must be slow. If racemization is fast, the result may be chiral enrichment followed by racemization to give a racemic mixture that would yield erroneous results.

Table VIII shows the results of the equilibrium dialysis/polarimetry on the three basic mutagenic ligand types. The bis-phenanthroline-dichlorochromium(III) complex displays the enrichment of the (-) isomer that would be expected for an intercalating complex. This means that the (+) isomer was bound preferentially to the DNA. The bis-bipyridyl-dichlorochromium(III) complex, as well, displays a small amount of enrichment of the (-) isomer but only about 15% of the phenanthroline complex. This lower degree of enrichment suggests that bipyridyl ligands are not nearly as efficient for intercalation as phenanthroline ligands. Or it may be that there is less chiral specificity for this complex and both isomers bind virtually equally well. If this is a valid assessment, it can be readily explained by the planarity of the different ring systems. This lower degree of enrichment may also explain why nothing was observed with the electrophoretic mobility of this complex. The tris-bipyridyl complex shows a slight enrichment of the (+) isomer although the degree of this enrichment is not terribly significant. These results, although tenuous, support the minor groove binding theory reported previously for this complex.<sup>110</sup>

Table VIII: Chiral enrichment of Cr(III) isomers after dialysis against DNA.

<u>Complex<sup>A</sup></u>	<u>Optical Rotation</u>	<u>DNA Interacting Isomer</u>
Cr(phen) <sub>2</sub> Cl <sub>2</sub>	-10.8° ± 0.4°	(+)
Cr(bpy) <sub>2</sub> Cl <sub>2</sub>	-1.8° ± 0.3°	(+)
Cr(bpy) <sub>3</sub>	+0.5° ± 0.2°	(-)
Cr(en) <sub>2</sub> Cl <sub>2</sub>	-0.6° ± 0.2°	(+)

A= complexes not shown have either not been measured or have no optical isomers.

### Spectrophotometric Changes Upon Intercalation

Changes in the spectrophotometric behavior of the metal complexes in the presence of DNA is another method to look for the interactions of the metal-ligand complex with DNA. Previously, it has been shown that upon intercalation, the intensity of the metal-ligand charge transfer band in the ultraviolet or visible spectrum is attenuated.<sup>68</sup> This phenomenon is based on the fact that when an unordered absorbing complex becomes ordered, in this case by intercalation between the DNA base pairs, the absorbance maximum is decreased (a hypochromic shift is observed).

Figures 65 and 66 show the results of the UV-VIS spectrophotometric work

on the two of the mutagenic Cr(III) species.

The  $\text{Cr}(\text{bpy})_2\text{Cl}_2$  complex shows a marked decrease in the absorbance when in the presence of DNA. The absorbance of the metal MLCT in the presence of DNA is 65% of that seen without added DNA. The  $\text{Cr}(\text{bpy})_3$  complex shows no obvious change in the MLCT absorbance either with or without the presence of DNA.

This work, and that shown previously, allows us to say unequivocally that the phenanthroline complexes of chromium interacts with DNA to intercalate in a coplanar manner between the bases. The bipyridyl complexes probably have a degree of intercalation but not nearly to the extent of the phenanthrolines. Upon addition of a third bulky ligand, as with the tris-bipyridyl case, no intercalatory interaction is seen.

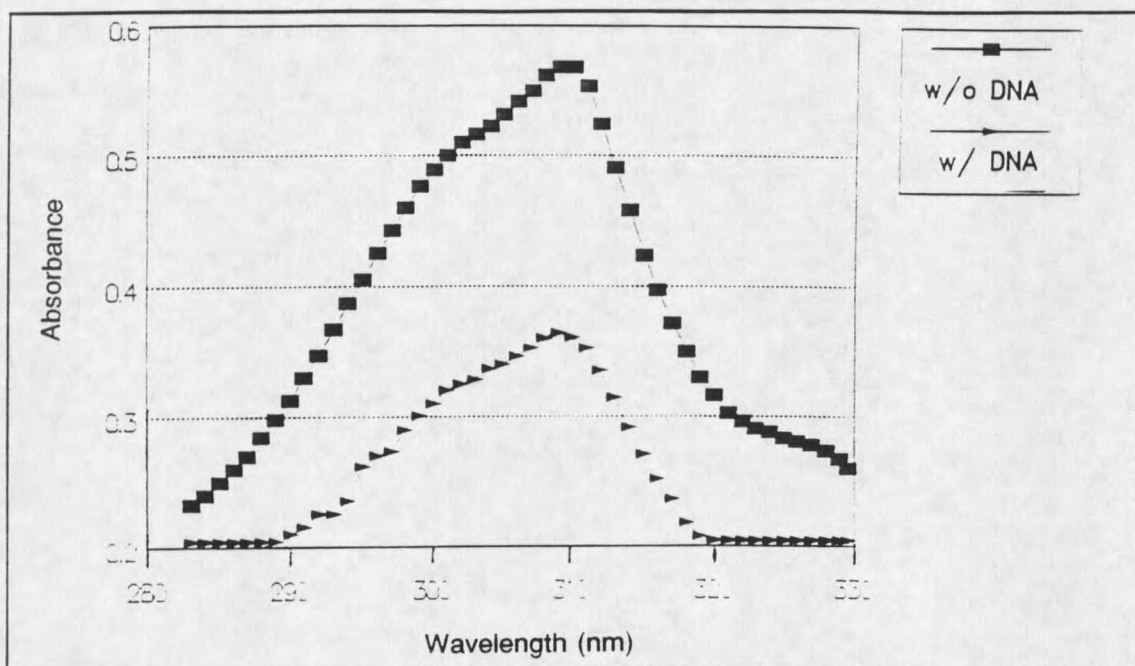


Figure 65: Ultraviolet absorption of  $\text{Cr}(\text{bpy})_2\text{Cl}_2$  with and without the presence of DNA.

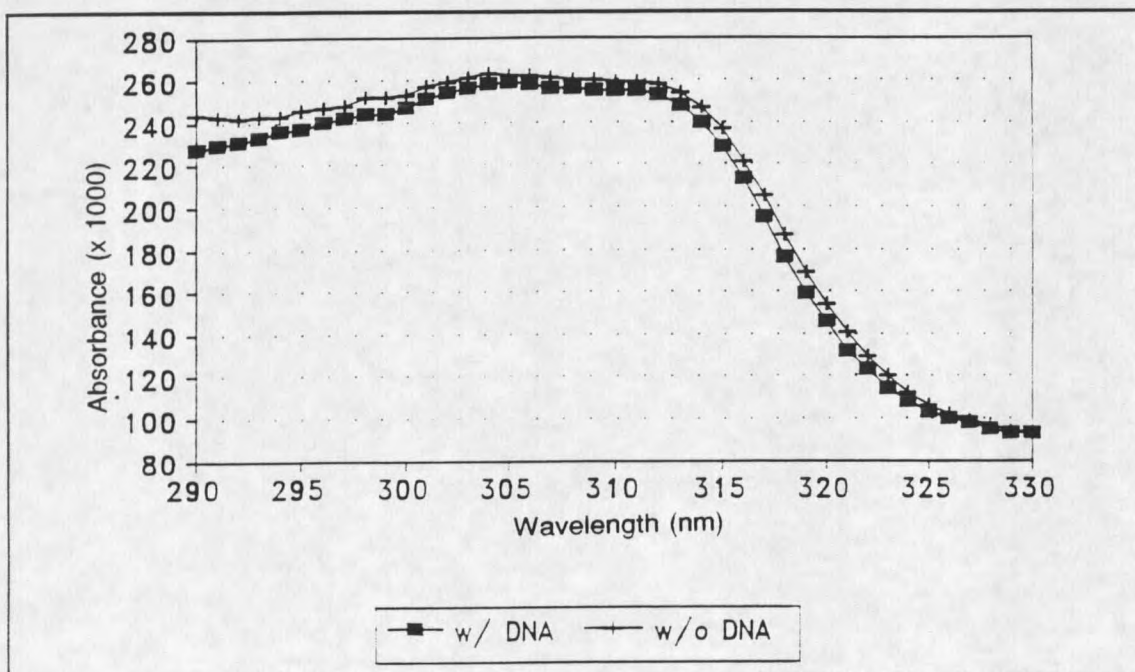


Figure 66: Ultraviolet absorption of  $\text{Cr}(\text{bpy})_3$  with and without the presence of DNA.

## SUMMARY

Prior to this work, the indications of *in vivo* biologically active Cr(III) compounds were considered, by most, to be artifacts of the assay systems. Those who accepted the indications of mutagenicity for these compounds attributed their activity to a differential ability to cross the cellular membrane in contrast to the common Cr(III) salts such as  $\text{CrCl}_3 \cdot 6\text{H}_2\text{O}$ . We believed, however, that there were fundamental differences in the physical characteristics of these compounds that could account for this difference in activity. The goal for this research was to discern, not only the different physical characteristics that separate the mutagenic and nonmutagenic Cr(III) species, but to also determine a mechanism by which the mutagenic species potentiate their activity.

An initial clue to the mechanism for these compounds was their preferential activity towards those *S. typhimurium* strains that are susceptible to oxidative damage. This preferential activity led us to believe that these complexes may have a mechanism involving an oxygen radical. To test this hypothesis, we developed an anaerobic Salmonella reversion assay as well as an anaerobic SOS response assay. In both assay systems, with the Cr(III) compounds, we observed that the activity was dependent on the presence of oxygen which is consistent with an oxygen radical mechanism of DNA damage.

To test whether there was a dependence on membrane permeability on activity, a series of different mutagenic and nonmutagenic Cr(III) complexes were assayed. This work was performed for us by Dr. Marguerite Sognier of the

University of Texas, Galveston. In mammalian cells, the uptake of Cr(III) compounds demonstrates that membrane permeability, at least with these complexes, is not the single controlling factor in their biological activity. In fact, those complexes that were taken up the easiest were the nonmutagenic Cr(III) complexes whereas the mutagenic complexes showed a much lesser degree of membrane permeability. This work tends to demonstrate that the biological activity of these complexes is based on a physical attribute of the metal-ligand complex and not on a simple membrane permeability basis.

To determine what physical characteristic the mutagenic complexes possess versus the nonmutagenic complexes, we assayed these complexes in the cyclic voltammeter. The presumption from which we chose cyclic voltammetry was that if an oxygen radical is responsible for the mechanism of damage, this implies that the complex must have redox kinetics consistent with being a cyclical electron donors. While the results from these data are not as straightforward as simple reversible and irreversible kinetics, it does show that the mutagenic complexes have redox kinetics consistent with an ability for these complexes to serve as cyclical electron donor. The nonmutagenic complexes have shown irreversible redox kinetics and more negative reduction potentials than the analogous mutagenic complexes. This difference between the mutagenic and nonmutagenic complexes may be the physical characteristic that controls the biological activity of Cr(III) complexes.

Oxygen radicals leave a characteristic "footprint" when reacted with DNA. The interaction of oxygen radicals with DNA can be characterized using a variety of assays. We chose a plasmid relaxation assay to show the interaction of oxygen radicals with supercoiled DNA to form the relaxed form of DNA. Electrophoretic gels of supercoiled plasmid DNA in the presence of the mutagenic and nonmutagenic Cr(III) species have shown that, in vitro, the mutagenic species, when in the presence of a reductant, tend to relax supercoiled plasmid DNA. The nonmutagenic species have shown only background amounts of relaxation of plasmid DNA in this assay.

The interaction of Cr(III) species with DNA is an important aspect of the overall mechanism of DNA damage. Oxygen radicals, to be efficient DNA damagers, must be produced in close proximity to the DNA. The spatial orientation of these complexes of DNA were measured using a variety of techniques. The results of these techniques tend to infer that the bis-phenanthroline complex is a very effective intercalating agent, the bis-bipyridyl complex probably intercalates although not nearly as effectively as the phenanthroline complex. The tris-bipyridyl complex, however, does not appear to intercalate but interacts mainly through coulombic attraction or minor groove stacking.

The model then, that we propose for mutagenic Cr(III) species, has a ligand directed activity that succeeds in endowing the metal-ligand complex with both redox characteristics compatible with oxygen radical generation as well as an

ability for interaction with DNA to spatially orient the complex at the DNA surface.

Several conclusions can be drawn from this work. It is possible that these mutagenic Cr(III) complexes mimic those compounds formed intracellularly from the reduction of Cr(VI) and may have a direct bearing on the carcinogenic potential of this oxidation state. The fact that certain anti-tumor drugs, such as bleomycin, have a similar mechanism of DNA damage and interaction may allow us to develop metal complexes that have both specificity of DNA interaction and a mechanism of DNA damage that can be "tuned" to cellular reduction potentials by changes in the metal-ligand complex. These results also suggest that environmental risk assessment based solely on one or two metal-ligand complexes does not guarantee that all complexes of that metal will be biologically analogous.

## LITERATURE CITED

- 1) Langard, S. (1990) *Am. J. Ind. Med.*, 17, 189.
- 2) Langard, S. (1988) *Sci. Total Environ.*, 71, 341.
- 3) Royle, H. (1975) *Environ. Res.*, 10, 39.
- 4) Acheson, E.D., Codwell, R.H., & Jolles, B. (1970) *Br. Med. J.*, 35, 358.
- 5) Langard, S. & Norseth, T. (1975) *Br. J. Ind. Med.*, 32, 62.
- 6) National Institute of Occupational Safety and Health. Occupational Exposure to Chromium(VI), pp. 23-121. Washington DC: Us Department of Health Education and Welfare, 1975.
- 7) Anderson, R.A. & Kozlovsky, A.S. (1985) *Am. J. Clin. Nutr.*, 41, 1177.
- 8) Warchola, R.J. (1986) Geology of the Beartooth Uplift and Adjacent Basins, Montana Geological Society and Yellowstone Bighorn Research Associate Joint Field Conference and Symposium, pp. 239-252.
- 9) Clark Fork Superfund Sites Master Plan, U.S. Environmental Protection Agency, November, 1990.
- 10) Leonard, A., & Lauwerys, R.R. (1980) *Mutat. Res.*, 76, 227.
- 11) Jénnette, K.W. (1981) *Environ. Health Perspect.*, 40, 233.
- 12) Sirover, M. A. (1981) *Environ. Health Perspect.*, 40, 163.
- 13) Nishioka, H. (1975) *Mutat. Res.*, 31, 185.
- 14) Sirover, M.A. & Loeb, L.A. (1976) *Science*, 194, 1434.
- 15) Rossman, T.G., Molina, M., & Meyer, L.W. (1984) *Environ. Mutagen.*, 6, 59.
- 16) Connett, P.H., & Wetterhahn, K.W. (1983) *Struct. Bonding* 54, 93.
- 17) Bianchi, V., Celotti, L., Lanfranchine, G., Majone, F., Marin, G., Montaldi, A., Sponza, G., Tamino, G., Venier, P., Zantedesci, A., & Levis, A.G. (1983) *Mutat. Res.*, 117, 279.

- 18) Langerwerf, J.S.A., Bakkeren, H.A., & Jongen, W.M.T. (1985) *Ecotox. Environ. Safety*, 9, 92.
- 19) DeFloro, S., & Wetterhahn, K.E. (1989) *Life Chem. Rep.*, 7, 169.
- 20) Tsapakos, M.J., Hampton, T.H., & Wetterhahn, K.E. (1983) *Cancer Res.*, 43, 5662.
- 21) Sugiyama, M., Wang, X.W., & Costa, M. (1986) *Cancer Res.*, 46, 4547.
- 22) Sugiyama, M., Patierno, S.R., Cantoni, D., & Costa, M. (1986) *Mol. Pharmacol.*, 29, 606.
- 23) Warren, G., Schultz, P., Bancroft, D., Bennett, K., Abbott, E., & Rogers, S. (1981) *Mutat. Res.*, 90, 111.
- 24) Beyersmann, D., Koester, A., Buttner, B., & Flessel, P. (1984) *Tox. and Env. Chem.*, 8, 279.
- 25) Warren, G. (1981) 2nd Symposium on Bioassays of Environmental Mixtures, EPA, Plenum Press, New York.
- 26) Garcia, J.D., & Wetterhahn, K.E. (1981) *J. Inorg. Biochem.*, 14, 281.
- 27) Shi, X., & Dalal, N.S. (1989) *Biochem. Biophys. Res. Comm.*, 163(1), 627.
- 28) Aiyar, J., Berkovits, H.J., Floyd, R.A., & Wetterhahn, K.E. (1991) *Environ. Health Perspect.*, 92, 53.
- 29) Aiyar, J., Berkovits, H.J., Floyd, R.A., & Wetterhahn, K.E. (1990) *Chem. Res. in Toxicol.*, 3(6), 595.
- 30) O'Brien, P., Barrett, J., & Swanson, F. (1985) *Inorganica Chimica Acta.*, 108, L19.
- 31) Aiyar, J., Borges, K.M. Floyd, R.A., & Wetterhahn, K.E. (1981) *Toxicol. Environ. Chem.*, 22, 135.
- 32) Shi, X., & Dalal, N.S. (1990) *Arch. Biochem. Biophys.*, 277, 342.
- 33) Kawanishi, S., Inoue, S., & Sano, S. (1986) *J. Biol. Chem.*, 261(13), 5952.
- 34) Jones, P., Kortenkamp, A., O'Brien, P., Wang, G., & Yang, G. (1991) *Arch. Biochem. Biophys.*, 286, 652.

- 35) Ozawa, T., & Hanaki, A. (1990) *Biochem. Int.*, 22, 343.
- 36) Rosenberg, B., Van Camp, L., Troski, J., & Mansour, V.H. (1969) *Nature*, 222, 385.
- 37) Zwelling, L.A., & Kohn, K.W. (1979) *Cancer Treatment Reports*, 63(9-10), 1439.
- 38) Bancroft, D.P., Lepre, C.A., & Lippard, S.J. (1990) *J. Am. Chem. Soc.*, 112, 6860.
- 39) Salles, B., Butour, J.L., Lesca, C., & Macquet, J.P. (1983) *Biochem. Biophys. Res. Commun.*, 112(2), 555.
- 40) Ciccarelli, R.B., Solomon, M.J., Varshavsky, A., & Lippard, S.J. (1985) *Biochemistry*, 24, 7533.
- 41) Pinto, A.L., & Lippard, S.J. (1985) *Proc. Natl. Acad. Sci. USA*, 82, 4616.
- 42) Fram, R.J., Cusick, P.S., Wilson, J.M., & Marinus, M.G. (1985) *Mol. Pharmacol.*, 28, 51.
- 43) Guttenplan, J.B., & Milstein, S. (1982) *Carcinogenesis*, 3(3), 327.
- 44) Loveless, A. (1969) *Nature*, 223, 206.
- 45) Singer, B. (1979) *J. Natl. Cancer Inst.*, 62, 1329.
- 46) Gerchman, L.L. & Ludlam, D. (1973) *Biochim. Biophys. Acta.*, 308, 310.
- 47) Magee, P.N., Montesano, R., & Preussman, R. (1976) Chemical Carcinogens, ACS Monograph Series, in Searle, C.E.(ed) 173, American Chemical Society, Washington, DC, pp.491-625.
- 48) Hince, T.A., & Neale, S. (1977) *Mutat. Res.*, 46, 1.
- 49) Caspary, W.J., Lanzo, D.A., & Niziak, C. (1982) *Biochemistry*, 21, 334.
- 50) Hassan, H.M., & Fridovich, I. (1978) *J. Biol. Chem.*, 253, 8143.
- 51) Hassan, H.M., & Fridovich, I. (1979) *J. Biol. Chem.*, 254, 10846.
- 52) Hassan, H.M., & Fridovich, I. (1979) *Arch. Biochem. Biophys.*, 196, 385.

- 53) Fridovich, I. (1975) *Annu. Rev. Biochem.*, 44, 147.
- 54) Halliwell, B. (1987) *FASEB J.*, 1, 358.
- 55) Cheson, B.D., Curnutte, J.T., & Babior, B.M. (1977) *Prog. Clin. Immunol.*, 3, 1.
- 56) Kellogg, E.W., & Fridovich, I. (1977) *J. Biol. Chem.*, 252, 6721.
- 57) Pryor, W.A. (1988) *Free Radical Biology and Medicine*, 4, 219.
- 58) Tullius, T.D. (1987) *Nature*, 343, 267.
- 59) Weinfeld, M., Soderlind, K.M. (1991) *Biochemistry*, 30, 1091.
- 60) Shigenaga, M.K., Ames, B.N. (1991) 10, 211.
- 61) Walker, G.C. (1985) *Annu. Rev. Biochem.*, 54, 425.
- 62) Haber, F., & Weiss, J. (1934) *Proc. R. Soc. A.*, 147, 332.
- 63) Fenton, H.J.H. (1894) *J. Chem. Soc.*, 65, 899.
- 64) Marshall, L., Reich, K.A., Graham, D.R. & Sigman, D.S. (1981) *Biochemistry*, 20, 244.
- 65) Chen, X., Rokita, S.E., & Burrows, C.J. (1991) *J. Am. Chem. Soc.*, 3570.
- 66) Torreilles, J., Guerin, M.C., & Slaoui-Hasnaoui, A. (1990) *Free Rad. Res. Commun.*, 11(1-3), 159.
- 67) Iyer, V.N., & Szybalski, W. (1964) *Science*, 145, 55.
- 68) Barton, J.K., Danishefsky, A.T., & Goldberg, J.M. (1984) *J. Am. Chem. Soc.*, 106(7), 2172.
- 69) Rehmann, J.P., & Barton, J.K. (1990) *Biochemistry*, 29, 1701.
- 70) Howe-Grant, M., Wu, K.C., Bauer, W.R., & Lippard, S.J. (1976) *Biochemistry*, 15(19), 4339.
- 71) Barton, J.K., & Raphael, A.L. (1985) *Proc. Natl. Acad. Sci. USA*, 82, 6460.
- 72) Cupo, D.Y., & Wetterhahn, K.E. (1985) *Cancer Res.*, 45, 1146.

- 73) Geiger, W.E. (1985) *Progress in Inorganic Chemistry*. Vol. 33, Lippard, S.J. (Ed), John Wiley & Sons, New York. pp.275-352.
- 74) Earley, J.E., & Cannon, R.D. (1965) *Transition Metal Chemistry*, Carlin (ed), Marcel Dekker, Inc., New York, pp.34-89.
- 75) Burstall, F.H., & Nyholm, R.S. (1952) *J. Chem. Soc.*, 3570.
- 76) Garner, C.S., & House, D.A. (1970) *Transition Metal Chemistry*, Carlin, R.L. (ed), Marcel Dekker, Inc., New York, pp. 59-295.
- 77) Sprintschnick, G., Sprintschnik, H.W., Kirsch, P.P., & Whitten, D.G. (1977) *J. Am. Chem. Soc.*, *99*(15), 4947.
- 78) Gillard, R.D., & Mitchell, P.R. (1976) *Inorganic Syntheses*, Vol. 13, McGraw-Hill, New York, pp. 184-186.
- 79) Rollinson, C.L., & Bailar, J.C. (1946) *Inorganic Syntheses*, Vol. 2, McGraw-Hill, New York, pp. 196-202.
- 80) Kyuno, E., Kamada, M., & Tanaka, N. (1967) *Chem. Soc. Jpn. Bull.*, *40*, 1848.
- 81) Bigelow, J.H. (1946) *Inorganic Syntheses*, Vol. 2, McGraw-Hill, New York, pp. 203-205.
- 82) Levin, D.E., Hollstein, M., Christman, M.F., & Ames, B.N. (1984) *Methods in Enzymol.*, *105*, 249.
- 83) Maron, D.M., & Ames, B.N. (1983) *Mutat. Res.* *113*, 173.
- 84) *Experiments in Molecular Genetics*, Cold Spring Harbor Laboratory.
- 85) Bonsteel, R.A. (1986) *A Micro Computer Controlled High Speed High Resolution Cyclic Voltammeter*, M.S. Thesis.
- 86) Enke, G.G., Ramaley, L., & Brubaker, R.L. (1963) *Anal. Chem.*, *35*, 1088.
- 87) Sawyer, D.T., & Roberts, J.L. (1974) *Experimental Electrochemistry for Chemists*, John Wiley and Sons, New York.
- 88) Maniatus, T., Fritsch, E.F., & Sambrook, J. (1982) *J. Molecular Cloning: A Laboratory Manual*, Cold Spring Harbor, New York.

- 89) Douglas, B., McDaniel, D.H., & Alexander, J.J. (1983) *Concepts and Models of Inorganic Chemistry*, John Wiley and Sons, Inc., New York. pp. 270-275.
- 90) Herzog, S., & Taube, R. (1962) *Z. Chem.*, 2, 208.
- 91) Elschner, B., & Herzog, S. (1958) *Arch. Sci. Geneva*, 11, 160.
- 92) Konig, E., & Fischer, H. (1962) *Z. Naturforsch*, 17, 1063.
- 93) Brown, I.M., Weissman, S.I. (1963) *J. Am. Chem. Soc.*, 85, 2528.
- 94) Vlcek, A.A. (1963) *Prog. Inorg. Chem.*, 5, 353.
- 95) Warren, G., Abbott, E., Schultz, P., Bennett, K., & Rogers, S. (1981) *Mutat. Res.*, 88, 165.
- 96) Ames, B.N. (1971) *Chemical Mutagens, Principles and Methods of Their Detection*, A. Hollaender (ed) Plenum, New York, Vol. 1, pp. 267-282.
- 97) Zakrzewski, S.F. (1991) *Principles of Environmental Toxicology*, American Chemical Society, Washington, D.C.
- 98) Soignet, D.M., & Hargis, L.G. (1972) *Inorg. Chem.*, 11(10), 2349.
- 99) Soignet, D.M., & Hargis, L.G. (1973) *Inorg. Chem.*, 12(4), 877.
- 100) Baker, B.R., & Dev Mehta, B. (1965) *Inorg. Chem.*, 4(6), 848.
- 101) Nadler, S.D., Dick, J.G., & Langford, C.H. (1985) *Can. J. Chem.*, 63, 2732.
- 102) Tanaka, N., & Sato, G. (1963) *Nature*, 197, 176.
- 103) Tanaka, N., Ebatta, E., & Sato, G. (1963) *Bull. Chem. Soc. Jpn.*, 36, 922.
- 104) Taube, H., & King, E.L. (1954) *J. Am. Chem. Soc.*, 76, 4056.
- 105) Inskip, R.G., & Bjerrum, J. (1961) *Acta Chem. Scand.*, 15, 62.
- 106) Josephsen, J., & Schaffer, C.E. (1970) *Acta Chem. Scand.*, 24, 2929.
- 107) Maki, N., Shimura, Y., & Tsuchida, R. (1958) *Bull. Chem. Soc. Jpn.*, 31, 413.

- 108) Mascio, P.D., Wefers, H., Do-Thi, H., Lafleur, M.V.M., & Sies, H. (1989) *Biochim. Biophys. Acta*, 1007, 151.
- 109) Standeven, A., & Wetterhahn, K.E. (1991) *Carcinogenesis*, 12(9), 1733.
- 110) Purrugganan, M.D., Kumar, C.V., Turro, N.J., & Barton, J.K. (1988) *Science*, 241, 1645.

## APPENDIX

### Conversion of Cyclic Voltammetry Output to Microamps

Data points generated by the Forth based *runcv* program must be converted into microamps prior to graphing versus the potential area scanned. This was accomplished by first using a program called *CD1X*. This program takes the raw CV data and converts it into a single column ASCII text file. At this point, the file is in the Apple Dos 3.3 format. To manipulate this data, the file must be converted into an IBM compatible ASCII text file. This was accomplished using a program called *Crossworks*. *Crossworks* takes an Apple Dos ASCII file and first converts into Apple ProDos format. It then converts the file into an IBM compatible ASCII text file that is transmitted from the Apple computer to an IBM compatible. This process gives you a single column ASCII text file of CV data points. At this point, the file can be imported into a spreadsheet program such as Quattro Pro.

The imported ASCII text at this time consists only of data points which must be converted to microamps. This was accomplished by using a macro created by Dr. Richard Geer and Dr. Penny O'Connor. The macro allows input of the CV calibration data (discussed below) and then uses this data to convert the data points into their corresponding microamp values. The voltages are inputted by hand by knowing the potential range scanned as well as how many mV/data point resolution was used. A working graph for each scan is produced and can then be

merged for the total number of scans of the complex.

Calibration of the instrument prior to running is necessary to obtain accurate current readings. This is accomplished within the *runcv* program itself. A submenu under the *runcv* program is *calibrate instrument*. The calibrate instrument program is a menu driven program that generates a hard copy of the calibration data needed in data point conversion macro. The steps to generate the calibration file are given below.

1) Go to Calibrate Instrument on Runcv menu.

2) A to D Conversion Tables

- a) connect x input from A to D converter to ground.
- b) connect x output to x input.
- c) hook voltmeter to x input and hook other side to ground.
- d) input mV readings into computer (from voltmeter).

3) D to A Voltage

- a) 1 enter
- b) 2 enter
- c) 3 enter
- d) 4 enter

4) Enter 6 on menu to return to Calibration menu.

- a) 3 enter (on calibration menu)
- b) 5 enter (input calibration resistance of 10040)
- c) 8 enter (takes you back to runcv menu)

While calibration is proceeding, the calibration file is printed out automatically. A sample of the calibration file is shown in the following pages.

## ATOD Gain Tables

Gain #	GDAC Num.	+ATOD		-ATOD		Ref.V Scale	ATOD ZOS
		Ref.V	Span	Ref.V	Span		
0	4095	10110	-1633	-9940	1606	1	-1
1	2576	6360	-1634	-6360	1633	1	-2
2	1625	4020	-1637	-4010	1634	1	-4
3	1024	2530	-1637	-2530	1633	1	-5
4	644	1599	-1643	-1595	1633	1	-10
5	409	1019	-1651	-1015	1641	1	-22
6	258	6450	-1658	-6410	1642	10	-27
7	163	4120	-1674	-4080	1648	10	-51
8	102	2610	-1696	-2560	1663	10	-85
9	65	1698	-1719	-1640	1669	10	-114
10	41	1112	-1793	-1053	1691	10	-192
11	26	7380	-1754	-6800	1730	100	-294
12	17	5120	-1631	-4540	1752	100	-417
13	11	3640	-1391	-3070	1822	100	-657
14	7	2610	-1070	-2030	1903	100	-978
15	5	2110	-727	-1540	1982	100	-1321
16	4	1830	-496	-1260	2023	100	-1552
17	3	1590	0	-1020	2101	100	-2048
18	2	13200	0	-7400	1411	1000	-2048
19	1	10500	0	-4800	0	1000	-2048

## Initial Potential DAC

Positive output:

span full scale... 10122 mV zero offset... -6 mV

Negative output:

span full scale... -9965 mV zero offset... 0 mV

## Step Potential DAC

Positive output:

span full scale... 10085 mV zero offset... -6 mV

Negative output:

span full scale... -10064 mV zero offset... 0 mV

## X Output DAC

Positive output:

span full scale... 10110 mV zero offset... 6 mV

Negative output:

span full scale... -9934 mV zero offset... 0 mV

## Y Output DAC

Positive output:

span full scale... 10073 mV zero offset... -6 mV

Negative output:

span full scale... -10163 mV zero offset... 0 mV

Positive Cell Offset is 0 MV  
 Negative Cell Offset is 0 MV

## CV Sweep Rate Table

## Negative Sweep Direction

Sweep rate Number	Sweep Rate mV/sec	End of Test Voltage, mV	Reps of 40ms TI
0	12	489	1000
1	12	495	1000
2	18	712	1000
3	40	792	500
4	70	836	300
5	121	1213	250
6	173	1659	240
7	227	2086	230
8	290	2551	220
9	397	3331	210
10	505	4037	200
11	616	4680	190
12	746	5219	175
13	976	5269	135
14	1206	5256	109
15	1439	5238	91
16	1705	5250	77
17	2177	5225	60
18	2647	5293	50
19	3125	5250	42
20	3663	5275	36
21	4616	5355	29
22	5572	5349	24
23	6539	5231	20
24	7621	5162	17
25	9535	5721	15
26	11429	5943	13
27	13350	6408	12
28	13436	5912	11
29	13450	5380	10
30	13450	5380	10
31	13450	5360	10

## CV Sweep Rate Table

## Positive Sweep Direction

Sweep rate Number	Sweep Rate mV/sec	End of Test Voltage, mV	Reps of 40ms TI
0	13	501	1000
1	13	501	1000
2	4	149	1000
3	-20	-408	500
4	-53	-637	300
5	-106	-1065	250
6	-159	-1523	240
7	-213	-1956	230
8	-276	-2426	220
9	-386	-3243	210
10	-495	-3961	200
11	-606	-4605	190
12	-737	-5162	175
13	-972	-5249	135
14	-1204	-5249	109
15	-1442	-5249	91
16	-1712	-5273	77
17	-2197	-5273	60
18	-2674	-5348	50
19	-3154	-5298	42
20	-3705	-5335	36
21	-4674	-5422	29
22	-5648	-5422	24
23	-6622	-5298	20
24	-7719	-5249	17
25	-9655	-5793	15
26	-11581	-6022	13
27	-12558	-6028	12
28	-12589	-5539	11
29	-12625	-5050	10
30	-12610	-5044	10
31	-12580	-5032	10

Reference Voltage is -4989 mV

Calibration resistor is 10040 ohms

Cell current as voltage is -4147 mV

Current scale factor is 1000

V to I conversion is 1198 microA/10000 mV

**Plasmid Preparation Solutions****Solution I**

10 mg lysozyme (added fresh on ice)  
0.1 ml 0.5 M EDTA pH 8.0  
0.625 ml 2.0 M Tris-HCl  
4.5 mg Glucose  
4.2 ml dH<sub>2</sub>O

**Solution II**

0.8 g NaOH  
1 g SDS  
100 ml dH<sub>2</sub>O

**Solution III**

6ml 5.0 M Potassium Acetate  
1.15 ml Glacial Acetic Acid  
2.85 ml H<sub>2</sub>O

**5X TBE**

54 g Tris base  
27.5 g Boric Acid  
20 ml 0.5 M EDTA  
1 L H<sub>2</sub>O

**TE**

10 mM Tris-HCl  
1.0 mM EDTA

**6X Agarose Gel Loading Buffer**

.15 g Ficoll  
0.4 ml 0.5 M EDTA  
0.6 ml 10X TBE  
2.5 mg Xylene Cyanol (optional)  
2.5 mg of Bromophenol Blue

T<sub>50</sub>NaOAC

1.3 ml 2.0M Tris (pH 8.0)

1.7 ml 3.0 M NaOAC

Salmonella Reversion Assay**M9 buffer (5X)**64 g Na<sub>2</sub>HPO<sub>4</sub>·7H<sub>2</sub>O15 g KH<sub>2</sub>PO<sub>4</sub>

2.5 g NaCl

5.0 g NH<sub>4</sub>Cl1.0 L dH<sub>2</sub>O

Histidine.HCl

**Minimal Glucose Plates**

15 g Agar

20 ml 50X VB Salts

40% glucose

930 ml dH<sub>2</sub>O**Top Agar**

6.0 g Agar

5.0 g NaCl

1.0 L dH<sub>2</sub>O**Vogel-Bonner (VB) Salts (50X)**670 ml dH<sub>2</sub>O10 g MgSO<sub>4</sub>·7H<sub>2</sub>O

100 g Citric Acid

500 g K<sub>2</sub>HPO<sub>4</sub>175 g NaH<sub>2</sub>NH<sub>4</sub>PO<sub>4</sub>·4H<sub>2</sub>O**Histidine/Biotin Solution**

30.9 mg D-Biotin

24.0 mg L-Histidine.HCl

250 ml dH<sub>2</sub>O**Ampicillin Plates**

15 g Agar

910 ml dH<sub>2</sub>O

20 ml VB salts

50 ml 40% glucose

10.0 ml of 2g/400ml

6.0 ml 0.5 mM biotin

3.15 ml of 8mg/ml ampicillin

**Ampicillin/Tetracycline Plates**Same as above but  
additionally:

0.25 ml of 8mg/ml

tetracycline

**LB Agar Plates**

10 g Bacto Tryptone

5 g Bacto Yeast Extract

10 g NaCl

15 g Agar

1.0 L dH<sub>2</sub>O**Z Buffer**0.06 M Na<sub>2</sub>HPO<sub>4</sub>·7H<sub>2</sub>O0.04 M NaH<sub>2</sub>PO<sub>4</sub>·H<sub>2</sub>O

0.01 M KCl

0.001 M MgSO<sub>4</sub>·7H<sub>2</sub>O

0.05 M Mercaptoethanol

MONTANA STATE UNIVERSITY LIBRARIES



3 1762 10198976 0